Copolymer Adsorption and the Effect on Colloidal Stability

promotoren: Dr. M.A. Cohen Stuart,
hoogleraar in de Fysische Chemie met bijzondere
aandacht voor de Kolloïdchemie

Dr. G.J. Fleer,
persoonlijk hoogleraar bij het Laboratorium
voor Fysische Chemie en Kolloïdkunde

Henri D. Bijsterbosch

Copolymer Adsorption and the Effect on Colloidal Stability

Proefschrift
ter verkrijging van de graad van doctor
op gezag van de rector magnificus
van de Landbouwuniversiteit Wageningen,
Dr. C.M. Karssen,
in het openbaar te verdedigen
op vrijdag 6 februari 1998
des namiddags te half twee in de aula.

CIP-DATA Koninklijke Bibliotheek, Den Haag

Bijsterbosch, Henri Derk

Copolymer adsorption and the effect on colloidal stability /
Henri Derk Bijsterbosch - [S.l. : s.n.]
Thesis Wageningen - with refs. - with summary in Dutch
ISBN 90-5485-790-0
Subject headings: polymer adsorption / colloidal stability

printing: Grafisch Service Centrum, Wageningen

Het in dit proefschrift beschreven onderzoek is financieel ondersteund door het Innovatiegericht Onderzoek Programma verf (IOP-v)

Stellingen

1. Een goede indicatie voor de mate van sterische stabilisatie van een colloïdale dispersie kan doorgaans verkregen worden door de geadsorbeerde hoeveelheid polymeer te meten.

   Dit proefschrift: hoofdstuk 6

2. Voor de sterische stabilisatie van colloïdale dispersies zijn adsorberende diblokcopolymeren geen wondermiddel.

   Dit proefschrift: hoofdstuk 3 en 6

3. De kinetiek van polymeeradsorptie krijgt wetenschappelijk gezien nog relatief weinig aandacht terwijl het in industriële toepassingen juist een zeer belangrijke rol speelt.

4. Gonçalves da Silva et al. verklaren de hysterese in oppervlaktedruk bij compressie en decompressie van een polystyreen-polyethyleenoxide monolaag met conformatieveranderingen en verstrengeling van de polyethyleenoxide ketens. De onomkeerbaarheid van de hysterese is echter beter te verklaren met verlies van ketens uit de monolaag.

   A.M. Gonçalves da Silva et al., *Langmuir*, 1996, 12, 6547
   Dit proefschrift hoofdstuk 2

5. De soms zeer tegenstrijdige beoordelingsrapporten die geschreven worden over een artikel dat voor publicatie is aangeboden, geven aan dat de acceptatie van een manuscript vaak ook in belangrijke mate een kwestie van smaak is.

6. Dat het promotieregelement van verschillende universiteiten ten aanzien van de stellingen niet hetzelfde is, is op z'n minst jammer te noemen.

7. De managementkwaliteiten die in veel personeelsadvertenties voor universitaire wetenschappers van de sollicitant verlangd worden, kunnen een verarming van de wetenschap betekenen omdat de wetenschappelijke kwaliteit hierdoor relatief minder zwaar weegt.

8. Het aan de industrie verplicht opleggen van milieu-eisen stimuleert het industrieel en wetenschappelijk onderzoek naar alternatieve produkten en produktiemethoden.

9. Het uitspreken van de Engelse taal zou een stuk eenvoudiger zijn wanneer de letters die toch niet uitgesproken hoeven worden, ook niet opgeschreven zouden zijn.

10. Dat wasmiddelen al zo vaak vernieuwd en verbeterd zijn suggereert ten onrechte dat ze nu toch wel perfect zullen zijn.

Stellingen behorend bij het proefschrift: "Copolymer adsorption and the effect on colloidal stability" van Henri D. Bijsterbosch, Landbouwuniversiteit Wageningen, 6 februari 1998.

Contents

Chapter 5

Chapter 6

Copolymer adsorption and the effect on colloidal stability

Chapter 1 - Introduction

Colloidal dispersions

Before introducing the subject of this thesis we give an example to illustrate the practical relevance. Our example is paint. The process of paint-making and its application involves a number of consecutive steps. The most frequently used pigment particles in paint are solid titanium oxide (titania) particles, often covered with a surface layer of silicium oxide (silica) or aluminium oxide. In the first step of paint-making grinding of the pigment powder consisting of dry agglomerates occurs in the presence of a liquid. The particles must be wetted by and stabilised in the solvent. This is achieved by adding long molecules that adsorb onto the surface and prevent the pigment particles from aggregating: a so-called *sterically stabilised colloidal dispersion* is obtained; what this means and how this can be achieved will be explained further on in this introduction. The second step in paint-making involves the addition of binders, cross-linkers and other additives. Then the dispersion is mixed with other paint dispersions, in order to make paints with a variety of features like colour, gloss and durability. The paint is then stored, during which it must remain stable, and is applied to a substrate for protection and decoration. After application of the wet paint, the solvent evaporates and the binder should form a strong film which keeps the pigment particles together.[1] The subject of this thesis is mainly relevant for the first step described above, dispersing the oxide pigment particles, but the choice of materials has also consequences for the following processes. Below we give a brief introduction to the most important terms encountered in the underlying science.

A paint with finely dispersed particles in a liquid is an example of a *colloidal system.* The variety of colloidal systems in nature and in industrial applications is enormous, but the common feature is the presence of (at least) two components, one of which has at least in one direction a dimension of roughly 1 nm to 1 μm.[2] A direct consequence of this small particle size is that the interface between the components is very large. One of the components forms a continuous phase in which the other component is dispersed. With these characteristics in mind, we may recognise many other colloidal systems in the world surrounding us. Classical examples are ink, milk, clouds, surfactant solutions, foam and smoke. Colloidal phenomena play a very important role in the living world as

well. The presence of particles in body fluids like blood and lymph, the membranes that surround the cells, proteins that regulate the processes in the body, and also DNA, which stores our genetic information, are all colloidal in nature. The components in these examples are either solid, liquid, or gas. In the following we will mainly consider colloidal dispersions of solid particles in a liquid continuous dispersion medium.

Solid particles in a colloidal dispersion attract each other by Van der Waals forces which, if these forces were the only ones acting, would result in aggregation of the particles. In order to prevent this aggregation the particles must also have some repulsive force that has a longer range than the attractive Van der Waals force. If no aggregation occurs the colloidal dispersion is stable. The repulsive force necessary for colloidal stability can be achieved in two ways: *electrostatically* and *sterically*. A schematic representation of electrostatic and steric stabilisation is given in Figure 1.

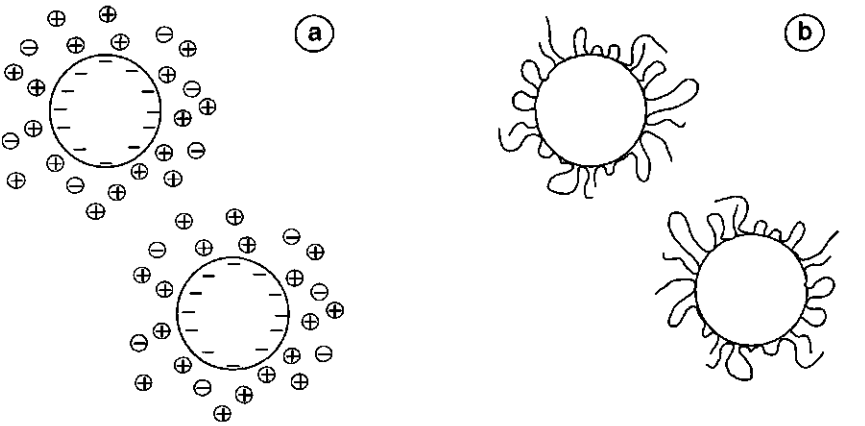

Figure 1. Electrostatically (a) and sterically (b) stabilised particles.

Electrostatic stabilisation can be obtained if the particles carry a surface charge.[3] In water, this is frequently the case. The presence of a charged surface layer leads to the formation of a diffuse layer of counter-charge in solution which ensures electroneutrality. Upon the approach of two charged particles the diffuse layers start to overlap which results in an electrostatic repulsive force. If the extension of the repulsive force is larger than the range of the Van der Waals attraction, the dispersion will be stable. The spatial extension of the electrostatic repulsion depends on the concentration of ions in solution. Increase of the ion concentration causes the diffuse layer to become thinner and makes

the stabilisation less effective. This phenomenon plays an important role in, for example, the settling of clay in a river-mouth when river water containing electrostatically stabilised clay particles mixes with salt water from the sea.

Steric stabilisation can be brought about by *polymers* attached to the surface of the particles.[4] These polymers are long macromolecules built from a large number of repeating units. The overlap of polymer layers up the approach of two particles results in a strong repulsion. If the polymer layers are thick enough they can prevent the particles from aggregation by the Van der Waals forces. The phenomenon of steric stabilisation was already used by the Egyptians in ancient times, although they probably did not realise. They prepared ink by dispersing carbon soot in a solution of naturally occurring polymers like gum arabic. The gum provided the steric stabilisation of the colloidal carbon particles.

As stated above, a polymer is built from a large number of repeating units, so-called monomers or segments. The properties of a polymer hardly change upon addition or removal of a few units. If the monomers are all of the same type the polymer is a *homopolymer*. If different types of monomers occur in the same macromolecule such a polymer is referred to as a *copolymer*. We can distinguish different types of copolymers with a different distribution of monomers in the molecule (see Figure 2). Two classes of copolymers are used in the studies described in this thesis: *block copolymers* and *graft copolymers*. In linear block copolymers the different types of segments are separated in long homopolymer blocks. Thus, in a diblock copolymer a homopolymeric block consisting of one type of monomers is connected with another block in which the monomers are of a different type than in the first block. Graft copolymers, also called comb polymers, on the other hand, consist of a long homopolymer main chain to which side chains (grafts or "teeth") consisting of another type of segments are grafted.

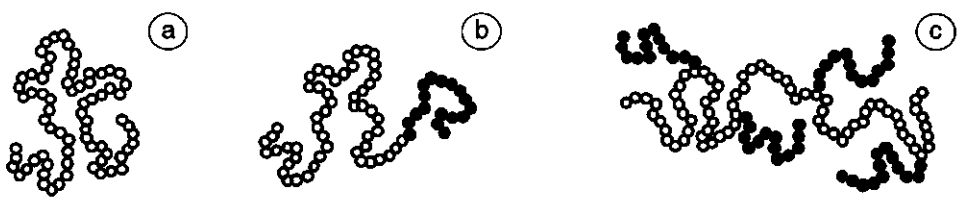

Figure 2. Schematic representation of different polymer types: homopolymer (a), diblock copolymer (b), graft or comb copolymer (c)

The segments of a polymer can be charged, in which case the polymer is called a polyelectrolyte. When polyelectrolytes are used for the stabilisation of charged colloidal particles, both steric and electrostatic contributions are involved. The electrostatic repulsion may then originate from both the particle surface and from the polyelectrolyte.[5,6] In this thesis we only consider uncharged polymers.

Polymer adsorption

As discussed before a colloidal dispersion has a large interfacial area. Such an interface has a high amount of *surface Gibbs energy,* which is (loosely) defined as the excess of the Gibbs energy of an interface between two unlike materials as compared to the bulk. The fact that an interface has a higher Gibbs energy than the bulk implies that, roughly speaking, the various kinds of molecules prefer to be surrounded by their own kind. The existence of an interface forces some molecules to be in contact with another type of molecules, which is unfavourable. A colloidal system therefore tends to decrease its Gibbs energy, hence its interfacial area. In a liquid-in-liquid or in a liquid-in-gas colloidal dispersion decrease of the interfacial area can be achieved by coalescence of many small droplets into fewer large droplets: a dispersion with big droplets has a lower surface area than one with small droplets (if the total amount of dispersed phase is kept constant). For solid-in-liquid dispersions coalescence is not possible as the solid particles can not easily change their shape. However, also aggregation of particles, which may be seen as particles clumping together without changing their individual shape, decreases the amount of solid-liquid interface as part of the surfaces of different particles make close contact in an aggregate.

Even without aggregation it is possible to decrease the surface Gibbs energy. When the dispersion contains another component which has affinity for the surface, the Gibbs energy may be decreased by the accumulation of these molecules at the interface. The molecules must then have some affinity for both the solid phase and the dispersion medium. For example, if the liquid is polar and the particles are apolar then we expect that a molecule with an intermediate polarity will decrease the surface Gibbs energy by accumulating at the interface. This accumulation of material at an interface is referred to as *adsorption.* Adsorption of molecules is very common in colloidal systems and is, for example, important when we clean our dishes. Apolar greasy substances on dishes are not soluble in (polar) water. Yet, we can remove the greasy material by using surfactants. Surfactants are bipolar: they have an apolar moiety and a polar head group which often carries a charge. When added to the dish-water the surfactants prefer the interface

between water and greasy material because they can adopt an orientation in which the polar head group is directed towards the water, whereas the apolar part is in contact with the oil. As a result the surface Gibbs energy is decreased and greasy substances become dispersed in water. The charge of the polar group provides these greasy colloidal particles with a stabilising diffuse electrical layer.

As discussed above adsorption is driven by a decrease of the surface Gibbs energy. Adsorption is, however, opposed by a decrease of *translational entropy* of the adsorbed molecules. In solution the molecules have considerable freedom to move. At the interface this freedom is restricted, which gives rise to a decrease of the translational entropy of the system. The balance between the decrease of surface Gibbs energy and the increase of entropy, which gives the *total Gibbs energy* of the system, determines whether adsorption will occur. If the total Gibbs energy decreases adsorption is likely to happen. The translational entropy per segment in a polymer chain is considerably lower than that of a small molecule of the same chemical type. This is caused by the fact that the monomer units in a polymer molecule have already lost much of their freedom to move through the solution because they are chemically linked to each other. The gain in surface Gibbs energy upon adsorption, on the other hand, is roughly equal for polymers and small molecules of the same chemical type. Consequently, adsorption of polymer molecules is more likely to occur than that of small molecules.[7]

Besides the translational entropy another kind of entropy plays an important role for the behaviour of polymers: *configurational entropy*. Although the translational entropy of polymers is relatively low, they have a considerable amount of configurational entropy: the freedom to vary the relative positions of the segments.[8] In solution the polymer molecules continuously change their conformation. The average overall conformation is a more or less spherical random coil. If a polymer chain adsorbs it will have part of its segments in contact with the surface. However, the adsorbed polymer layer does not form a rigid structure: the chains retain a large degree of their configurational freedom by also here changing the relative position of their segments. Consequently, the adsorbed layer is a dynamic state in which the segments that are in contact with the surface (trains), continuously change position with non-adsorbed segments (loops and tails). When two surfaces covered with an adsorbed polymer layer approach each other, the polymer chains become confined between the surfaces. As the polymer wants to keep its entropy as high as possible, the chains do not want to overlap or change their shape towards a flat and dense conformation. The adsorbed layers thus provide a repulsive force which keeps the surfaces separated, which is the principle of steric stabilisation.

Polymer layer thickness

A colloidal dispersion of particles covered with an adsorbed polymer layer is only stable if the range of the repulsive forces is larger than that of the attractive Van der Waals forces. As we have seen above the steric repulsion is a consequence of the decrease in entropy upon "squeezing" the polymer layers. The range of the repulsive force is more or less proportional to the thickness of the polymer layer, which must therefore be large enough to impart colloidal stability. If this thickness is smaller than the range of the attractive forces and no other repulsive forces are present, we may encounter a situation where the dispersion is not stable but the aggregation between the particles is slowed down compared to the aggregation rate of bare particles without any form of protection.

For effective steric stabilisation the polymer must adsorb strongly on the particle surface and form a thick layer. Diblock copolymers can meet these two requirements. As described before these polymers contain two homopolymeric blocks of a different type of segments. When we choose one relatively short block that has a high affinity for the surface and another long block which prefers the dispersion medium, we expect a thick adsorbed layer. This situation in which only one of the blocks has affinity for the surface and the other prefers the dispersion medium may be referred to as *surface-selectivity.* Surface-selective adsorption of diblock copolymers has been studied extensively during the last ten years, theoretically as well as experimentally. We now have a rather complete picture of the behaviour of diblock copolymers at interfaces.[9-14]

Upon adsorption of diblock copolymers the adsorbing block will form a relatively thin layer on the surface. This block is also denoted as the *anchor* as it anchores the polymer molecule to the surface. The non-adsorbing blocks form a rather dilute and extended layer repelled by the surface. The non-adsorbing block is commonly referred to as *buoy* as it "floats" into the solution but can not diffuse away as it is anchored to the surface by the adsorbing block. The relative length of the blocks is of great importance for the structure of the polymer layer. This can be seen from Figure 3 where we plot the adsorbed amount as a function of the block copolymer composition and give a schematic representation of the adsorbed layer for four different block copolymer compositions. The total length of the diblock copolymer chain is taken to be constant in this example.

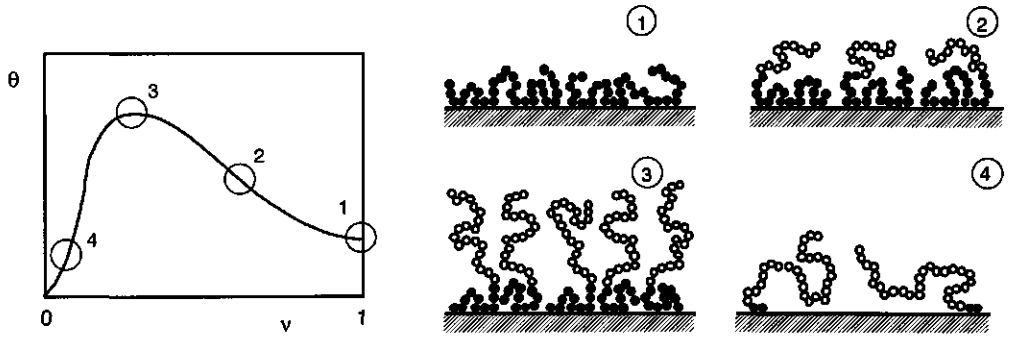

Figure 3. A graph of the adsorbed amount θ as a function of the fraction of anchor segments in the block copolymer v, and a sketch of the adsorbed layer for four different block copolymer compositions.

When the adsorbing anchor block is long, on the right side of the graph in Figure 3, the adsorption is limited by saturation of the anchoring layer. The adsorbed layer is very similar to that of an adsorbing homopolymer (situation 1), and only small non-adsorbing buoy blocks protrude into the solution (situation 2). The lateral repulsion between these buoy blocks, which originates from the entropic tendency to preserve the random coil conformation, is then weak compared to the adsorption energy. When we decrease the relative length of the anchor block, from right to left in the graph of Figure 3, we see that the adsorbed amount increases. The total mass of adsorbed anchor segments remains more or less constant but as the anchor blocks become smaller more chains must be adsorbed to keep the number of adsorbed segments constant. Therefore not only the length but also the number of buoy blocks protruding into the solution increases. The lateral repulsion between the buoy blocks increases as well but is still weak compared to the adsorption energy. When the length of the anchor block is further decreased, under a simultaneous increase of the length of the buoy, we find a maximum in the adsorbed amount. In this maximum the lateral repulsion between the non-adsorbed chains is very high and the buoy blocks are forced to adapt a stretched configuration as they are still attached to the surface by the anchor block (situation 3). This situation with highly stretched polymers is often referred to as a *brush*. The conformation and lateral pressure of such a brush has received much attention in literature.

When the length of the anchor block becomes very small and only a few segments are left to adsorb on the surface, the anchor blocks will no longer be able to fill the surface completely with an adsorbed layer (situation 4). The number and the length of the buoy blocks is now very high and the lateral repulsion in the buoy layer becomes more

important than the gain in adsorption energy; the adsorbed amount decreases accordingly.

From Figure 3 we see that the amount and the thickness of adsorbed diblock copolymers can be much higher than that of an adsorbing homopolymer of the same length. The extension of the repulsive force of an adsorbed diblock copolymer layer is thus also greater than that of the homopolymer. We therefore expect that diblock copolymers are good steric stabilisers.

A similar graph as in Figure 3 can be obtained with the use of graft copolymers. If we consider a graft copolymer with an adsorbing backbone and non-adsorbing side chains, the adsorbed amount as a function of the graft copolymer composition also shows a maximum at a certain composition. At this composition the relatively long grafts protrude into the solution in a stretched configuration forming a brush layer with high lateral pressure, similar to diblock copolymer brushes.

If the backbone of the graft copolymer has no affinity for the surface but the copolymer adsorbs with the side chains we also expect a maximum in the adsorbed amount as a function of the copolymer composition. At this maximum the polymer is firmly attached to the surface with the grafts and the polymer backbone is expected to form loops between the anchor points. The adsorbed layer again forms a dense brush although there are in this case no tails but only loops. A schematic representation of diblock and graft copolymer brushes is given in Figure 4.

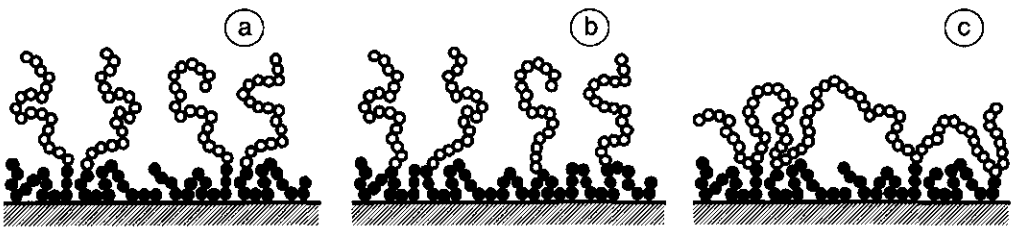

Figure 4. Brushes of diblock copolymers (a), graft copolymers with adsorbing backbone (b), and graft copolymers with adsorbing grafts and non-adsorbing backbone (c).

In Figure 4 the ratio of adsorbing to non-adsorbing segments is constant, the graft length and the graft density of the copolymer is in this case such that a comparison with the diblock copolymer is possible.The structure of the adsorbed layer of diblock copolymers

(Figure 4a) and that of a graft copolymer with an adsorbing backbone (Figure 4b) is very similar. A difference between the brushes formed by diblock copolymers and by graft copolymers with a non-adsorbing backbone (Figure 4c) is that the backbone loops prevent that the brush becomes very thick.

So far, we only considered selective adsorption of polymers: only one of the blocks has affinity for the surface. In real systems, however, often both blocks have affinity for the surface. The properties of the adsorbed layer for this *non-selective adsorption* are determined by the competition for anchoring sites between the two blocks. This aspect has hardly been addressed in the literature.

Kinetics of adsorption

Above, we only discussed the equilibrium state of an adsorbed polymer layer: the average conformation at which the system has a minimum Gibbs energy. However, the equilibrium state may not be obtained on the experimental time-scale, especially in industrial applications, where the time available for different processes is limited. The kinetics of adsorption determine how fast the equilibrium is obtained. Again, we use paint-making as an example, in this case to illustrate that time is a very important parameter. The pigment particles must be sterically stabilised in the grinding process. This process is immediately followed by mixing with other dispersions and additives. If the pigment is not yet completely stabilised in the grinding step, aggregation may occur during the following steps, leading to bad performance of the paint.[1] It is therefore very important that the grinding time is long enough to assure that the polymers form a thick and stabilising layer around the pigment particles. The time needed is determined by the adsorption kinetics. The kinetics of adsorption can give us more insight in the intermediate structures of the polymer layer before equilibrium. It may well be possible that a stabilising layer is formed on a very short time-scale, whereas the time to reach the equilibrium state takes much longer. On the other hand, we may encounter a situation where the equilibrium state is the same as in the former example but that the time required for the formation of the stabilising layer is very long. Knowledge about the adsorption kinetics is therefore important as it may determine the outcome of a process.

In the adsorption kinetics of polymers we can distinguish three processes: transport of the polymer from the dispersion medium towards the surface, attachment to the surface, and reconformation of the adsorbed polymer. For flexible homopolymers the attachment and reconformation of the molecule are generally very fast and the adsorption rate is determined by transport towards the surface. All polymer chains arriving at the surface will

adsorb until the surface is saturated and a plateau adsorbed amount is found. The adsorption kinetics of copolymers is more intricate than that of flexible homopolymers. During the formation of an adsorbed diblock copolymer layer the density in the brush becomes very high. The dense brush layer forms a barrier which makes it difficult for newly arriving molecules to bring their anchor block in contact with the surface. The anchor blocks have to diffuse through this barrier before they can adsorb. This diffusion process can be very slow and the equilibrium state may only be reached after a long time.

Another aspect which is important for the kinetics of adsorption is the solvent type. A copolymer can be solubilised in a solvent in which only one of the blocks is soluble whereas the other block dislikes the solvent. The solvent is then generally referred to as a *selective* solvent. A block copolymer dissolved in a selective solvent will form aggregation structures above a certain concentration of polymer in solution. The non-soluble blocks are clustered together and are surrounded by a layer of solvated chains. These structures, commonly denoted *micelles*, are in equilibrium with the solution which still contains a very low concentration of single polymeric chains. In Figure 5 we sketch the conformation of diblock copolymer molecules in a non-selective solvent (a) and in a selective solvent (b).

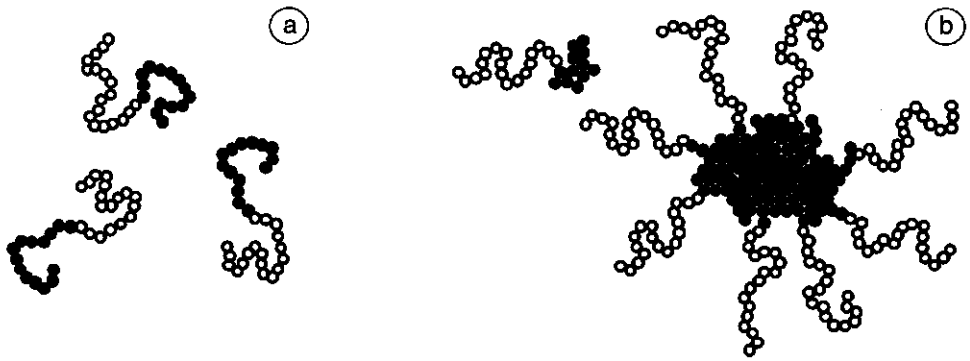

Figure 5. Sketch of the conformation of diblock copolymer molecules in a non-selective solvent (a) and in a selective solvent (b).

If only the non-soluble block has affinity for a surface the adsorption is most likely to proceed by the attachment of single chains. As the concentration of these polymer chains is very low the kinetics of adsorption may be very slow. However, there is a continuous

exchange of single polymeric chains between micelles and solution. If this exchange is fast compared to the adsorption process, the micelles can be seen as a reservoir which supplies new polymer molecules. The exchange kinetics of these micellar systems is therefore very important for the kinetics of polymer adsorption.

Outline of the thesis

The main aim of the work described in this thesis is to study the effect of different types of copolymers on the stability of aqueous oxide dispersions. In order to obtain a better insight in steric stabilisation we first study the relations between the adsorbed amount and layer thickness, and between the type of polymer and the adsorbed amount. We also pay attention to the adsorption kinetics.

In Chapter 2 we describe the properties of a diblock copolymer layer spread on a liquid-air interface. The lateral pressure and the thickness of the buoy layer formed on the surface is measured as a function of the adsorbed amount. The thickness is determined with help of neutron reflectivity measurements. The results are compared with theoretical predictions.

In Chapter 3 we present a study on the non-selective adsorption of two series of diblock copolymers from an aqueous solution on a macroscopically flat silicium oxide surface. The adsorbed amounts in this study and in that of Chapters 4 and 5, are measured with an optical reflectometer. We perform self-consistent field calculations for comparison with the experimental data.

The kinetics of adsorption of diblock copolymers can be very slow if the polymers form micelles in solution. This subject is addressed in Chapter 4. We compare the adsorption rates with the theoretical flux of copolymer molecules towards the surface for a series of four diblock copolymers with the same block length ratio but different molar masses. In this way we gain insight in factors that determine the adsorption kinetics.

In Chapter 5 we compare the adsorption of graft copolymers with an adsorbing backbone and non-adsorbing side chains to the reverse situation of adsorbing side chains and a non-adsorbing backbone. The results are compared with theoretical predictions from literature.

The effect of the polymers used in Chapters 3 to 5 on the stability of an aqueous silicium oxide dispersion is described in Chapter 6. The time-dependent increase of the average hydrodynamic radius of silicium oxide aggregates in the absence of stabilising forces is

measured. The increase of this radius in time is a good indication of the aggregation rate of the dispersion. The effect of polymer on the stability of the dispersion is studied by adding polymer to the dispersion and recording the aggregation rate. The stabilising effect of the polymers is compared with the adsorbed amount, and good correlation is found.

References

(1) Patton, T. C. Paint flow and pigment dispersion. A rheological approach to coating and ink technology; John Wiley & Sons: New York, 1979.

(2) Lyklema, J. Fundamentals of interface and colloid science I. Fundamentals; Academic Press: London, 1991.

(3) Kruyt, H. R. Colloid Science. Part I. Irreversible systems; Elsevier: Amsterdam, 1952.

(4) Napper, D. H. *Polymeric stabilisation of colloidal dispersions*; Academic Press: London, 1983.

(5) Israëls, R. PhD-thesis, Wageningen Agricultural University, 1994.

(6) Hoogeveen, N. G. PhD-thesis, Wageningen Agricultural University, 1996.

(7) Fleer, G. J.; Cohen Stuart, M. A.; Scheutjens, J. M. H. M.; Cosgrove, T.; Vincent, B. Polymers at Interfaces; Chapman & Hall: London, 1993.

(8) Flory, P. J. Principles of polymer chemistry; Cornell University Press: Ithaca NY, 1953.

(9) Marques, C. M.; Joanny, J. F.; Leibler, L. *Macromolecules* **1988**, 21, 1051.

(10) Marques, C. M.; Joanny, J. F. *Macromolecules* **1989**, 22, 1454.

(11) Van Lent, B.; Scheutjens, J. M. H. M. *Macromolecules* **1989**, 22, 1931.

(12) Evers, O. A.; Scheutjens, J. M. H. M.; Fleer, G. J. *J. Chem. Soc., Faraday Trans.* **1990**, 86, 1333.

(13) Wu, D. T.; Yokoyama, A.; Setterquist, R. L. *Polymer J.* **1991**, 23, 711.

(14) Cosgrove, T.; Phipps, J. S.; Heath, T. G.; Richardson, R. M. *Macromolecules* **1991**, 24, 94.

Chapter 2

Tethered adsorbing chains: neutron reflectivity and surface pressure of spread diblock copolymer monolayers

Spread monolayers of diblock copolymers of styrene and ethylene oxide at the air-water interface were studied by surface pressure measurements and neutron reflectivity, as a function of coverage σ and chain length N. The surface pressure data have three regions, one at low coverage, where a relatively sharp increase due to increasing intermolecular interaction is found, a more gently increasing part at intermediate coverage, where the poly(ethylene oxide) block gradually desorbs to form a brush, and a sharply increasing part at high coverage, where the brush is compressed. The neutron reflectivity measurements, taken in the intermediate and high coverage region, confirm the presence of a brush with a thickness scaling, by approximation as $N\sigma^{1/3}$. These brushes could be compressed by a factor of about 5 without desorption occurring. The observations are in good agreement with numerical calculations based on a mean field lattice model for terminally anchored, adsorbing chains. These calculations predict a gradual change in the average configuration from a flat, adsorbed state to a brush consisting of stretched chains.

Introduction

In many natural and technical processes the presence of polymers at surfaces and interfaces plays a crucial role.[1,2] Block copolymers are particularly interesting because the blocks can be chosen to give the molecule a pronounced amphiphilic character. In view of this, the properties of interfacial layers formed by block copolymers have received considerable attention.[3] Scaling theories[4,5] and self-consistent-field (SCF) theories[6,7] predict the volume fraction profile of the polymer at the interface, as well as the excess free energy (surface pressure). At sufficiently high chain densities a brush is formed, the structure and surface pressure of which have been considered in detail. Several experimental studies have been carried out to test the theoretical predictions. Most of these focused on solid-liquid (e.g., mica-solvent[8] or silica-solvent[9,10]) interfaces. Unfortunately, the interfacial chain density, an important parameter in the theory, cannot be controlled very well for these systems. A better approach is to use liquid-air (or liquid-liquid) interfaces on which a known quantity of polymer can be spread. The chain density can then be varied continuously by compression or expansion of the interface. Liquid interfaces are generally very smooth and therefore ideal for reflectivity studies. In addition, the surface pressure is experimentally accessible, which is not the case for solid-liquid interfaces.

A few earlier studies have exploited this idea.[11-14] Though interesting data on the brush extension (in a limited range of relative compressions) have been obtained, the use of a non-soluble block that spreads on the liquid surface made it more difficult to analyse the surface pressure in terms of behaviour of the soluble block only. Another interesting case which has not been studied extensively is that of an end-attached chain capable of adsorbing at the liquid-air interface. In this case, the soluble chains should form a flat adsorbed layer ("pancake") in the low density limit, whereas they should desorb and form a stretched configuration ("cigar") at sufficiently high coverage.[15] So far, the development of a brush from initially adsorbed chains has not been studied experimentally, and this motivates the present work.

For our study we used a series of polystyrene-poly(ethylene oxide) (PS-PEO) diblock copolymers with varying length of the PEO block. Since PS is known not to spread on water, we expect this block to anchor the chain firmly to the interface, yet to contribute very little to the surface pressure. We should then see essentially the pressure from the soluble, brush-forming PEO block. Furthermore, PEO is known to adsorb weakly to the air-water interface.[16] In order to get a complete picture, both structural (neutron

reflectivity) studies and surface pressure measurements as a function of surface coverage were carried out.

Theory of terminally-attached polymers

We first consider the simple system of non-adsorbing polymers, each consisting of N segments, that are attached by one end to the interface. At low grafting density σ (number of polymer chains per unit area) the polymer chains do not interact laterally, and each chain forms a coil-like structure stuck to the interface. This is often referred to as a *mushroom*. At higher σ, lateral repulsion develops, and the chains begin to stretch. In the strongly stretched state this is called a *brush*. The height H of the brush and the volume fraction profile $\varphi(z)$ have been predicted theoretically. We summarise here the analytical self-consistent-field (SCF) theory.[6,7] In this treatment, a mean-field approximation is usually made, which implies that all interactions within a layer parallel to the interface are averaged. The SCF theory as used here assumes that the chains can be described by a flexible Kuhn model, i.e. as consisting of segments of length l. By taking into account all possible conformations, each weighted with its Boltzmann probability factor, the equilibrium distribution of a polymer-solvent system at the interface is calculated. Nearest-neighbour interactions between polymer segments and solvent molecules are taken into account by the Flory-Huggins parameter χ.

If the volume fraction of polymer is not too large (< 0.2), $\varphi(z)$ can be described by a parabolic profile[6,7]

$$\varphi(z) = \frac{3}{2}\overline{\varphi}\left(1 - \frac{z^2}{H^2}\right) \tag{1}$$

where $\overline{\varphi} = l^3\sigma N/H$ is the average volume fraction of the polymer brush which depends on σ, the number of grafted polymer molecules per unit area

$$\overline{\varphi} = \eta \ell^{4/3}\sigma^{2/3} \tag{2}$$

Here, $\eta = (\pi^2/72pv)^{1/3}$, p is the stiffness parameter, and $v = 1-2\chi$ is the excluded volume parameter. The brush height also depends linearly on the number N of segments in the chain

$$H = \eta^{-1} N \ell^{5/3}\sigma^{1/3} \tag{3}$$

For the surface pressure of the brush one finds[7]

$$\frac{\pi}{kT} = \left(N^{-1} + \frac{3}{5}v\overline{\varphi} \right)\overline{\varphi}H\ell^{-3} = \sigma\left(1 + \frac{3}{5}v\overline{\varphi}N\right) \qquad (4)$$

where k is the Boltzmann constant and T the temperature. This equation only holds for not too large volume fractions, as does equation (1).

For the description of our experimental system, the above expressions are not enough. This is because the analytical SCF brush theory assumes that the polymer segments are repelled by the surface, whereas we have a system where the soluble chain is attracted by the air-water interface.

One way to study end-attached adsorbing chains is to carry out calculations based on a numerical version of the SCF lattice theory.[17] In these calculations it is possible to assign an adsorption energy to segments in contact with the interface, so that adsorption occurs. Typically, the surface pressure and the structure of the interface as a function of σ are obtained. It is important to realise that in the SCF approach the coverage is always uniform and lateral inhomogeneities are ignored. In Figure 1 we present results of a set of such calculations for which we used a cubic lattice.

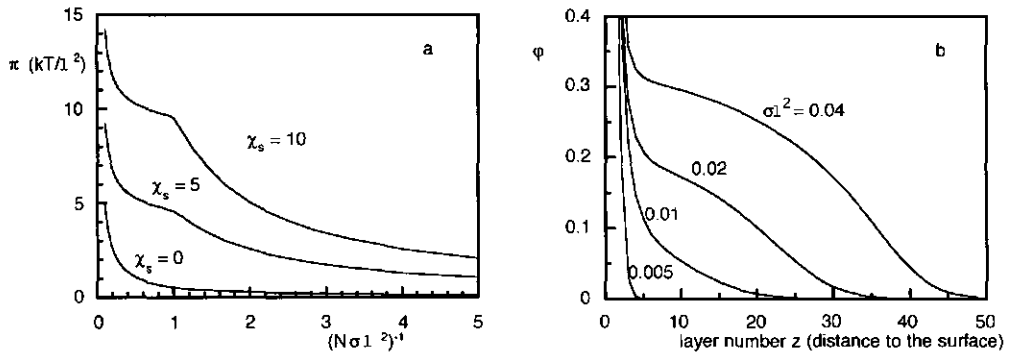

Figure 1. Surface pressure, $\pi(kT/l^2)$, as a function of the number of segments per unit of area, $(N\sigma l^2)^{-1}$, for different adsorption energies χ_S (a) and the volume fraction profile at four different coverages of the surface and an adsorption energy $\chi_S = 5$ (b). The polymers are end-attached, N = 250, $\chi = 0.45$.

Inspection of Figure 1a shows that when the polymer chains do not adsorb ($\chi_s = 0$), the surface pressure is a continuously increasing function of surface coverage. This is the osmotic pressure of the brush for which we can write equation (4). For adsorbing chains the pressure rises more steeply with increasing chain density and we find an inflection point at a coverage of $(N1^2\sigma)^{-1} = 1$. Beyond this point there is a much weaker increase. At very high compressions, however, the pressure rises very steeply again. At the inflection point, the coverage (in number of segments per unit of area) appears to be independent of the chain length. For adsorbing chains the surface pressure is clearly a build up of two contributing effects. The first contribution is from the adsorption energy of the chains, this part is increasing until it reaches a pseudo-plateau as the surface layer is filled with polymer segments. The second contribution is the osmotic pressure of the brushes. The adsorption part of the pressure at the inflection point is proportional to the segmental adsorption energy, χ_s, which is to be expected since this point marks the onset of desorption.

In Figure 1b the density profile of the adsorbed layer perpendicular to the interface is given. We observe a gradual thickening of the layer confirming the gradual desorption upon compression. The brush formation can be seen from the shape of the volume fraction profiles; at increasing coverage the shape becomes more parabolic, the profile which is to be expected for real brushes.

The pancake-cigar scenario has also been considered by means of scaling arguments.[3,4,15,18] It was predicted that when the chains are sufficiently long and the adsorption not too weak, the polymer layer may undergo a first order phase transition between the adsorbed and the stretched state. We return to this point in the discussion.

Experimental

Materials

The block copolymers were synthesised in the group of Dr. G. Riess, Mulhouse, France by sequential anionic polymerisation.[19] They were kindly given to us by T. Jensma, Univ. of Toronto, Canada. All five block copolymers contain a poly(styrene) block of constant length of about 38 monomers. The poly(ethylene oxide) part consists of respectively 90, 148, 250, 445 and 700 monomers. The PEO homopolymer was supplied by Polymer Laboratories Ltd., UK.

Table 1. Characteristics of the polymers used

polymer	M_W (PS)	M_W (PEO)	N (PEO)	M_W/M_n
ZGH-1	4000	3 950	90	1.21
ZGH-2	4000	6 500	148	1.15
ZGH-3	4000	11 000	250	1.20
ZGH-4	4000	19 600	445	1.17
ZGH-5	4000	30 800	700	1.25
PEO-23	-	23 000	523	1.08

The block copolymers have been characterised by gel permeation chromatography and H-NMR in Dr. Riess' group.[19] The results are shown in Table 1 together with the characteristics of the PEO homopolymer as provided by the manufacturer. In Table 2 the neutron scattering parameters of PS and PEO are given.

Table 2. Scattering parameters of polystyrene (PS) and poly(ethylene oxide) (PEO)

	PS	PEO
molar mass monomer with respect to hydrogen, M	104	44
density, ρ [10^3 kgm^{-3}]	1.04	1.10
scattering-length density, Γ[10^{-3} nm^{-2}]	1.76	0.75
bond length, l[nm]	0.25	0.33

Surface pressure measurements

The surface pressure isotherms were obtained by using a Teflon Langmuir film balance with a moving barrier. The surface pressure was measured continuously by means of two separate Wilhelmy plate tensiometers, one with a platinum plate and one with a paper strip.

The polymers were dissolved in chloroform at a concentration of about 1 g/l. After deposition of the polymer solution with help of a precision microsyringe, the chloroform was allowed to evaporate for 8 minutes. The (de)compression rate was kept constant at 30 mm^2/s, and the temperature was 296 (±0.5) K.

Neutron reflectometry

For the neutron reflectivity experiments, polymer was spread on D_2O in a Teflon trough of 255 x 105 mm. The polymers were dissolved in chloroform (0.5 g/l), and required quantities of this solution were carefully deposited on the surface with help of a precision microsyringe.

The reflectivity measurements were performed at the neutron reflectometer ROG installed at IRI, Delft, The Netherlands.[20,21] The reflection angle was set to 15.0 mrad. At this angle the minimum wavelength for total reflection from pure D_2O is 1.05 nm. The frame-overlap mirror was set at –21 mrad, giving a maximum wavelength in the incident beam of 1.2 nm. Hence, the wavelength region between 1.1 and 1.2 nm could be used to normalise the reflectivity to unity. The correction factor was typically 0.83. This differs from 1 because the diaphragm in front of the detector was set a little too narrow. The flight path of the neutrons from chopper to detector was 5355 mm. The chopper frequency was set at 25 Hz, so that in the wavelength region between 1.2 and 1.5 nm only the background count rate was recorded, which was found to be 0.015 neutrons/s. Two diaphragms in the beam were set at 3 and 1 mm, respectively, giving a footprint of 106 mm and an angular resolution of 2% (standard deviation). The measuring time per experiment was approximately 7 h.

Results

Surface pressure

The surface pressure curves were taken at compression and decompression. All curves were reproducible except the one taken at first compression. At second and next compression, the surface pressure isotherms for ZGH-2, ZGH-3, ZGH-4 and ZGH-5 were shifted to higher coverage with about 15, 15, 20, and 30 % compared to the first compression, respectively. This shift only concerns the part of the curve before the first inflection point at a surface pressure of about 10 mN/m. Beyond this inflection point there is no difference between the first and following compressions.

An explanation can be the possible formation of aggregates in the surface at first compression. The amphiphilic polymers could cluster together forming flat surface micelles with a polystyrene corona and a poly(ethylene oxide) outer layer. We were not able to check whether such small aggregates are formed. Another more likely explanation is the presence of free homopolymer PEO in the block copolymer samples.

As this soluble homopolymer is not anchored, it is pushed out of the surface layer into the solution at first compression. The presence of free homopolymer seems to be confirmed by GPC measurements of the same samples, where a component lacking an UV-detectable PS content was found.[22] From the neutron reflection data, we found a coverage that was somewhat lower than expected, also a confirmation of the loss of (homo)polymer. In the results presented here the surface pressure isotherm obtained at first compression is neglected.

Experimental results for the surface pressure vs surface area per polymer are presented in Figure 2a. For a better comparison with Figure 1a, the surface pressure vs. surface area per monomer is plotted in Figure 2b.

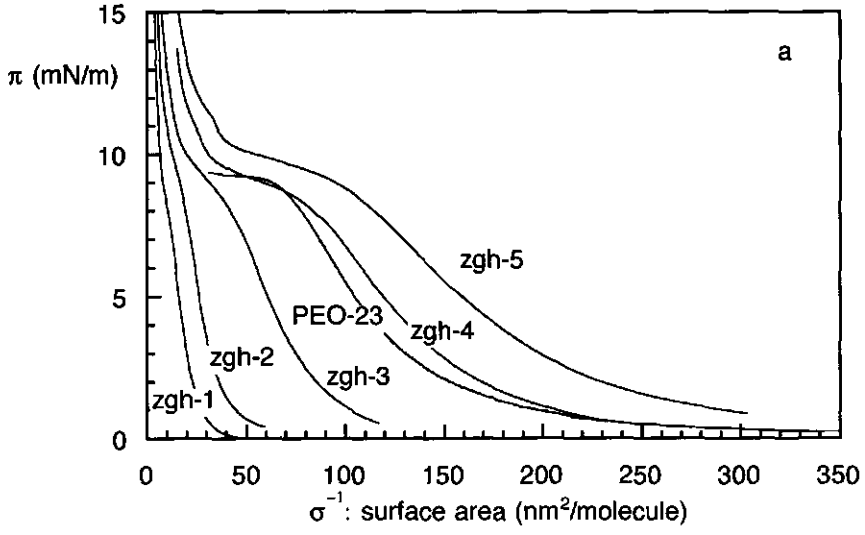

Figure 2a. Surface pressure, π(mN/m), as a function of the surface area per polymer molecule, σ^{-1}.

In the figures several regions can be distinguished. At low coverage, the pressure is very low, as should be expected for an ideal 2D gas of polymers. The surface pressure at low coverage can simply be seen as a two dimensional osmotic pressure for which a simple expression is, $\pi = \sigma RT$. This would give very low surface pressures over the whole experimental range. Hence, the increase in pressure that is measured experimentally is entirely due to lateral interaction.

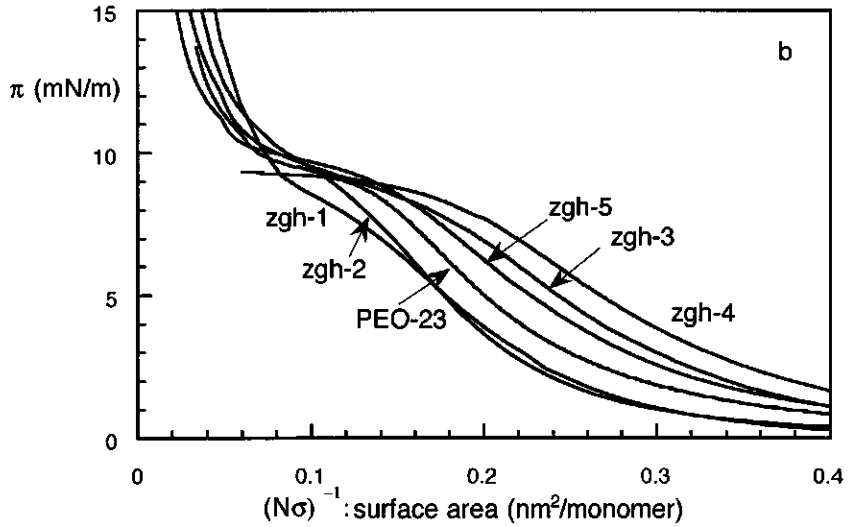

Figure 2b. Surface pressure, π(mN/m), as a function of the surface area per monomer ethylene oxide, $(N\sigma)^{-1}$.

The most conspicuous feature of the curves in Figures 2a and 2b is that they show a distinct leveling off at a pressure of about 10 mN/m. This (pseudo)plateau extends over roughly a factor of 3 in compression. It is worth mentioning that the pressure at the onset of the plateau is very close to that of a saturated PEO solution.[16] With numerical self-consistent-field calculations we also found the same plateau value for a saturated solution of adsorbing chains as that for the adsorption energy part of grafted chains.

When PEO is spread on water and subsequently compressed, one finds a curve which again levels off at about 10 mN/m. In Figure 2 the surface pressure vs area per monomer is also given for a PEO homopolymer. Because the PEO homopolymer is not anchored to the surface, it does not exhibit the steep rise at high compression. In addition, we found that the coverage (in units of mass per area) at the onset of the plateau is approximately constant; at least it does not depend in a systematic way on the PEO chain length (Figure 2b). From the position of the onset of the plateau, about 0.15 nm^2 per monomer, it can be seen that the segment length l is 0.4 nm.

From the low coverage region the excluded volume parameter υ for a 2D chain can be obtained by plotting the surface pressure against the area per monomer on a double logarithmic scale.[23] This is done in Figure 3.

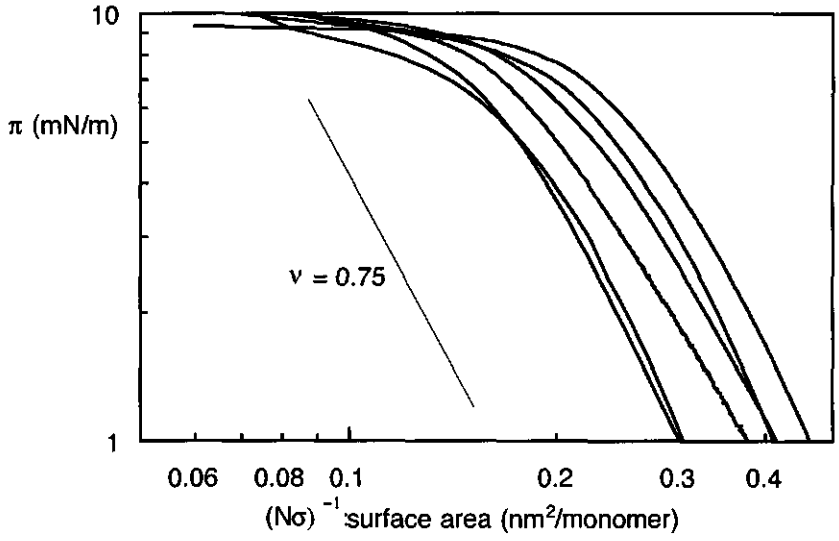

Figure 3. Surface pressure, π(mN/m), vs surface coverage, σ^{-1}, plotted on a double-logarithmic scale.

The (initial) slope y of the curves at low coverage is given by: $y = 2\upsilon/(1 - 2\upsilon)$. For a 2D self-avoiding walk (SAW), υ is theoretically predicted to be 3/4. This would lead to a slope of –3 in the plot. For comparison we indicate this slope in Figure 3. It can be seen that the SAW model is consistent with the data both for PEO homopolymer and block copolymers. Hence, PEO in the surface layer behaves as a 2D chain in a good solvent, this is in agreement with other experimental results.[24]

Neutron reflectometry

By way of example, neutron reflectivity curves for pure D_2O and from D_2O with a layer of ZGH-5 compressed to a density of 9.1 nm^2 per molecule are shown in Figure 4. The D_2O curve is almost a pure Fresnel curve, but the curve for the polymer film has the expected pattern with wiggles. We interpret the reflectivity curves as follows.

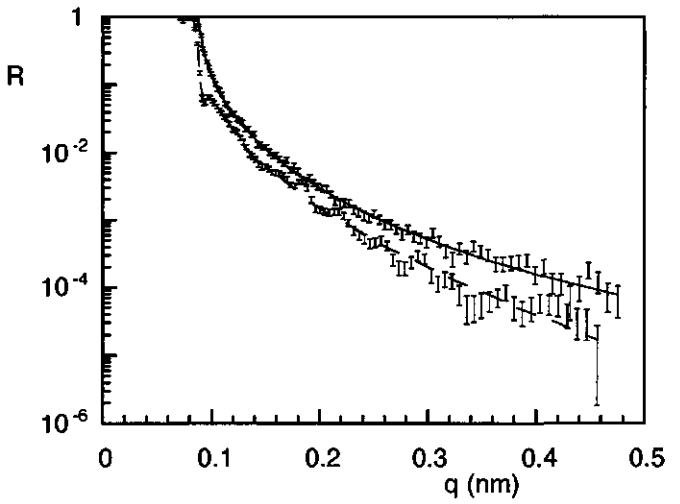

Figure 4. Reflectivity, R, as function of the vertical component of the wave vector, q, for D_2O (error bars, full line) and ZGH-5 with 9.1 nm^2 per molecule (error bars, dashed line). The lines represent fits of the model to the data, with $\bar{\varphi}$ = 0.09 and H = 47 nm.

As the model for the density profile of the PEO block, in the range of high compression, where we expect to have a brush, we adopt the parabolic shape now generally accepted as the one to be theoretically expected.[1] This gives:

$$\Gamma(z) = 0 \qquad z < 0$$

$$\Gamma(z) = \Gamma_b - \frac{3}{2}(\Gamma_b - \Gamma_e)\bar{\varphi}(1 - z^2/H^2) \qquad 0 \le z \le H$$

$$\Gamma(z) = \Gamma_b \qquad z > H$$

where Γ_b is the scattering length density of deuterated water and Γ_e that of PEO. An example for $\bar{\varphi}$ = 0.1 and H = 50 nm is shown in Figure 5. The 'gap' produced by the polymer is not very large, so that very accurate measurements must be performed. The gap is proportional to the average density $\bar{\varphi}$; hence, it becomes less visible for smaller values of this parameter. The dashed line represents the actual scattering length density of the polymer if the PS anchors and some PEO at the surface are also taken into account. The solid line is the model where the PS anchors and the PEO monolayers are modeled by a roughness at the surface. It is obvious that the difference in detail due to the neglect of the anchors and adsorbed PEO segments is hardly noticeable. For this

reason, the neutron reflection experiments can be performed most successfully in the region of high compression, where the brush is well developed.

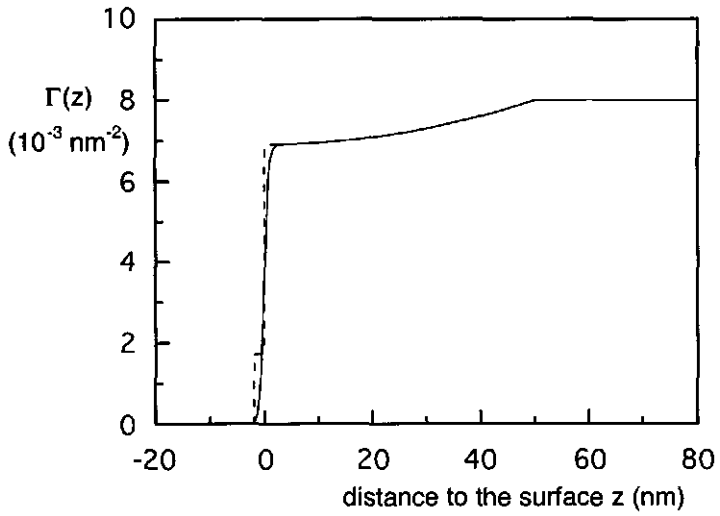

Figure 5. Example of a scattering length profile for $\bar{\varphi}$ = 0.1 and H = 50 nm: fitted (full line) and actual profile (dashed line).

For the purpose of data analysis, the scattering length density profile was discretised in 20 layers of thickness H/20 each, from which the reflectivity was calculated using recursive relations.[25] The reflectivity data were then fitted by varying model parameters. The parameters that were fitted are Γ_b, $\bar{\varphi}$, H, and the roughness at the surface, σ_s. The fit procedure is discussed by De Haan et al.[26] The errors in the parameters are calculated as the 68.3% confidence intervals. The data could be fitted easily with the model as discussed above. The correlation between the fit parameters H and $\bar{\varphi}$ varied between –0.2 and –1. The smallest (and therefore the best) correlation was obtained at the highest compression (smallest value of σ^{-1}). When $\bar{\varphi}$ H was less than 0.5 nm (corresponding to an adsorbed amount of approximately 0.5 mg/m^2, $(N\sigma)^{-1}$ = 0.15 - 0.2), it was not possible to distinguish between a large $\bar{\varphi}$ and a small H or *vice versa*. In this case the correlation between these two fit parameters was almost –1. For ZGH-2 only the measurement at the largest σ gave a solution where the correlation between the fit parameters was less than –0.9. Measurements on ZGH-1 were for similar reasons omitted. The weighted mean-square deviation of the fits to the data, χ^2, varied between 1

and 2 for the various measurements. The roughness at the surface was fitted to be approximately 1 nm. The fitted average volume fractions and brush heights as a function of the available surface area per molecule, σ^{-1}, are shown in Figures 6 and 7, respectively.

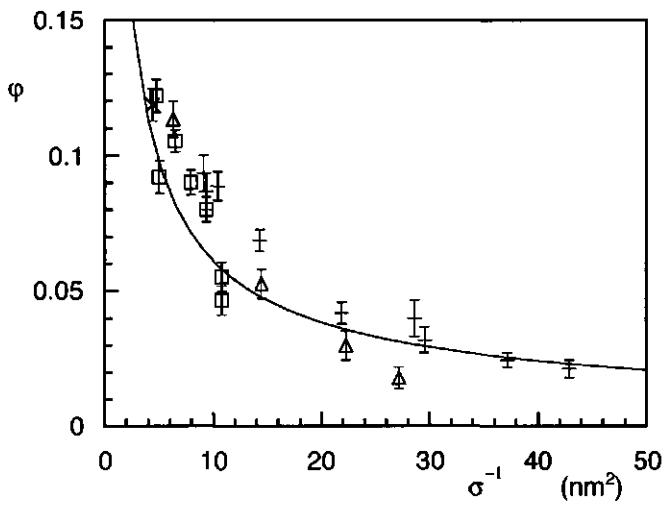

Figure 6. Average volume fraction, $\bar{\varphi}$, as a function of available area per molecule, σ^{-1}, for different polymers: ZGH-2 (asterisks); ZGH-3 (squares); ZGH-4 (triangles); ZGH-5 (plusses). The line corresponds to equation (2) of the model described in the text.

The $\bar{\varphi}$ - and H-data were then fitted to equations (2) and (3), using pv and l as the variables. The best fits, with $l = 0.34 \pm 0.02$ nm and pv = 0.08 ± 0.02, are given by the lines included in Figures 6 and 7. For the full range of segment numbers as used here, the theory can describe the data quite well. Note that the independence of $\bar{\varphi}$ on N, the number of segments, is reproduced remarkably well. The values found for l and pv are in agreement with the literature values for the monomer length of ethylene oxide (0.33 nm) and the χ-value for PEO in water (0.45).[1]

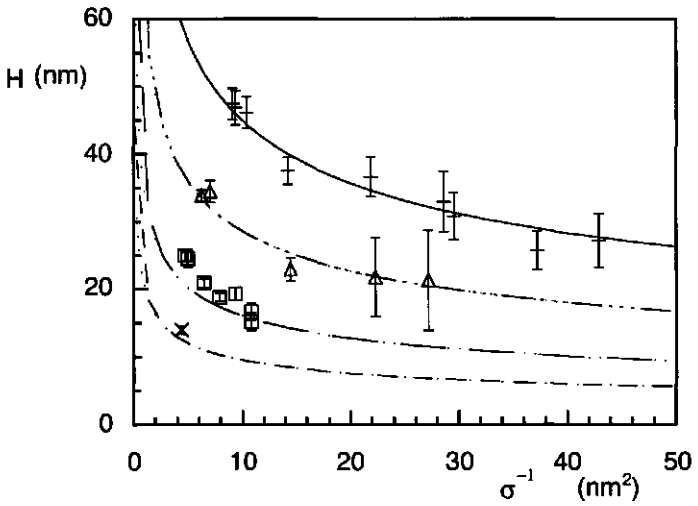

Figure 7. Brush height, H, as a function of available area per molecule, σ^{-1}, for different polymers: ZGH-2 (asterisks); ZGH-3 (squares); ZGH-4 (triangles); ZGH-5 (plusses). The lines correspond to equation (3) of the model described in the text.

In order to determine the power law dependencies of the average volume fraction and the brush height on the surface coverage more exactly, we plotted the experimental results on a double logarithmic scale in Figures 8 and 9. As can be seen from these figures the dependencies seem to be somewhat higher than theoretically predicted in equations (2) and (3): 0.80 and 0.41, respectively. Again, the best fits to equations (2) and (3) are included in the diagrams (dashed lines).

For the brush height, divided by $\sigma^{1/3}$, we found that the power law dependency on the number of segments is 0.90, somewhat lower than predicted in theory.

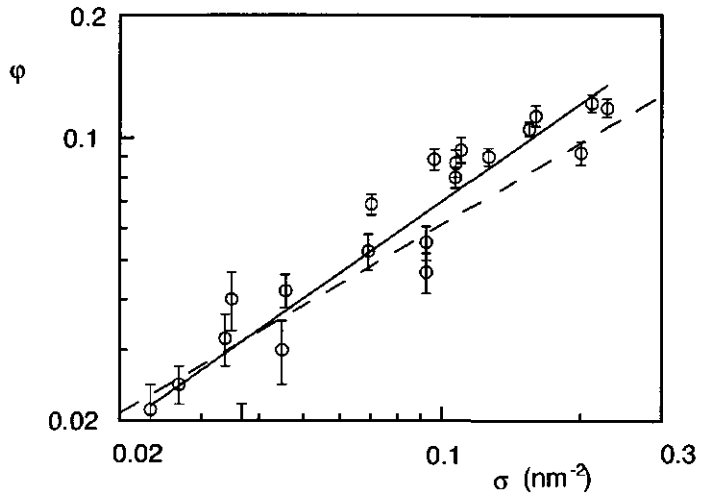

Figure 8. Average volume fraction, $\overline{\Phi}$, as a function of available area per molecule, σ^{-1}, plotted on a double logarithmic scale. The fitted line has a power exponent of 0.80. The dashed line corresponds to equation (2) of the model described in the text.

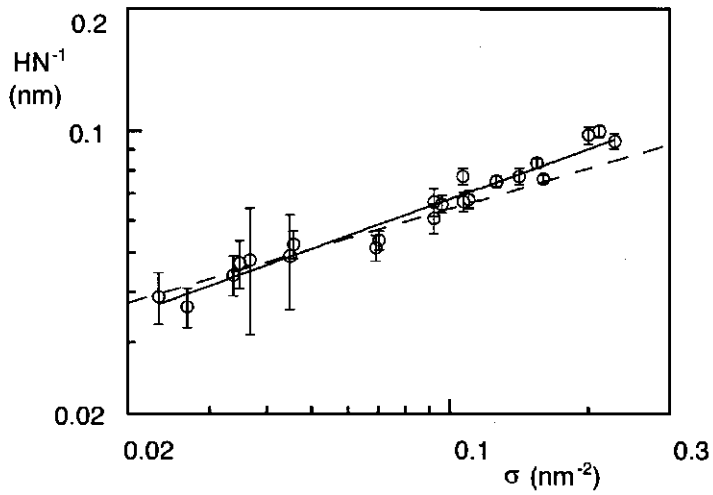

Figure 9. Brush height, H, divided by N, as a function of available area per molecule, σ^{-1}, plotted on a double logarithmic scale. The fitted line has an exponent of 0.41. The dashed line corresponds to equation (3) of the model described in the text.

Discussion

Surface pressure: the transition

The surface pressure data are most likely explained by the scenario that has been sketched in Figure 10.

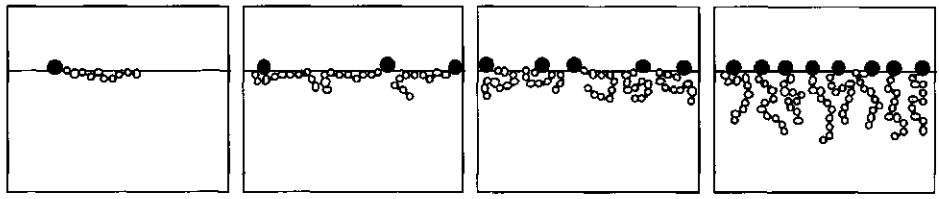

Figure 10. Sketch of a diblock copolymer at the air-water surface with, from left to the right, increasing values of surface coverage σ.

At low coverage, the PEO block spreads on the water surface (forming a 'pancake'). Since PS is known not to spread, the PS blocks will form small, compact globules. Upon compression, the pancakes start to interact, and the pressure goes up. When the pressure reaches a value of approximately 10 mN/m, the surface density of PEO has reached its plateau, and upon further compression the PEO blocks begin to desorb, thereby gradually forming a kind of brush or cigar. Eventually, all PEO segments have left the surface and, only the PS block remains anchored at the surface. From this point on, the fully developed brush stretches further upon lateral compression.

The formation of the brush can also be seen as a transition between two states: a pancake-cigar transition.[15] As mentioned above, this transition has been considered in detail, using scaling arguments, by Alexander in his pioneering paper on end-grafted chains.[4] More recent work concerning this subject has been done by Ligoure.[18] It is claimed that under certain conditions the pancake-cigar transition is a first order phase transition. This would mean that polymer chains in a flat pancake-like structure coexist with chains stretched normal to the surface ("cigar"). There should then be a concomitant flat part in the surface pressure vs area curve.

Alexander also gives the condition under which the phase transition is expected to occur. The adsorbed amount $N1^2\sigma$ should be within the following range:

$$(N\chi_s^6)^{1/7} > N1^2\sigma > \chi_s^{1/2} \qquad (5)$$

For our experimental system we have N = 90 up to 700, l = 0.4 and χ_s can be estimated from Figure 2: at the onset of the pseudo-plateau the surface pressure is about 10 mN/m. With l = 0.4 this gives an adsorption energy χ_s = 0.4 per segment. As this is only the effective part of the adsorption energy, we have to add the critical adsorption energy (0.2) to get the total adsorption energy. This gives for the total adsorption energy χ_s = 0.6 per segment (in units of kT). The calculation of the adsorption energy from the surface pressure (surface free energy), only holds for infinite sharp interfaces. For interfaces with a finite width, as in any practical system, there is an extra entropic contribution to the free energy. The above estimation of χ_s is therefore the lower limit, we expect χ_s to be somewhat higher.

When we compare the variables of our system to equation (5), we infer that our experimental data may well include the relevant range.

As can be seen from figure 2, we do find a leveling off of the surface pressure beyond the inflection point. It is tempting to ascribe this phenomenon to the first order phase transition predicted theoretically. However, the pressure continues to increase upon compression, which should not be the case for a true first order phase transition. Moreover, we studied the compressed surface by Brewster angle microscopy, searching for domains of coexisting phases. We were unable to detect such domains: the entire surface had a completely homogeneous appearance on a length scale of a few micrometers. Hence, it seems that a first order phase transition does not occur in our experimental system.

We now reconsider the numerical SCF calculations. In these calculations the parameters can be easily chosen in such way that the condition of equation (5) is obeyed. Since the chain density in these calculations is kept uniform, any unstable situations should show up as a loop in the pressure-area curve, but this is not found: a first order phase transition is not predicted. For the calculations, a large range of χ_s is checked and the number of segments was varied up to 1000. When the structure of the layer is considered, we observe a gradual thickening of the layer (Figure 1b), confirming the gradual desorption upon compression. The brush formation can be seen from the shape of the volume fraction profiles; at increasing coverage the shape becomes gradually more parabolic.

From Figure 2b, it can be noticed that despite the low adsorption energy for the experimental system ($\chi_s \approx 1$), a clear inflection point is seen. At such a low adsorption energy, the inflection point as found by numerical SCF calculations is hardly noticeable. Obviously, the osmotic pressure of the brush is overestimated in the SCF calculations.

The question now arises, why does the SCF theory give results qualitatively different from the scaling analysis? In a SCF analysis all conformations are considered in a mean field (lateral fluctuations are neglected). In a scaling analysis, the lateral fluctuations are included but other types of fluctuations, such as the position of the end points in the brush, are not. The different types of fluctuations included in the two approaches can perhaps be the reason of the different outcome of the two theories.

Another explanation can be the evolution of the brush profile adopted by scaling analysis.[18] This appears to be different from the one found with SCF calculations. Ligoure postulates that the formation of the brush starts at the interface in the proximal part of the adsorbed layer profile, so that the brush develops outward from the surface; a self-similar adsorbed layer structure remains present but is gradually 'consumed' and pushed outward.

In the SCF calculations we observe that as the brush becomes more dense, the profile in the central part of the profile falls off much less steep and becomes parabolic. These changes occur primarily on the dilute side of the central regime (near the distal part of the profile). Both the proximal part of the profile and the distal regime remain intact. However, as in the Ligoure scenario the distal regime shifts gradually to higher z. Hence the initial and final situations are the same for the two calculations, but the path postulated by Ligoure is quite different from the one that emerges from our calculations, and apparently the free energies associated with either path are also different.

Both in experiment as in SCF calculations, the surface pressure results show an inflection point at $N\sigma l^2 \approx 1$. The pseudo-plateau after the inflection has a slope that is independent of N when the horizontal axis is expressed in unit of area per segment (Figures 1a and 2b). This means that for very large N, the surface pressure isotherm, expressed in unit area per molecule, gives an almost flat pseudo-plateau. In the limit of $N \rightarrow \infty$, the pseudo-plateau of the isotherm may then become near horizontal, but a Van der Waals loop, characteristic for a real first order transition, is then not expected. This last point cannot be checked numerically because the SCF calculations are limited to relatively low N.

Neutron Reflectivity: the brush

The neutron reflectivity data give rise to some discussion. The approximation introduced through equation (1) may not be valid. For example, the volume-fraction profile may not be parabolic. In a theta solvent the profile shape changes to $\varphi(z) = 4\ \bar{\varphi}\ /\pi(1-z^2/H^2)^{1/2}$ [17]. This profile was also used to fit the data, and found to fit equally well and $\bar{\varphi}$ is the same.

H is 10% smaller than with the parabolic profile. However, in a theta solvent theoretically both H and $\bar{\varphi}$ are proportional to $\sigma^{1/2}$, which is not reproduced by the measurements. It is not possible to get a good fit with a rectangular volume fraction profile. Because the volume fractions are very small, the measurements are not very sensitive to the exact profile shape, but shapes deviating strongly from the parabola can be excluded. If more information about the volume fraction profile is required, measurements extending to larger q-values have to be performed.

The fitted power law dependencies of the average volume fraction profile and the brush height on σ are somewhat higher than predicted. On the other hand, the fits to equations (2) and (3) seem to be rather well. An explanation for too high dependencies could be that, at low surface coverages, the measurements become less accurate and a deviation to lower average volume fraction and brush height is found, thereby giving rise to a higher power law dependency. For the brush height we find a dependency on N that is slightly lower than predicted. This can possibly be explained by the relatively short chains we used in these experiments, yet a real brush may not have been developed.

Nevertheless, within the experimental error, the dependencies of the average volume fraction and the brush height on σ and N seem to be as predicted theoretically.

Conclusions

Spread monolayers of diblock copolymers of styrene and ethylene oxide at the air-water interface were studied by surface pressure measurements and neutron reflectivity. The surface pressure data do not show a flat part in the isotherms, the pressure is increasing over the entire experimental range. In the area range used for neutron reflectivity the brush compression factor was about 5. At low coverage the adsorbing PEO block forms a flat pancake like structure at the surface. Upon compression the PEO is pushed out of the surface layer into the solution to form a cigar or brush structure, firmly anchored by the PS block. During this process the thickness H of the polymer layer scales, by approximation, as $N\sigma^{1/3}$.

The numerical SCF calculations do not confirm the first order phase transition predicted earlier.[3,18] We have shown that this may be due to the scenario of how the brush develops. The scenario used in scaling analysis and the one found by numerical SCF calculations are different.

The experimental data seem to support the gradual transition predicted by the SCF theory, rather than the first order phase transition. Although this does not rule out the

possibility that such a transition exists (e.g., for very long chains), it makes it unlikely that it will be easily found experimentally.

Note

After publication of this chapter in Langmuir (*Langmuir* **1995** *11* 4467) it appeared that the calculation of the surface pressure as presented in Figure 1a was not correct. In our SCF calculations we assumed that the surface pressure is equal to minus the excess surface Gibbs free energy. Currie et al. have shown that we have to add the product of the grafting density times the derivative of the excess surface Gibbs free energy towards the grafting density. [27] Nevertheless, the shape of the curve in Figure 1b does hardly change; the conclusions in this chapter remain the same. However, the value of the adsorption energy used to obtain surface pressure curves which are in agreement with experiments is around 1. This value is equal to the experimental value, indicating that in SCF calculations the brush contribution is not overestimated, as suggested in the discussion of this chapter.

References

(1) Fleer, G. J.; Cohen Stuart, M. A.; Scheutjens, J. M. H. M.; Cosgrove, T.; Vincent, B. *Polymers at Interfaces*; Chapman & Hall: London, 1993.

(2) Ulman, A. *Ultrathin organic Films*; Academic Press: San Diego, CA, 1991.

(3) Halperin, A.; Tirrel, M.; Lodge, T. P. *Adv. Polym. Sci.* **1992**, *100*, 31.

(4) Alexander, S. *J. Phys.* **1977**, *38*, 983.

(5) De Gennes, P. G. *Macromolecules* **1980**, *13*, 1069.

(6) Milner, S. T.; Witten, T. A.; Cates, M. E. *Macromolecules* **1988**, *21*, 2610.

(7) Zhulina, E. B.; Borisov, O. V.; Priamitsyn, V. A. *J. Colloid Interface Sci.* **1990**, *137*, 495.

(8) Hair, M. L.; Guzonas, D.; Boils, D.; Tripp, C. *Macromolecules* **1992**, *24*, 2434.

(9) Auroy, P.; Auvray, L.; Léger, L. *Phys. Rev. Lett.* **1991**, *66*, 719.

(10) Mansfield, T. L.; Iyengar, D. R.; Beaucage, G.; McCarthy, T. J.; Stein, R. S. *Macromolecules* **1995**, *28*, 492.

(11) Kent, M. S.; Lee, L. T.; Farnoux, B.; Rondelez, F. *Macromolecules* **1992**, *25*, 6240.

(12) Saville, P. M.; Gentle, I. R.; White, J. W.; Penfold, J.; Webster, J. R. P. *J. Phys. Chem.* **1994**, *98*, 5935.

(13) Richards, R. W.; Rochford, B. R.; Webster, J. R. P. *Faraday Discuss.* **1994**, *98*, 263.

(14) Lee, L. T.; Factor, B. J.; Kent, M. S.; Rondelez, F. *Faraday Discuss.* **1994**, *98*, 139.

(15) Halperin, A. *Macromol. Rep.* **1992**, *A-29*, 107.

(16) Cao, B. H.; Kim, M. W. *Faraday Discuss.* **1994**, *98*, 245.

(17) Wijmans, C. M.; Scheutjens, J. M. H. M.; Zhulina, E. B. *Macromolecules* **1992**, *25*, 2567.

(18) Ligoure, C. *J. Phys. II France* **1993**, *3*, 1607.

(19) Hruska, Z.; Hurtrez, G.; Walter, S.; Riess, G. *Polymer* **1992**, *33*, 2247.

(20) Van Well, A. A.; De Haan, V. O.; Frederikze, H. *Physica B* **1994**, 217.

(21) De Haan, V. O.; De Blois, J.; Van der Ende, P.; Frederikze, H.; Van der Graaf, A.; Schipper, M. N.; Van Well, A. A.; Van der Zanden, J. *Nucl. Instrum. Methods A* .

(22) d'Oliveira, J. M. R. *personal communication* .

(23) Vilanove, R.; Poupinet, D.; Rondelez, F. *Macromolecules* **1988**, *21*, 2880.

(24) Kawaguchi, M.; Komatsu, S.; Matsuzumi, M.; Takahashi, A. *J. Colloid Interface Sci.* **1984**, *102*, 356.

(25) Parratt, L. G. *Phys. Rev.* **1954**, *95*, 359.

(26) De Haan, V. O.; Drijkoningen, G. G. *Physica B* **1994**, *198*, 24.

(27) Currie, E. P. K.; Leermakers, F. A. M.; Cohen Stuart, M. A.; Fleer, G. J. *Macromolecules* **1997**, *submitted.*

Chapter 3

Non-selective adsorption of block copolymers and the effect of block incompatibility

The adsorbed amount and the hydrodynamic layer thickness of two series of block copolymers and the corresponding homopolymers on silica were determined. We used diblock copolymers of poly(vinyl methyl ether) and poly(2-ethyl-2-oxazoline) and tri- and diblock copolymers of poly(2-methyl-2-oxazoline) and poly(ethylene oxide). The diblock copolymers of poly(ethylene oxide) and poly(2-methyl-2-oxazoline) were obtained by polymerisation of 2-methyl-2-oxazoline initiated by the tosylate of poly(ethylene glycol) monomethyl ether. The difference between the adsorption energies of the segments is found to be small: the block copolymer adsorption is non-selective. The adsorbed amount as a function of block copolymer composition shows a maximum at a composition where the longest block is also the strongest adsorbing block. The adsorbed amounts and the layer thicknesses are relatively low. Similar results are obtained with numerical self-consistent field calculations for non-selective adsorption for the case when the different blocks are incompatible. The typical anchor-buoy structure of the adsorbed layer is maintained, be it less explicit than found for selective adsorption.

Introduction

Polymers play an important role in many industrial and natural processes and in various applications. One of the relevant features is their interfacial behaviour. It has long been recognised that polymers can change the properties of colloidal dispersions. For example, they can be used for controlled flocculation or, conversely, for steric stabilisation. Much experimental and theoretical attention has been paid to the different aspects of polymer adsorption; for a detailed survey we refer to recent reviews.[1,2]

In this paper we consider the adsorption of block copolymers, in which the various kinds of segments are distributed in blocks along the chain. Because of their dualistic character, block copolymers may be amphiphilic; they behave very differently from homopolymers.

Much attention has been paid to the adsorption of block copolymers in which one of the blocks does adsorb to a surface whereas the other block does not have any affinity for that surface; this situation may be referred to as surface-selectivity. From these theoretical[3-5] and experimental[6-11] studies we now have a rather complete picture of the behaviour of block copolymers at interfaces. Upon adsorption of diblock copolymers the adsorbing anchor block will form a relatively thin layer on the surface, whereas the non-adsorbing blocks form a rather dilute and extended buoy layer. The relative length of the blocks is of great importance for the structure of the polymer layer. When the adsorbing anchor block is long, the adsorption is limited by saturation of the anchoring layer; the lateral repulsion between the buoy blocks is then weak compared to the adsorption energy. Decreasing the relative length of the anchor will enhance the adsorbed amount because the total mass of adsorbed anchor segments remains more or less constant and the relative contribution of the buoy segments to the adsorbed amount increases. This behaviour is sometimes denoted the anchor regime.

When the relative length of the anchoring block is further decreased we find a cross-over to the buoy regime: the lateral repulsion between the buoy blocks is now more important than the gain in adsorption energy of the anchor blocks, and the total adsorbed amount decreases with decreasing anchor length. In Figure 1a this scenario is illustrated by plotting the adsorbed amount (θ^a) as a function of the block copolymer composition for different total chain lengths N. Figure 1b gives the volume fraction profiles ($\varphi(z)$) of the two blocks in the maximum, for N = 100. These figures were calculated with a self-consistent-field theory,[5] but the same qualitative results are obtained with other theories.[3] The total length clearly affects the adsorption behaviour of the block

copolymer. With increasing length the maximum becomes more pronounced and shifts to a lower fraction ν_A of anchor segments A. For the longer chains a smaller fraction of anchor segment is needed to give long enough anchor blocks to secure attachment. From the volume fraction profiles (Figure 1b) it is seen that almost all anchor segments can be found in the first few layers next to the surface. The buoy segments, on the other hand, avoid contact with the surface and form an extended layer. This extended layer, in which the polymers are stretched away from the surface,[12] can be important for the steric stabilisation of colloidal dispersions.[13]

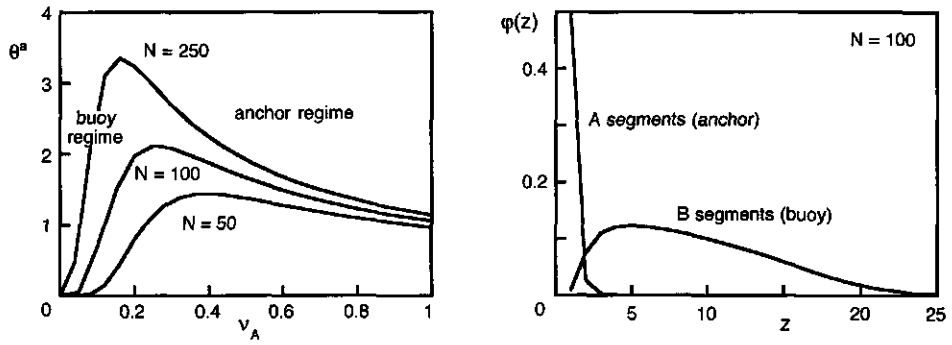

Figure 1. The adsorbed amount (θ^a) as a function of block copolymer composition for different chain lengths, ν_A is the fraction A segments of the total number of segments (a), and the volume fraction profiles ($\varphi(z)$) of the two blocks in the maximum for N=100, z is the distance to the surface in number of lattice layers (b). Adsorption energy of the A segments, χ_{sA}, is 2 kT, all other interaction parameters are zero. Calculated with help of a SCF theory using a cubic lattice.

Adsorption of block copolymers can take place from a solvent that is either non-selective or selective. Figure 1 was calculated for a non-selective solvent in which both blocks are equally soluble. In a selective solvent one of the blocks can be insoluble and the block copolymers may form micelles in solution. The qualitative features for a non-selective and for a selective solvent in which the anchor blocks do not dissolve, are expected to be roughly the same (i.e., like in Figure 1).[14,15] However, when in a selective solvent the soluble block (i.e., the micellar corona) does adsorb, it is very likely that associative adsorption occurs and that micellar structures accumulate at the surface.[15-17] This scenario can be very complex and the kinetic parameters probably influence the final conformation of the adsorbed polymer.[18-20] We have to keep in mind that the picture as given in Figure 1 is for a system at equilibrium. In natural processes and in certain

experiments such equilibrium conditions may not be attained, especially so when the solvent is selective.

Above, we sketched the situation for selective adsorption, where one of the blocks is adsorbing and the other has no affinity for the surface. In real systems, however, often both blocks of a diblock copolymer can adsorb to a surface. We may denote this situation as non-selective adsorption. The properties of the adsorbed layer are now determined by the competition for anchoring sites between the two blocks. So far, this competition between two adsorbing blocks within one polymer has not been studied in detail. In a few papers this aspect has been considered,[5,21] but when the difference between the adsorption energies of the two segment types is relatively high the behaviour is not greatly different from that of selective adsorption. In this paper we describe the adsorption of two different sets of block copolymers at the silica-water interface. For the two types of segments in these copolymers, the difference in adsorption energy for the surface turned out to be rather low. We used a series of diblock copolymers of poly(vinyl methyl ether) and poly(2-ethyl-2-oxazoline) and a series of di- and triblock copolymers of poly(ethylene oxide) and poly(2-methyl-2-oxazoline). We measured the adsorbed amount with optical reflectometry as well as the hydrodynamic layer thickness with dynamic light scattering. In order to get a complete picture, also numerical self-consistent field calculations were carried out. In this theoretical modelling special attention is paid to the effect of incompatibility of the two blocks within the polymer. So far, this aspect has hardly received any attention in the literature.

Experimental

Materials

We used four types of homopolymers: poly(vinyl methyl ether) (PVME), poly(2-methyl-2-oxazoline) (PMeOx), poly(2-ethyl-2-oxazoline) (PEtOx) and poly(ethylene oxide) (PEO). The block copolymers were three PVME-PEtOx and three PMeOx-PEO diblock copolymers, as well as two triblock copolymers of PMeOx and PEO, where the ether block forms the middle part. The structural formulas of typical representatives of these polymers are given in Figure 2. The PEtOx and PMeOx homopolymers were synthesised and kindly given to us by F. Derks (DSM, The Netherlands). The PVME homopolymer is a commercial product (Scientific Polymer Science), as is PEO (Polymer Laboratories). The block copolymers of PVME and PEtOx were synthesised[22] and kindly made available by Dr. J. Riffle (Virginia State University, USA). The triblock copolymers of PMeOx and PEO were synthesised by cationic polymerisation of the oxazoline block,

starting with a bifunctional PEO homopolymer macro-initiator.[23] The synthesis of the diblock copolymers of PMeOx and PEO is different because we had to start with a monofunctional PEO. As this synthesis has not been described earlier in the literature, we give the procedure in the next section.

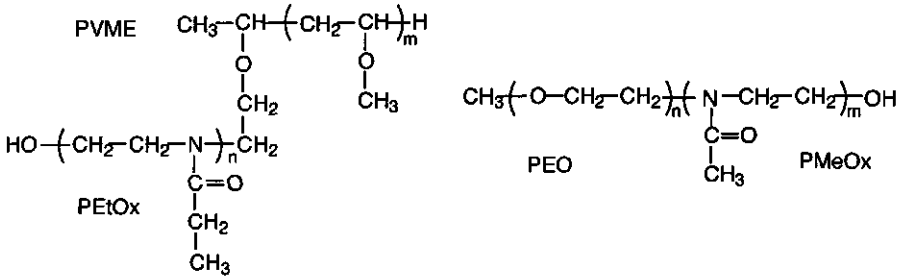

Figure 2. Structural formulas of some of the polymers used. The PMeOx living end group is not specially treated, in the aqueous environment the ring structure is probably opened and end functionalised with a hydroxyl group.

Table 1. Molecular (block) structure, molar mass, and refractive index increment of the polymers used; the molar mass of PVME-PEtOx 17 has not been determined, indicated is the target molar mass during synthesis.

sample	M_w kg mol^{-1}	dn/dc cm^{3}g^{-1}	sample	M_w kg mol^{-1}	dn/dc cm^{3}g^{-1}
PVME	99	0.146	PMeOx	6.0	0.160
PVME-PEtOx 63	15.7-9.2	0.152	PMeOx-PEO 89	5.8-0.75	0.157
PVME-PEtOx 42	7.5-10.3	0.155	PMeOx-PEO 67	4.3-2.1	0.152
PVME-PEtOx 17	2.0-8.0	0.158	PMeOx-PEO 17	1.0-5.0	0.140
PEtOx	6.0	0.161	PMeOx-PEO-PMeOx 75	3.0-2.0-3.0	0.154
			PMeOx-PEO-PMeOx 57	1.3-2.0-1.3	0.150
			PEO	7.1	0.136

Some of the characteristics of the polymer samples used are given in Table 1. The number in the sample name for the block copolymers gives the percentage of the first block in the total molar mass, for which we choose the block with the highest affinity for

the surface. As we shall see, PVME adsorbs more strongly than PEtOx, and PMeOx more strongly than PEO. The commercial homopolymer PVME has a high polydispersity (M_w/M_n = 2.1). All the other polymers were synthesised by living ionic polymerisation and therefore the molar mass distributions are relatively narrow. The value of the refractive index increment dn/dc for the PEO homopolymer was taken from literature,[24] the values for the other homopolymers were obtained with the group contribution method as described by van Krevelen.[25] The refractive index increments for the block copolymers were calculated from the homopolymer values, assuming additivity of the refractive index. Polymer solutions were made up by dissolving the dry material in de-ionised water, and were stored in a refrigerator. Measurements of the adsorbed amount and the hydrodynamic thickness were performed at room temperature.

Synthesis of PMeOx and PEO diblock copolymers

Commercial poly(ethylene glycol) monomethyl ether (PEO monomethyl ether) (M_w = 750, 2000 and 5000 from Fluka) was dried in vacuo at 60°C in the presence of phosphorous pentoxide for 24h. Benzene was dried over sodium wire and distilled under nitrogen. Tosyl chloride was purified by sublimation under reduced pressure. Acetonitrile was dried over CaH_2 and distilled under nitrogen. 2-Methyl-2-oxazoline was purified by distillation over KOH pellets and CaH_2 under nitrogen. n-Butyl lithium (1.6 M solution in hexane from Aldrich) was used as received.

Poly(ethylene glycol) monomethyl ether was converted to the corresponding tosylate ester in analogy to a reported procedure for the synthesis of α,ω-ditosylated PEO.[26] First the alcohol end group was converted into the lithium alcoholate with a stoichiometric amount of n-butyl lithium (n-BuLi) in benzene, followed by the reaction with tosyl chloride; the reaction scheme is given in the top line of Figure 3. As a typical example of the synthesis of PEO monotosylate (TsPEO), the preparation of a TsPEO sample with a molar mass of 2100 g mol^{-1} is described. A solution of 30 g of PEO monomethylether (M_w = 2000 g mol^{-1}) in 300 ml of benzene was cooled to 5°C under nitrogen. Under stirring, 10.3 ml of a 1.6 M solution of n-butyl lithium was added rapidly followed by 3.43 g of tosyl chloride, dissolved in 30 ml of benzene. The resulting mixture was stirred overnight at room temperature. The lithium chloride precipitate was filtered off, the filtrate evaporated in vacuo until dryness and the residue dissolved in 40 ml of dry ethanol at room temperature. The solution was cooled to –18 °C for 1h and the resulting precipitate was filtered off under dry nitrogen on a cooled glass filter. After drying in vacuo at 60°C in the presence of phosphorous pentoxide for 24h, 30.9 g of TsPEO was obtained. Three samples were synthesised, with molar masses of 740, 2100, and 5200 g mol^{-1},

respectively, all samples have an end group functionality of 1.0. The molar masses and the end group functionalities were determined by the integral ratio of the tosyl to ethylene peaks in the 500 MHz ^{1}H-NMR spectra in $CDCl_3$. The polydispersity index M_w/M_n, measured by GPC, using a PL-Gel 10 MIX Å column, $CHCl_3$ as eluent, and calibration on PS standards, was 1.1 for all three samples.

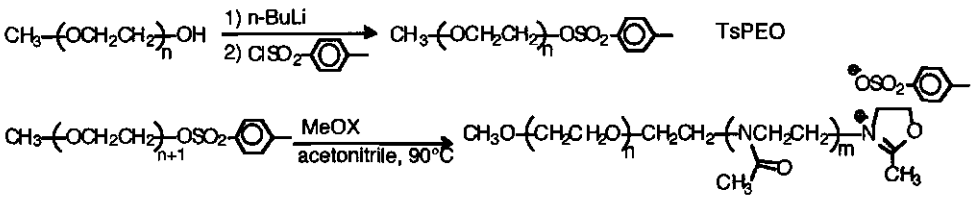

Figure 3. Reaction scheme for the synthesis of diblock copolymers of PEO and PMeOx. The top line gives the conversion of poly(ethylene glycol) monomethyl ether to the corresponding tosylate ester. This ester is used as a macro-initiator for the polymerisation of 2-methyl-2-oxazoline, as indicated in the bottom lines.

The monofunctional TsPEO was used as a macro initiator for the polymerisation of 2-methyl-2-oxazoline (MeOx), as indicated in the bottom lines of Figure 3. In this way AB block copolymers consisting of an A-block of PEO and a B-block of poly(2-methyl-2-oxazoline) (PMeOx) were obtained in analogy to a reported procedure for the synthesis of analogous ABA block copolymers of the same block segments.[23] As a typical example, the preparation of PMeOx-PEO 67 is described. TsPEO with M_w = 2000 g mol^{-1} (3.3 g, 1.5 mmol) was transferred into a 100 ml "heavy wall glass tube" containing 30 ml of acetonitrile under nitrogen. MeOx (6.7 ml, 79 mmol) was added and the tube was sealed and heated to 90°C. After 20h, the reaction mixture was cooled and poured into 2 l of diethyl ether. The precipitated block copolymer was isolated by decantation and purified by reprecipitation from chloroform solution in diethyl ether. The pale yellow solid was dried in vacuo at 60°C in the presence of phosphorous pentoxide for 24h. The yield was 9.5 g. In this way the three PMeOx-PEO diblock copolymer samples indicated in Table 1 were synthesised. The molar masses were determined by the integral ratio in the 500 MHz ^{1}H-NMR spectra in $CDCl_3$. The ratio M_w/M_n was 1.2 for all three samples, as measured by GPC, using a Waters Styragel HT 10^3 Å (10) + 10^4 Å (10) column, N-methyl pyrrolidon (80°C) as eluent, and calibration on PS standards. The yield, calculated as %-conversion of the MeOx polymerisation, was between 95 and 97 %.

Comparison of the GPC analysis of one of the AB block copolymers with that of the original TsPEO prepolymer (Figure 4) shows that a considerable increase in the molar mass has occurred and that the reaction mixture contains no unreacted macro-initiator.

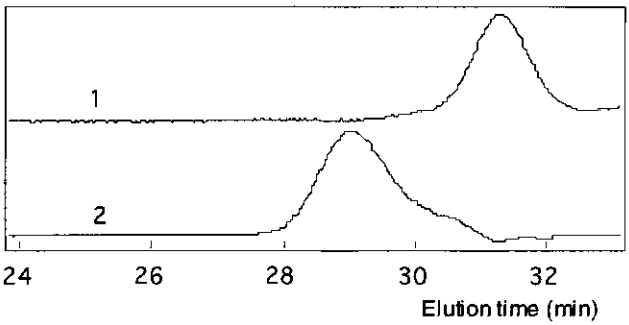

Figure 4. GPC analysis of PEO-PMeOx 67 (trace 2) and its prepolymer TsPEO (M_W = 2100 g mol^{-1}) (trace 1), using a refactive index detector.

Reflectometry

The adsorbed amounts of polymer were measured in a reflectometer with a stagnation-point flow-cell as described in detail by Dijt et al.[27] Here we give only a brief summary. Schematically the set-up of the reflectometer is shown in Figure 5. A polarised laser beam is reflected by the oxidised silicon substrate in the cell. The reflected beam is split into its parallel and perpendicular components by means of a beam splitter and both components are detected separately. The signal S is then defined as $S = I_p/I_s = f\, R_p/R_s$, where I_p and I_s are the intensities of the parallel and the perpendicular components of the reflected polarised laser beam, respectively, f is a constant which can be found by calibration, and R_p and R_s are the reflectivities of the parallel and the perpendicular components. Upon adsorption of polymer the signal changes by an amount ΔS, and the relative change $\Delta S/S_0$ is proportional to the adsorbed amount Γ provided Γ is not too high. The sensitivity, i.e., the ratio $\Gamma/(\Delta S/S_0)$, can easily be calculated from a suitable optical model. This sensitivity depends on the thickness of the oxide layer d_{ox}, on the refractive indices of silicon, silica and solution (n_{si}, n_{ox}, and n_s, respectively), and on the refractive index increment dn/dc of the polymer in solution. Other parameters that influence the sensitivity are the angle of incidence θ_i and the wavelength λ of the laser beam. The values used were d_{ox} = 110 nm, n_{si} = 3.8, n_{ox} =1.46, n_s = 1.333, θ_i = 70.5°, λ = 632.8 nm. The values of dn/dc are indicated in Table 1.

Macroscopically flat silicon wafers from Aurel GmbH (Germany) were used. By thermal oxidation, we obtained an SiO_2 layer with a thickness of about 110 nm. Strips cut from this wafer were cleaned by oxidation by UV-ozone, and could be cleaned and reused many times.

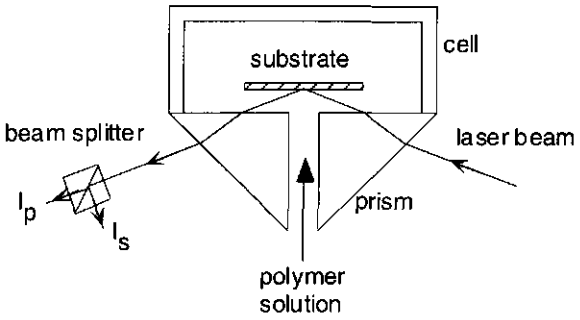

Figure 5. Schematic set-up of a reflectometer with a stagnation-point flow-cell.

Dynamic light scattering

The hydrodynamic thickness of the adsorbed polymer layer was measured by dynamic light scattering. The radius of a colloidal silica particle covered with polymer was compared to that of a bare particle, and the difference was taken as the hydrodynamic thickness of the adsorbed polymer layer. We used a colloidal Ludox silica with a hydrodynamic diameter of 39 nm, purchased from Du Pont.

Calculations

Scaling theories[3,14] and self-consistent mean field theories (SCF)[5,15] have proven to be very useful in describing block copolymer adsorption. Here we used a numerical SCF method first developed by Scheutjens and Fleer for homopolymer adsorption[1,28,29] and later adapted for block copolymer adsorption by Evers et al.[5] In order to investigate whether there is an effect of the chain stiffness, calculations for both flexible and stiff polymers were done. In the latter case a second order Markov approximation[30] was used. In the calculations the composition of an AB block copolymer was varied by changing the numbers of A and B segments, keeping the total number of segments constant. We chose a rather small number of segments (N = 100) in order to make it possible to compare the results qualitatively with the experimental system, in which we

used block copolymers with a rather low molar mass. The calculations were done on a cubic lattice.

Results and Discussion

Homopolymer adsorption

In reflectometry experiments the adsorbed amount is measured as a function of time. This gives a good opportunity to study the kinetics of polymer adsorption. It is assumed that when the variation in the signal has the same order of magnitude as that of the baseline drift, the system is at equilibrium. Of course, this may not be generally true because in some systems equilibrium may only be obtained on much longer time scales than those needed for reflectometry (typically of the order of minutes, with a maximum of a few hours). However, for our experimental system the above assumption is expected to hold, since we are dealing with small, rather flexible polymers which do not form any micellar structure in solution, as evidenced by dynamic light scattering on the polymer solutions. For monodisperse homopolymer solutions of PEtOx, PMeOx and PEO atconcentrations of 10 mg l^{-1}, a plateau in the adsorbed amount is reached within one minute. We also find a very sharp transition from a linear (transport-limited) regime to saturation, in agreement with other results for flexible polymers.[27] For the 10 mg l^{-1} solution of polydisperse PVME the adsorption curve as a function of time is different. The slope of the linear part is lower due to the lower diffusion coefficient of this polymer, which has a much higher molar mass than the other polymers used in these experiments. The transition to saturation is less sharp. This is a general feature of polydisperse polymers.[1,27] In the initial linear part of the curve, all chain lengths present in the polydisperse polymer solution contribute to the adsorption. However, the plateau values of the polymers with different molar mass are not equal, the short polymers having a lower adsorbed amount in the plateau. The contribution of the short chains to the adsorption can never exceed the plateau of these short polymers, whereas the longer chains can reach a higher level. Hence, the short chains are displaced by the longer chains, and the adsorption curve of a polydisperse polymer solution is thus more rounded than that of a monodisperse sample.

For two of the homopolymers we measured the final adsorbed amounts after saturation on silica as a function of the polymer concentration. The resulting adsorption isotherms, for PVME and PEtOx, respectively, are given in Figures 6 and 7.

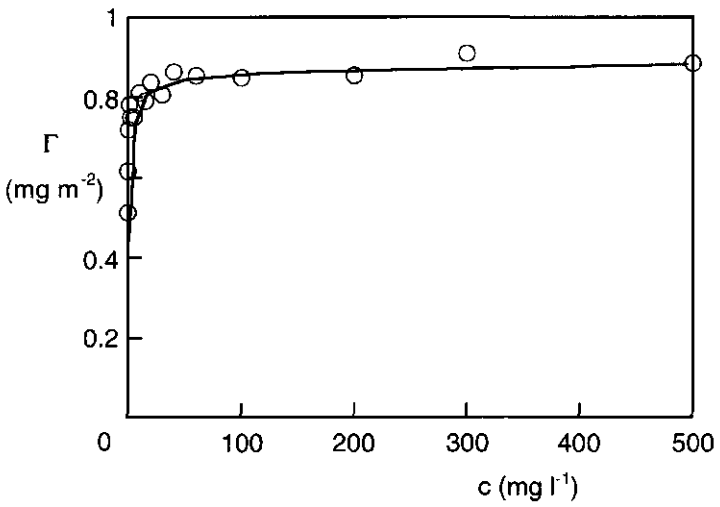

Figure 6. Adsorption isotherm of PVME on silica at pH = 6, as measured by reflectometry.

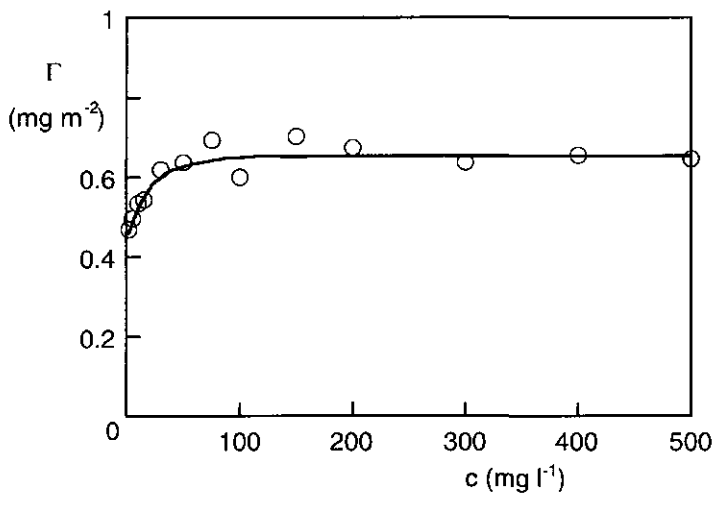

Figure 7. Adsorption isotherm of PEtOx on silica at pH = 6, as measured by reflectometry.

The error in the result of one reflectometry experiment can be rather large, up to 10 percent deviation from the average. It is therefore necessary to do many experiments to obtain accurate results. Although the measurements for the adsorption isotherms were only done twice, the general trends are clear. The high-affinity isotherms we see in Figures 6 and 7 are characteristic for long polymers. Only for very low polymer concentrations (less than 2 mg l^{-1}) is the equilibrium adsorbed amount lower than that in the plateau of the isotherm. This feature is not necessarily unambiguous, because reflectometry is less accurate at extremely low concentrations due to the long time needed for one measurement in our experimental set-up.

We did not measure a full adsorption isotherm for PEO, because in this case literature data[31] are available. PEO gives also a high affinity isotherm[31] with a plateau starting well below 10 mg l^{-1}. We may assume that the same holds for PMeOx. Hence, a polymer concentration of 10 mg l^{-1}, which we used as the standard in the experiment, may be assumed to be sufficient to reach the plateau of the adsorption isotherm. The adsorbed amounts at this concentration are 0.78, 0.56, 0.53 and 0.36 mg m^{-2} for PVME, PEtOx, PMeOx and PEO, respectively. Dijt et al.[27] found for the same PEO sample with the same technique an adsorbed amount of 0.41 mg m^{-2} which agrees, within experimental error, with our results. Chen et al.[32] used a solution depletion method to determine the adsorption isotherms for a series of PEtOx with different molar mass on colloidal silica. Our result for PEtOx with M_w = 6000 fits well in their results, even though we used a quite different technique.

The adsorption of PEO and PEtOx presumably proceeds by hydrogen bonding of the ether or carbonyl oxygen with surface silanol groups.[31] The adsorption of the other polymers is also likely to be driven by hydrogen bonding since they all have an oxygen which can donate an electron pair for a hydrogen bond with the silica surface. Chen et al.[32] found that the segmental adsorption energy of PEtOx on silica was 5.1 kT in water. One way to check the role of the hydrogen bond, is to measure the adsorption as a function of the pH of the solution; at high pH there are less silanols so that hydrogen bonding is impeded. For PVME and PEtOx the results are given in Figure 8. Data by Van der Beek et al.[31] for PEO on colloidal silica have been included in this figure.

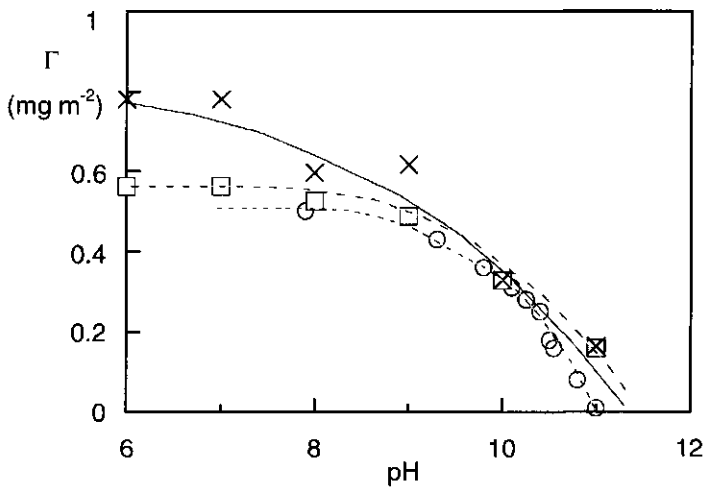

Figure 8. Adsorption of PVME (squares) and PEtOx (triangles) as a function of pH, as measured by reflectometry on a flat silica surface. The results found by Van der Beek et al. for PEO on a colloidal silica have been included (circles).

The shape of the curves is the same for the three homopolymers. The adsorbed amount is almost constant up to about neutral pH. When the polymer solution is made basic desorption occurs. At high pH (above pH around 11) no adsorption is found at all. As discussed by Van der Beek, the OH-ions in solution act as a displacer for the polymers since they deprotonate the silanols. Increasing the concentration of these ions, i.e., increasing the pH, lowers the effective adsorption energy of the polymers because the oxygens are no longer able to form hydrogen bonds with the surface. The adsorbed amount drops to zero around pH = 11. It can be seen from Figure 8 that a slightly higher pH is needed to displace all PVME and PEtOx than to displace all PEO. It is tempting to ascribe this to a higher adsorption energy for PVME and PEtOx. However, we have to be careful because the surfaces were different: the adsorption of PEO was measured on dispersed colloidal silica particles,[31] whereas we measured the adsorption of PVME and PEtOx on a flat silica wafer. It is conceivable that there might be slight differences in properties between these surfaces.

All homopolymers adsorb on silica and the difference in segmental adsorption energy is probably not high, as can be deduced from Figure 8. In order to assess which of two blocks within one block copolymer has the higher segmental adsorption energy, we

measured the adsorption from a mixture of two homopolymers and in sequential adsorption experiments. Even a small difference in adsorption energy between the segments could be enough to obtain a significant preferential adsorption of the more strongly adsorbing polymer, due to the co-operative nature of polymer adsorption: a small difference in adsorption energy per segment will nevertheless give a large difference per chain. Measurement of sequential adsorption or adsorption from a mixture can therefore indicate which polymer has the highest adsorption energy.[1]

We found that in a mixture of PVME and PEtOx the adsorbed amount at saturation is the same as obtained for the isolated PVME solution This suggests that no PEtOx does adsorb from the mixture, and would indicate that the adsorption energy of PVME on silica is higher than for PEtOx. However, PVME has a molar mass that is an order of magnitude higher than that of PEtOx. It is possible that the adsorption energy of PEtOx is slightly higher than of PVME but that the longer chain adsorbs preferentially because it loses less translational entropy (per unit of mass). Nevertheless, the most likely conclusion is that the adsorption energy of PVME is indeed higher than for PEtOx.

In the same way it was deduced that the adsorption energy of PMeOx is higher than that of PEO. In this mixture the molar masses were comparable (6000 and 7100 respectively) and the preference is therefore unambiguously determined by the segmental adsorption energy. All findings were confirmed by sequential measurements in which one of the polymers was adsorbed until a plateau was reached and then a solution of the second polymer was brought into contact with the surface. The height of the resulting adsorption plateau is determined by the polymer with the highest adsorption energy, i.e., PVME in a sequential adsorption experiment of PVME followed by PEtOx or reverse, and PMeOx for the combination of PMeOx and PEO.

Block copolymer adsorption

From the homopolymer results it was concluded that PVME has a higher adsorption energy than PEtOx but that the difference is small. In order to see what the consequences are for the adsorption of diblock copolymers composed of these two blocks, we measured the adsorbed amount of these block copolymers.

Figure 9 gives the adsorbed amount on silica as a function of the composition of the PVME-PEtOx polymer. All measurements were repeated several times and here we give only the average results. The circles correspond to the homopolymers (PEtOx on the left and PVME to the right), and the squares to the copolymers as given in Table 2. For the block copolymers the adsorption is clearly enhanced compared to the values for the

homopolymers, even though the molar mass of the homopolymer PVME is much higher than that of the block copolymers. Surprisingly, the position of the maximum is found at the side of the strongest adsorbing block: at this maximum the strongest adsorbing block is also the longest one. This is completely different from the situation sketched in Figure 1 for selective adsorption, where the maximum is found at a composition where the adsorbing block is smaller than the non-adsorbing block. The total length of the polymer affects the position of the maximum, but for lengths comparable to the molar mass of the polymers used in the experiments, the theoretical maximum is situated at a low fraction of adsorbing segments ν_A. We return to this apparent contradiction between theory and experiment in the section "Comparison with theory".

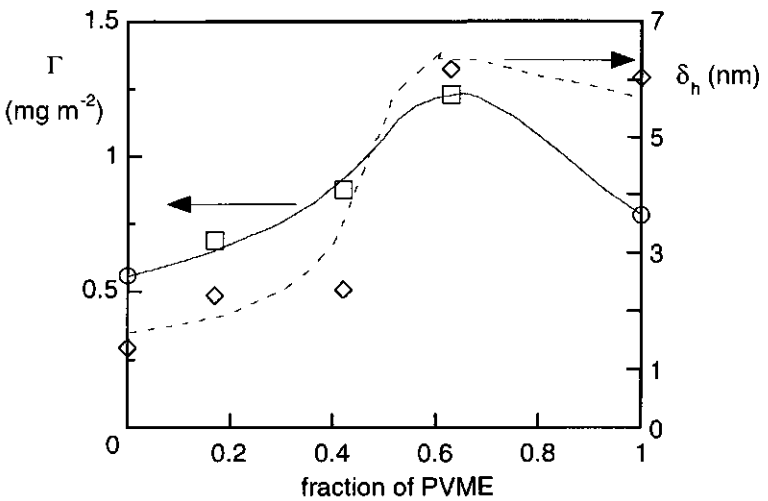

Figure 9. Adsorbed amount Γ (full line) of PVME-PEtOx diblock copolymers (squares) on silica as a function of polymer composition. The results for the homopolymers (circles) have been included. For all samples the hydrodynamic layer thickness δ_h on dispersed silica particles as measured by dynamic light scattering is also indicated (diamonds, dashed line).

For the set of block copolymers consisting of PMeOx and PEO blocks, the former has the highest segmental adsorption energy. Results for this system are plotted in Figure 10. Note that we used diblock (squares) as well as triblock (triangles) copolymers. We see, as for PVME-PEtOx block copolymers, that the adsorbed amount for the block copolymers is higher than for the homopolymers. The maximum in the adsorbed amount

is found at a high PMeOx fraction: again the strongest adsorbing block is also the longest one at the maximum, as in Figure 9. The maximum is not as pronounced as in Figure 9.

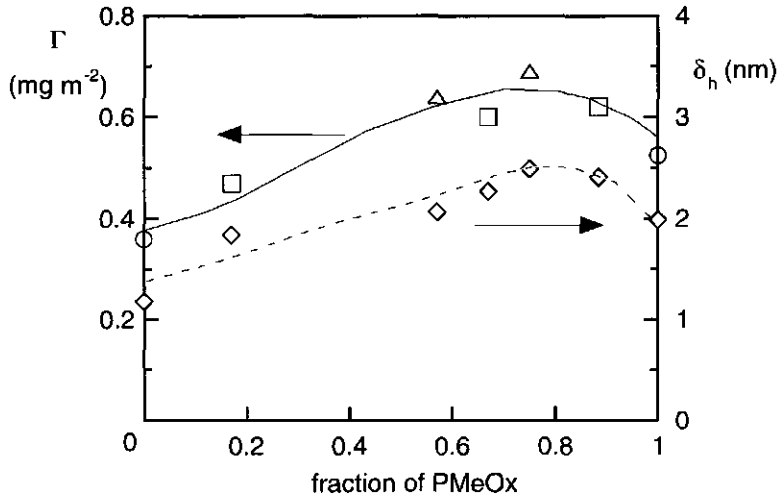

Figure 10. Adsorbed amount Γ (full line) of PMeOx-PEO diblock (squares) and triblock (triangles) copolymers on silica as a function of polymer composition. The results for the homopolymers (circles) have been included. For all samples the hydrodynamic layer thickness δ_h on dispersed silica particles as measured by dynamic light scattering is also indicated (diamonds, dashed line).

A remarkable feature in Figure 10 is that the adsorption of the triblock copolymers (triangles), having a less strongly adsorbing middle part, is even slightly higher than that of the diblock copolymers (squares). This is an unexpected result because a triblock copolymer, adsorbing with its two outer blocks has hardly any dangling tails and therefore looses more entropy than an adsorbing diblock copolymer with the same overall composition. Hence, one would expect that the total adsorbed amount of a triblock copolymer would be lower than that of a diblock copolymer. Our results do not agree with this expectation, so far we do not have an explanation for this.

Hydrodynamic layer thickness

In Figures 9 and 10, the hydrodynamic thicknesses of PVME-PEtOx and PMeOx-PEO polymer layers, respectively, are also included These layer thicknesses are less accurate than the adsorbed amounts, because there where sometimes problems with

the colloidal stability. For example, in a first series of experiments, the triblock copolymers of PMeOx and PEO, induced some flocculation of the silica dispersion. The end blocks of these polymers have a higher adsorption energy than the middle block; polymer bridging is therefore facilitated. For the diblock copolymers we did not observe flocculation, although it cannot be completely ruled out. Hence, the results in Figures 9 and 10 give an upper limit of the hydrodynamic layer thickness.

The layer thicknesses are in agreement to what could be expected regarding the adsorbed amount and the molar mass. The PVME homopolymer, which has a rather high molar mass of 99 000 g mol^{-1}, gives a thickness of about 6.0 nm, a value comparable with the one found for PEO with the same molar mass.[31] The other adsorbed homopolymers have very small layer thicknesses, as expected for these rather short polymers. The hydrodynamic thickness of the adsorbed block copolymers is higher than that of the homopolymers. The overall shape of the curves for the thickness and the adsorbed amount is very similar. Both in Figure 9 and 10, a maximum for the layer thickness is seen at a polymer composition in which the strongest adsorbing block is also the longest one. Polymer PVME-PEtOx 63, the diblock copolymer of PVME and PEtOx which gave the highest adsorbed amount, also has the thickest adsorbed layer (6.2 nm). This is only slightly above the value of PVME homopolymer but the molar mass of the latter is considerably higher.

We summarise the experimental finding as follows. The block copolymers show a higher adsorbed amount and a higher hydrodynamic thickness as compared to the homopolymers of similar molar mass. However, the effects are not as pronounced as found for selectively adsorbed block copolymers, which is probably related to the small difference in adsorption energies. Nevertheless, this kind of block copolymers is promising for the steric stabilisation of an aqueous dispersion, especially when fast equilibration is needed: these block copolymers do not have a kinetic barrier, since water is an non-selective solvent for these polymers so that no micelles are formed.

Comparison with theory

In our experiments we found a maximum for the adsorbed amount and the layer thickness as a function of the block copolymer composition. In this maximum, the strongest adsorbing block is also the longest one, which differs from the theoretical curve given in Figure 1. In this figure, we showed results for adsorbing A segments and non-adsorbing B segments in an athermal solvent. In our experimental system both blocks have a relatively high adsorption energy for the surface and the interaction parameters

between solvent and polymer and between the two blocks (block compatibility) may not be zero. In this section we try to find out whether SCF theory, taking these effects into account, can offer some help in interpreting the experimental findings.

We first consider the adsorption of an AB diblock copolymer from a non-selective, in this case athermal solvent, as described earlier by Evers et al[5]. We assigned a constant adsorption energy (2 kT) to the A segments and increased the adsorption energy of the B segments from zero to 2 kT. In the latter case there is no difference between the blocks and the copolymer behaves like a homopolymer for all compositions. Figure 11 gives the adsorbed amount θ as a function of the fraction ν_A of A segments, where ν_A is defined as $\nu_A = N_A/N$, with $N = N_A + N_B = 100$.

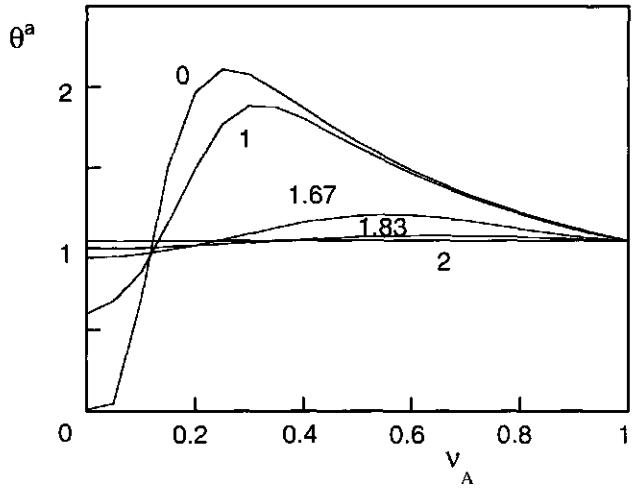

Figure 11. SCF calculations of the adsorbed amounts θ^a (expressed in equivalent monolayers) as a function of the fraction ν_A, for fully compatible blocks and an athermal solvent. Parameters: $\chi_{sA} = 2$, χ_{sB} is indicated, other χ-parameters are zero, $N = 100$.

For selective adsorption ($\chi_{sB} = 0$) we find the same maximum in the adsorbed amount as in Figure 1, i.e., at relatively low ν_A. When the adsorption energy of the B segments is increased, the maximum becomes less pronounced and shifts to higher ν_A. More importantly, for small differences in adsorption energy the maximum is found at a composition where the A block is longer than the B block. Obviously, the maximum disappears when there is no difference in adsorption energy ($\chi_{sB} = 2$).

By assigning an adsorption energy to the B segments, we introduce competition between the A and B segments. The total adsorbed amount is determined by the balance between the gain in adsorption energy and the loss in translational and configurational entropy of the adsorbing chains. When the surface is not yet saturated with block copolymer, free polymers from the solution can adsorb with their A block at the cost of translational entropy of that polymer. When the B segments have also an adsorption energy, some of the B segments of a chain already adsorbed by its A segments attach to the surface. When this occurs, the total system will gain less energy ($\chi_{sB} < \chi_{sA}$) but at the same time lose less entropy as compared to the adsorption of additional free block copolymer. In both scenarios the free energy of the system will decrease and the competition between the two mechanisms is determined by a subtle balance involving the difference in segmental adsorption energy of A and B and the relative lengths of the blocks. When the difference decreases, relatively more B segments adsorb. As a consequence, the adsorbed amount decreases for almost all polymer compositions when the adsorption energy of B increases (but remains below that of A). Only at very low ν_A, below a crossover point in the *buoy regime*, does the adsorption increase, but it is relatively low in this region. The more weakly adsorbing B blocks must be long enough to compete with the A blocks for adsorbing sites. Decreasing the difference in segmental adsorption energy will decrease the necessity of a relatively long B block and therefore the maximum shifts to a higher ν_A, in other words to a shorter B block. The maximum disappears when the difference is zero ($\chi_{sA} = \chi_{sB}$).

We conclude that for small differences in adsorption energy the maximum is found at a composition where the A block is longer than the B block. However, the theoretical maximum is not as pronounced as the one we found experimentally. In order to investigate whether we can find a better qualitative agreement, we consider the influence of the solvency parameters (i.e., χ_{AO} and χ_{BO}) and of the block (in)compatibility (i.e., χ_{AB}).

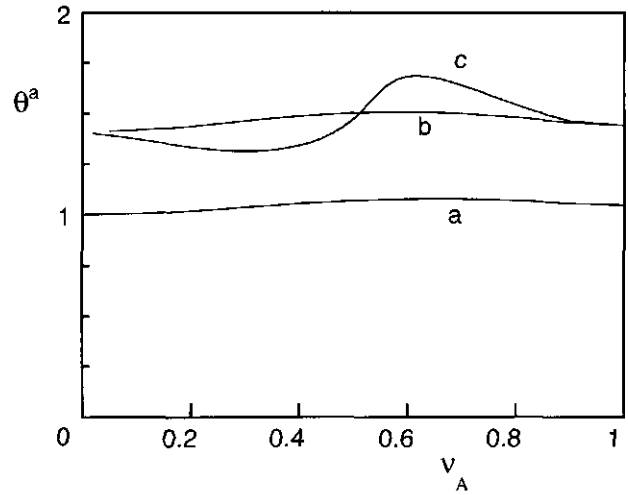

Figure 12. SCF calculations of the adsorbed amounts θ^a (expressed in equivalent monolayers) as a function of the fraction v_A, for fully compatible block (a and b) or incompatible blocks (c) from a poorer solvent. Parameters: $\chi_{sA} = 2$, $\chi_{sB} = 1.83$, $N = 100$, for curve a: $\chi_{AO} = \chi_{BO} = \chi_{AB} = 0$, for curve b: $\chi_{AO} = \chi_{BO} = 0.45$ and $\chi_{AB} = 0$, and for curve c: $\chi_{AO} = \chi_{BO} = \chi_{AB} = 0.45$.

In Figure 12 we give some results for a block copolymer with a small difference in segmental adsorption energy between the blocks ($\chi_{sA} = 2$ kT, $\chi_{sB} = 1.87$ kT). When we choose a positive interaction energy between the segments and the solvent ($\chi_{AO} = \chi_{BO} = 0.45$, curve b), the adsorbed amount is increased for all compositions of the block copolymer as compared to the adsorption from an athermal solvent (curve a). To reduce the amount of non-favourable polymer-solvent contacts, the solvent is expelled from the adsorbed layer. The lateral repulsion between the polymers is reduced and more chains can adsorb per unit area. The layer is more compact as compared to a layer adsorbed from an athermal solution. This can also be seen in the volume fraction profiles of the A and B blocks in the adsorbed layer for the two different solvencies (Figures 13a and b). These volume fraction profiles are given for compositions that give a maximum in Figure 12. In Figure 13a most segments of both blocks can be found in the first few layers close to the surface. Nevertheless, a small segregation can be seen as the B segments are relatively more extended in the solution than the A segments. In Figure 13b the fraction of A and B segments in the first layers is enhanced because the solvent is expelled from the adsorbed layer due to the repulsive interaction between the polymer segments and the solvent. The segregation between A and B segments, necessary for an anchor-buoy

structure of the adsorbed layer, is evolving: the B layer is slightly more extended into the solution than in Figure 13a.

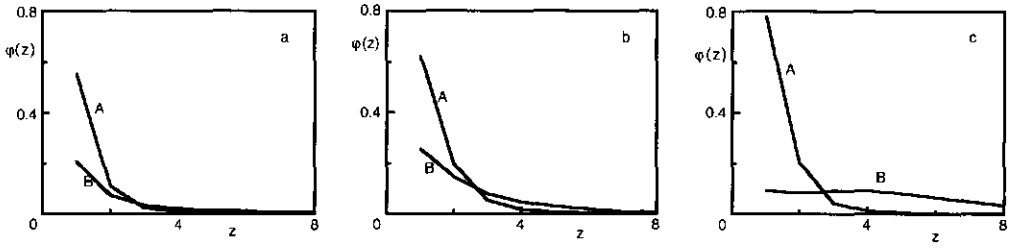

Figure 13. Volume fraction profiles ($\varphi(z)$) of the A and B blocks in the maxima of Figure 12, all parameters the same as in Figure 12.

When the solvent quality decreases, less anchoring segments are needed to keep the whole polymer attached to the surface in comparison with an athermal solution, which causes a shift in the position of the maximum to a slightly lower ν_A, and a slight increase in the relative height of the maximum (defined as the ratio between the adsorbed amounts in the maximum and at $\nu_A = 1$). These two effects due to the solvency (Figure 12) are, however, small in comparison to those occurring when the adsorption energies are varied (Figure 11).

When we assign a positive interaction energy to A-B contacts (i.e., the A and B blocks now become incompatible if they are long enough), the shape of the curve changes remarkably. The relative height of maximum is increased considerably, and a minimum appears at low ν_A. The minimum can be explained by considering the structure of the adsorbed layer. At low ν_A the A and B segments are forced to have many unfavourable contacts with each other in the mixed adsorbed layer; the total repulsive interaction energy is therefore high and the adsorption is decreased. The segregation, already seen in the volume fraction profiles in Figure 13b, is promoted by the incompatibility of the A and B blocks, so that the number of A-B contacts is further reduced. This effect is demonstrated in the volume fraction profiles of the A and B block given in Figure 13c. The first layer is almost completely occupied by adsorbed A segments, whereas most B segments form a more dilute buoy layer, extending away from the surface. A real anchor-buoy structure can be seen, although it is not as pronounced as in Figure 1b. The reason for this anchor-buoy structure is different from that in Figure 1b. In the latter case it is the difference in adsorption energy, in Figure 13c it is block incompatibility.

Statistically, the amount of unfavourable A-B contacts is the highest when both blocks are equal in size. For a block copolymer in which the A and B segments have the same segmental adsorption energy, and a positive AB interaction energy, this gives rise to a minimum in the adsorbed amount as a function of the polymer composition at $\nu_A = 0.5$ (result not shown). When the A and B segments have a slightly different adsorption energy the minimum is shifted to $\nu_A < 0.5$ and a maximum develops at $\nu_A > 0.5$, as seen in Figure 12c. The theoretical curve in Figure 12c is in qualitative agreement with the experimental results presented in Figures 9 and 10. Experimentally we do not find a minimum, but the number of available compositions of the block copolymers was rather low; it would be interesting to include samples with ν_A around 0.3.

The calculations presented above were performed with equally flexible blocks. In reality, however, the chain stiffness might well be different. It is an established fact that some polymers are rather flexible, whereas others are stiff due to large side groups or internal structures. We performed some SCF calculations where we assigned a positive bending energy to one of the blocks or to both blocks, along the lines reported in literature[1]. The effect of introducing chain stiffness appears to be very small and is definitely less pronounced than those of changing solvency and block incompatibility. The results of the theoretical calculations with stiff polymers are therefore not shown here.

Conclusions

The adsorption of two series of block copolymers and the corresponding homopolymers on silica was measured with reflectometry and the hydrodynamic layer thickness was determined by dynamic light scattering. All polymers adsorb by the same mechanism: hydrogen bonding between an oxygen of the polymer and a silanol group on the silica surface. The segmental adsorption energy is relatively high, of the order of 5 kT[32]. On the other hand, the *difference* between the segmental adsorption energies of the two blocks is low, giving rise to non-selective adsorption of the block copolymers. For two types of block copolymers used in this study, the adsorbed amount as a function of block copolymer composition shows a shallow maximum; at this maximum the longest block is also the strongest adsorbing block. The same trend is found for the hydrodynamic layer thickness. These findings differ from theoretical predictions concerning selective adsorption, where a pronounced maximum is found for a short anchor block.

With numerical self-consistent field calculations we demonstrated that the same trends as in our experimental findings can be predicted by theory. In non-selective adsorption, when the difference between the adsorption energies of the blocks is low, both blocks

compete for the same adsorption sites on the surface. When the differences in solvency are small and the blocks are compatible, only a very shallow maximum is seen at high fraction of A segments v_A. Assigning a positive interaction energy to the two different segments decreases the compatibility of the blocks. Due to this incompatibility, the blocks try to avoid each other, which promotes an anchor-buoy structure. This effect gives rise to a considerable increase of the adsorbed amount in the maximum as a function of the block copolymer composition. At this maximum the longest block is also the strongest adsorbing block. For this non-selective adsorption with incompatible blocks the typical anchor-buoy structure of the adsorbed layer, necessary for an effective steric stabilisation, is maintained, be it less pronounced than for selective adsorption. The buoy layer is far less extended into the solution.

The non-selectively adsorbed block copolymers show a higher adsorbed amount and a higher hydrodynamic thickness as compared to the homopolymers of similar molar mass. Even though the effects are not as outspoken as found for selectively adsorbed block copolymers, this kind of block copolymers is promising for the steric stabilisation of aqueous dispersions.

References

(1) Fleer, G. J.; Cohen Stuart, M. A.; Scheutjens, J. M. H. M.; Cosgrove, T.; Vincent, B. *Polymers at Interfaces*; Chapman & Hall: London, 1993.

(2) Kawaguchi, M.; Takahashi, A. *Adv. Colloid and Interface Sci.* **1992**, *37*, 219.

(3) Marques, C. M.; Joanny, J. F. *Macromolecules* **1989**, *22*, 1454.

(4) Munch, M. R.; Gast, A. P. *Macromolecules* **1988**, *21*, 1366.

(5) Evers, O. A.; Scheutjens, J. M. H. M.; Fleer, G. J. *J. Chem. Soc., Faraday Trans.* **1990**, *86*, 1333.

(6) Wu, D. T.; Yokoyama, A.; Setterquist, R. L. *Polymer J.* **1991**, *23*, 711.

(7) Cosgrove, T.; Phipps, J. S.; Heath, T. G.; Richardson, R. M. *Macromolecules* **1991**, *24*, 94.

(8) Parsonage, E.; Tirrell, M.; Watanabe, H.; Nuzzo, R. G. *Macromolecules* **1991**, *24*, 1987.

(9) Guzonas, D. A.; Boils, D.; Tripp, C. P.; Hair, M. L. *Macromolecules* **1992**, *25*, 2434.

(10) Guzonas, D.; Hair, M. L.; Cosgrove, T. *Macromolecules* **1992**, *25*, 2777.

(11) Webber, R. M.; Anderson, J. L. *Langmuir* **1994**, *10*, 3156.

(12) Halperin, A.; Tirell, M.; Lodge, T. P. *Adv. Polymer Sci.* **1992**, *100*, 31.

(13) Fleer, G. J.; Scheutjens, J. M. H. M. *Colloids Surfaces* **1990**, *51*, 281.

(14) Marques, C. M.; Joanny, J. F.; Leibler, L. *Macromolecules* **1988**, *21*, 1051.

(15) Van Lent, B.; Scheutjens, J. M. H. M. *Macromolecules* **1989**, *22*, 1931.

(16) Malmsten, M.; Linse, P.; Cosgrove, T. *Macromolecules* **1992**, *25*, 2474.

(17) Tiberg, F.; Malmsten, M.; Linse, P.; Lindman, B. *Langmuir* **1991**, *7*, 2723.

(18) Munch, M. R.; Gast, A. P. *Macromolecules* **1990**, *23*, 2313.

(19) Johner, A.; Joanny, J. F. *Macromolecules* **1990**, *26*, 5299.

(20) Huguenard, C.; Varoqui, R.; Pefferkorn, E. *Macromolecules* **1991**, *24*, 2226.

(21) Tripp, C. P.; Hair, M. L. *Langmuir* **1996**, *12*, 3952.

(22) Liu, Q.; Konas, M.; Davis, R. M.; Riffle, J. S. *J. Polymer Sci. Part A - Polymer Chem.* **1993**, *31*, 1709.

(23) Miyamoto, M.; Sano, Y.; Saegusa, T.; Kobayashi, S. *Eur. Polym. J.* **1983**, *19*, 955.

(24) Brandrup, J.; Immergut, E. H., Eds *Polymer Handbook, 3rd ed.*; Wiley and Sons: New York, 1989.

(25) Van Krevelen, D. W. *Properties of Polymers, Their Estimation and Correlation with Chemical Structure*; Elsevier: Amsterdam, 1976.

(26) De Vos, R. J.; Goethals, E. J. *Makromol. Chem., Rapid. Comm.* **1985**, *6*, 53.

(27) Dijt, J. C.; Cohen Stuart, M. A.; Hofman, J. E.; Fleer, G. J. *Colloids Interfaces* **1990**, *51*, 141.

(28) Scheutjens, J. M. H. M.; Fleer, G. J. *J. Phys. Chem.* **1979**, *83*, 1619.

(29) Scheutjens, J. M. H. M.; Fleer, G. J. *J. Phys. Chem.* **1980**, *84*, 178.

(30) Gorbunov, A. A.; Zhulina, E. B.; Skvortsov, A. M. *Polymer* **1982**, *23*, 1133.

(31) Van der Beek, G. P.; Cohen Stuart, M. A. *J. Phys. (Paris)* **1988**, *49*, 1449.

(32) Chen, C. H.; Wilson, J. E.; Davis, R. M.; Chen, W.; Riffle, J. S. *Macromolecules* **1994**, *27*, 6376.

Chapter 4

Adsorption kinetics of diblock copolymers on silica and titania from a micellar solution

The solution and adsorption behaviour of a seres of diblock copolymers of hydrophobic poly(dimethyl siloxane) and hydrophilic poly(2-ethyl-2-oxazoline) was studied. In an aqueous solution these block copolymers form large polydisperse micelles. The critical micellisation concentration is lower than 2 mg l^{-1}. The adsorption kinetics of these polymers onto macroscopically flat oxide surfaces was studied with reflectometry in stagnation point flow. Both blocks of the copolymers have affinity for silica and only the hydrophobic block has affinity for the titania surface. Nevertheless, the adsorption curves on silica and titania have similar features. The adsorption kinetics are affected by the exchange rate between micelles and free polymers. For short polymer chains the exchange rate is fast compared to the time necessary for diffusion across the diffusive layer. Before the micelles arrive at the surface they have already broken up into unimers. Because the cmc is very low, the experimental adsorption rate is determined by the diffusion of micelles towards the surface. For the longest polymer chain this is not the case: the exchange between micelles and unimers is relatively slow. The micelles do not adsorb directly, and the adsorption rate is determined by the exchange of polymers between micelles and solution. For all polymer samples the adsorption increases linearly as a function of time, up to very high adsorbed amounts where it reaches a plateau. The adsorbed amount on silica is considerably higher than found for titania. The poly(dimethyl siloxane) is more strongly anchored to the silica surface than to titania, the density of the adsorbed layer can therefore become higher.

Introduction

Polymers play an important role in many natural and technical processes. Especially their interfacial behaviour can have an enormous impact on the properties of materials.[1] For example, polymers are known for their ability to stabilise colloidal dispersions.[2] This steric stabilisation can be achieved when the polymers adsorb on the surface of the colloidal particles, and form a layer that is thick enough to overcome the attractive Van der Waals force. The thickness of the layer is mainly determined by the number and the length of the polymer chain ends (tails) protruding into the solution. For a thick and stabilising layer long tails are required, which have to be firmly anchored to the surface. In diblock copolymers these conditions can be met by using two different blocks where one block (*the anchor*) has a high affinity for the surface and the other block (*the buoy*) protrudes far into the solution in the form of a long tail. The adsorption of block copolymers has been extensively studied theoretically[3-8] as well as experimentally.[9-17]

In the adsorption of block copolymers the solvent plays an important role. If both blocks of the diblock copolymer are soluble, the solvent is called non-selective. If, however, only one of the blocks dissolves and the other does not, the solvent is selective, and the block copolymers may form micelles. In both types of solvents very thick layers can be built up, with the non-adsorbing block forming a dilute and extended buoy layer. In a non-selective solvent the anchor layer is swollen due to the presence of solvent molecules. In a selective solvent where the non-soluble block is the anchor, the anchor layer is thin and dense because the solvent is expelled. In both types of solvent a maximum in the adsorbed amount is found as a function of the block copolymer composition. When the polymer chains are long, this maximum will be found for a relatively short anchor block. The anchor block is then just long enough to keep the whole molecule attached to the surface and the relatively long tails can form a very extended dense layer, a so-called *brush*.[18] However, when in a selective solvent the soluble block is preferentially adsorbed an adsorbed layer of micelles or a bilayer may be formed. In the bilayer the soluble blocks are expected to form a swollen adsorbed layer close to the wall. A second, very dense layer may then be formed by the non-soluble blocks. Further away from the surface another layer of soluble blocks is thought to be built up, minimising the contacts between the solvent and the non-soluble block.[5] For a layer of adsorbed micelles the dense middle layer is not continuous and we may expect lateral inhomogeneities for that situation. A schematic presentation of possible structures of the adsorbed layer is given in Figure 1.

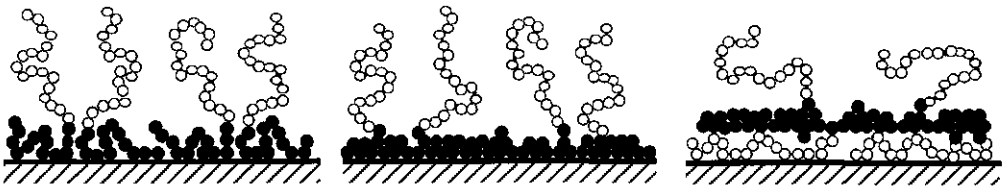

Figure 1. Possible structures of an adsorbed diblock copolymer layer. In the left hand side picture the anchor blocks (filled circles) are soluble and form a swollen layer, the non-adsorbing buoy blocks (open circles) protrude into the solution. In the middle picture, the anchor blocks are not soluble and form a melt at the surface. In the right hand side picture a (laterally homogeneous) bilayer is formed with a swollen anchor layer, a dense non-soluble middle layer and a layer of buoy blocks. In this case the soluble blocks (open circles) form both the anchor and the buoy layer.

The structures sketched for the adsorbed layer of block copolymers are those corresponding to equilibrium states. However, kinetic barriers can make it difficult or even impossible to reach this equilibrium state. In a non-selective solvent the osmotic pressure in the dense brush forms a barrier which makes it hard for additional polymer molecules to adsorb because they first have to diffuse through this brush. It can therefore take a very long time before equilibrium is reached. In a selective solvent where only the non-soluble block has affinity for the surface, an extra barrier is formed by the existence of a micellar corona of soluble blocks, which is repelled by the surface. The hydrophobic blocks then have to diffuse over a long distance through a non-favourable environment before they reach the surface. For such a system it may even take more time to reach the equilibrium state than for the adsorption from a non-selective solvent.

The kinetics of diblock copolymer adsorption is very important, especially for industrial purposes, where the time available for different processes is limited and non-equilibrium conditions may prevail. Obviously, in the study of block copolymer adsorption attention should not only be paid to the equilibrium state but also to the kinetics.

In this paper we consider the adsorption of amphiphilic diblock copolymers from an aqueous solution onto silicium dioxide (silica or SiO_2) and titanium dioxide (titania or TiO_2) surfaces. A series of four diblock copolymers of poly(dimethyl siloxane) (PDMS) and poly(2-ethyl-2-oxazoline) (PEtOx) was used. The block copolymers form micelles in solution. It turns out that both blocks have affinity for silica but only the hydrophobic block (PDMS) has affinity for the titania surface. The equilibrium adsorbed state for both surfaces is expected to be as drawn in the middle picture of Figure 1. However, before this equilibrium is attained, the structures of the adsorbed layers on silica and titania can

be different. The adsorption onto silica most probably proceeds by an intermediate structure of adsorbed micelles, because the corona has affinity for silica. When finally, by rearrangement of the micelles, the hydrophobic core has made contact with the surface, a saturated block copolymer layer may be formed in which the surface is completely covered by a dense layer of hydrophobic blocks and the hydrophilic chains protrude into the solution.

For adsorption of the micelles on titania a steric barrier has to be overcome: the micelle must bring its core into contact with the surface but is hindered by the existence of a non-adsorbing corona. Johner and Joanny used scaling arguments to show that the potential barrier of the corona is very high and that formation of the surface layer in this case proceeds by the attachment of free polymer chains or unimers, i.e., polymer molecules that are not in micelles.[7] The micelles act as a source which supplies unimers to the solution from where they can adsorb to the surface. Eventually, the adsorbed layer will probably be similar to that on silica. For the kinetics of adsorption the exchange rate between micelles and unimers is thus very important. The micelles can only act as a source for new unimers when the exchange rate is relatively fast as compared to the time the micelle is near the adsorbing surface. The exchange rate depends on many quantities among which are the solvent quality, the flexibility of the core, and the polymer block lengths. In our experimental system we used a series of four diblock copolymers differing in total length but with a constant weight ratio between hydrophilic and hydrophobic blocks. Within this series, the exchange rates of unimer molecules between micelles and solution will be strongly dependent on the total polymer length. The molar mass of the largest polymer is forty times higher than that of the smallest polymer. This will probably lead to micellar relaxation times that differ several orders of magnitude.[19] For the purpose of this study we hope that the shortest polymer chains have a micellar relaxation time that is fast compared to the contact time with the surface whereas that of the largest polymer molecules is much slower. Investigating the adsorption kinetics as a function of molar mass can give us more insight in the mechanism of diblock copolymer adsorption.

Micellar solutions of the polymers in water were characterised using dynamic light scattering and cryogenic transmission electron microscopy. The adsorption of these polymers onto macroscopically flat oxide surfaces was studied with reflectometry in the so-called stagnation point of an impinging jet flow cell. We were able to follow the time-dependent adsorption up to several hours after the onset of the experiment. For a comparison between the experimental adsorption rate and the theoretical flux of polymers towards the surface, it is necessary to know the flow pattern in the flow cell.

Before discussing the experimental results we calculate in the following section the flux of polymer molecules towards the surface, in particular in the stagnation point. A new feature in this treatment is that we include the exchange of unimers between micelles and solution.

Convective diffusion of polymer in a stagnation point flow

We want to know the flow behaviour of the solution in the experimental set-up and the resulting flux towards the surface under investigation. In the reflectometer used to measure the adsorption of the polymer, we have an impinging jet flow which was described extensively by Dabros and Van de Ven.[20] A schematic presentation of an impinging jet flow is given in Figure 2.

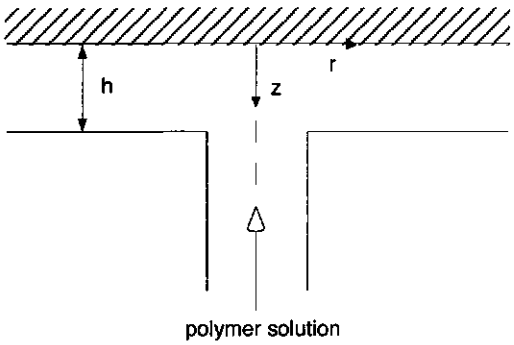

Figure 2. The geometry of the impinging jet flow cell. The polymer solution flows through the inlet tube with radius R, and enters the gap between two parallel surfaces separated by a distance h. The stagnation point is located at the top surface on the axis of symmetry (dotted line). The distance to that surface is z and the radial distance to the axis of symmetry is r.

The mass transport of particles in diluted suspensions towards the surface in the stagnation point of an impinging jet flow was calculated in detail by Dabros and Van de Ven.[20] When we consider the polymer coils in solution as particles, the same expressions hold for the flux of polymer molecules towards the surface in a stagnation point. The flow velocity vector near r = 0 can be written in cylindrical coordinates:

$$\vec{v} = \begin{pmatrix} v_r \\ v_z \\ v_\phi \end{pmatrix} = \begin{pmatrix} \alpha z r \\ -\alpha z^2 \\ \beta r z \end{pmatrix} \qquad (1)$$

where α and β are streaming intensity parameters. These can also be expressed as $\bar{\alpha}U/R^2$ and $\bar{\beta}U/R^2$, respectively, where U is the mean velocity in the tube at the outlet plane (z = h), and $\bar{\alpha}$ and $\bar{\beta}$ are dimensionless streaming intensity parameters. The value of these parameters depends on the Reynolds number Re, and on the geometric factors h and R, and can be found numerically.[20] The Reynolds number is related to the mean velocity, the radius of the tube and the kinematic viscosity ν through Re = UR/ν. For an impinging jet flow $\bar{\beta}$=0, for symmetry reasons. The total concentration c of polymer in the solution satisfies the continuity equation:

$$\frac{\partial c_i}{\partial t} = -\vec{\nabla}.\vec{F}_i + S_i(t) = -\vec{\nabla}.\left((c_i\vec{v}) - (D_i\vec{\nabla}c_i)\right) + S_i(t) = -\vec{v}\vec{\nabla}c_i + D_i\vec{\nabla}^2 c_i + S_i(t) = 0 \qquad (2)$$

where the subscript i indicates the polymeric species, i.e., i = u for unimers and i = m for micelles, t is time, $\vec{F}_i$ is the flux vector, and $\vec{\nabla}$. denotes the gradient operator. The flux has a convective term $c_i\vec{v}$, where $\vec{v}$ is the velocity vector, and a diffusive term $-D_i\vec{\nabla}c_i$, where D is the diffusion coefficient. We only consider incrompressible fluids, i.e., $c_i\vec{\nabla}.\vec{v} = 0$, and stationary states, i.e., $\partial c_i/\partial t = 0$. The total flux of polymer is given by the sum of the fluxes for unimers and micelles, the concentrations of which are coupled through the exchange of polymers between micelles and solution. This exchange is included as the source term $S_i(t)$, for which we can write:

$$S_u(t) = -S_m(t) = -k_s^- c_m + k_s^+ (c_u)^N \qquad (3)$$

The rate constants k_s^+ and k_s^- determine the 'on and off rate' of micelle formation, and N is the number of unimers per micelle. For the sake of clarity, we only consider two limits: the exchange is very slow or, conversely, very fast as compared to the time the micelles need to diffuse across the diffusive layer (of thickness δ_m) towards the surface.

Slow exchange rate

First, we consider the case that the exchange rate between unimers and micelles is very slow. The time τ_r a micelle needs for break up is then long compared to the time τ_m it takes for the micelle to travel across the diffusive layer towards the surface. The exchange term $S_i(t)$ may then be ignored, and equation (2) can be solved for both unimers and micelles separately. It can now be written as:

$$\vec{v}\vec{\nabla}c_i = D_i\vec{\nabla}^2 c_i \qquad \text{or} \tag{4a}$$

$$\alpha r z\frac{\partial c_i}{\partial r} - \alpha z^2\frac{\partial c_i}{\partial z} = D_i\left(\frac{\partial^2 c_i}{\partial r^2} + \frac{\partial c_i}{r\partial r} + \frac{\partial^2 c_i}{\partial z^2}\right) \tag{4b}$$

Close to the stagnation point we may neglect the variation in the r-direction and obtain:

$$-\alpha z^2\frac{\partial c_i}{\partial z} = D\frac{\partial^2 c_i}{\partial z^2} \tag{5}$$

Upon integrating this equation we find for $\partial c_i/\partial z$:

$$\frac{\partial c_i}{\partial z} = K_i\exp\left(\frac{-\alpha z^3}{3D_i}\right) = K_i\exp\left(\frac{-\overline{\alpha}\,\mathrm{Re}\,\nu z^3}{3D_i R^3}\right) \tag{6}$$

where K_i is a constant, to be determined from the boundary condition that the total change in concentration between $z = \infty$ and $z = 0$ is given by the difference between bulk concentration c_i^b and the 'subsurface concentration' of unadsorbed polymers c_i^s:

$$K_i = \frac{c_i^{\,b} - c_i^{\,s}}{\int_0^\infty \exp\left(\frac{-\alpha z^3}{3D_i}\right)dz} = p\left(c_i^{\,b} - c_i^{\,s}\right)\left(\frac{\alpha}{D_i}\right)^{1/3} \tag{7}$$

where the numerical constant p equals $9^{1/3}/\Gamma(1/3) \approx 0.776$. Here Γ denotes the gamma function[21]. The flux of polymer unimers and micelles towards the surface can now be written as

$$J_i = D_i\left(\frac{\partial c_i}{\partial z}\right)_{z=0} = D_i K_i = p\left(c_i^{\,b} - c_i^{\,s}\right)D_i^{\,2/3}\alpha^{1/3} = k_i\left(c_i^{\,b} - c_i^{\,s}\right) \tag{8a}$$

where the rate constant k_i is defined as

$$k_i = p\nu^{1/3}R^{-1}D_i^{\,2/3}\left(\overline{\alpha}\,\mathrm{Re}\right)^{1/3} \tag{8b}$$

For uncharged polymers with affinity for the surface we may expect that the initial attachment rate is much higher than the transport rate k_i, i.e., every polymer chain that arrives at the surface will adsorb immediately. Thus, for the initial stage of the adsorption we may assume that c_i^s is zero and $d\Gamma_i/dt$ equals the limiting flux $J_i^{max} = k_i c_i^b$. Upon adsorption the surface is gradually filled with polymer and the attachment rate decreases. When the attachment rate becomes slower than the transport rate c_i^s will

increase. Eventually, when the surface is completely occupied with polymer, c_i^s becomes equal to the bulk concentration. For a species which has no affinity for the surface the attachment rate is zero and c_i^s equals the bulk concentration. For a micellar system with a relatively slow exchange rate the total flux of polymer is simply given by the sum of the individual fluxes for unimers and micelles. When the corona of the micelles does not have affinity for the surface (but the hydrophobic block does), the micelles cannot contribute to the flux and the total flux is equal to the flux of unimers.

Fast exchange rate

As the other extreme we assume that the exchange rate between unimers and micelles is relatively fast. The micelle breaks up into free polymers before it has reached the surface. At concentrations below the cmc, the total flux of polymer is given by equation (8a) for unimers. Above the cmc, however, the micelles that are present can be seen as a reservoir that instantaneously supplies new unimers until the cmc is reached again. This supply will continue up to a distance $z = \Delta$ from the surface where the concentration of micelles drops to zero. From this point on the concentration of unimers decreases to become zero at the surface. We may now again take the source term $S_i(t)$ to be zero and solve equation (2) for unimers and micelles separately so that we obtain again equation (6) for $\partial c_i/\partial z$. However, the boundary conditions by which K_i is determined are different. For unimers, we have at the surface $c_u = c_u^s$, and at $z = \Delta$ the concentration is equal to c_u^b (the cmc). For the micelles, the concentration at $z \leq \Delta$ is zero, the concentration far away from the surface is equal to the bulk concentration c_m^b. This leads to the following expressions for K_u and K_m

$$K_u = \frac{c_u^b - c_u^s}{\int_0^{\Delta} \exp\left(\frac{-\alpha z^3}{3D_u}\right) dz} = \frac{\left(c_u^b - c_u^s\right) 3 \left(\frac{\alpha}{3D_u}\right)^{1/3}}{\Gamma'\left(\frac{1}{3}, 0, \frac{\alpha\Delta^3}{3D_u}\right)}$$

$$K_m = \frac{c_m^b}{\int_{\Delta}^{\infty} \exp\left(\frac{-\alpha z^3}{3D_m}\right) dz} = \frac{3c_m^b \left(\frac{\alpha}{3D_m}\right)^{1/3}}{\Gamma\left(\frac{1}{3}\right) - \Gamma'\left(\frac{1}{3}, 0, \frac{\alpha\Delta^3}{3D_m}\right)} \qquad (9b)$$

Here Γ' is a generalised incomplete gamma function.[21] The corresponding fluxes are obtained by multiplying $(\partial c/\partial z)_0$ and $(\partial c/\partial z)_\Delta$ with the diffusion coefficients D_u and D_m,

respectively. An additional boundary condition is obtained from the conservation of mass: the flux of unimers at $z = \Delta - \partial z$ equals the flux of micelles at $z = \Delta + \partial z$, where ∂z is infinitesimally small:

$$D_u\left(\frac{\partial c_u}{\partial z}\right)_{z=\Delta} - D_m\left(\frac{\partial c_m}{\partial z}\right)_{z=\Delta} = K_u D_u \exp\left(\frac{-\alpha\Delta^3}{3D_u}\right) - K_m D_m \exp\left(\frac{-\alpha\Delta^3}{3D_m}\right) = 0 \qquad (10)$$

Equations (9) and (10) can be solved numerically. We realise that the solution only gives a very rough description of the fluxes. Nevertheless, it can yield more insight in what occurs in real micellar systems. An impression of what will happen to the flux can already be obtained by taking a glance at equations (9) and (10). In a solution of amphiphilic polymers the ratio between the total polymer concentration and the cmc is very important for the total flux of unimers towards the surface. When the total polymer concentration ($c_p = c_u + c_m$) in the bulk is equal to or lower than the cmc, no micelles are present, Δ is infinitely large and K_m is zero. Consequently, equation (9a) reduces to equation (7) for unimers. Keeping the polymer concentration c_p constant but decreasing the cmc will induce the formation of micelles, Δ becomes finite and the flux of unimers at the surface is given by multiplying $(\partial c_u/\partial z)_0$ with the unimer diffusion coefficient D_u. Equation (9a) has to be used for K_u. A further decrease of the cmc, while keeping c_p constant, will decrease Δ until this distance becomes infinitesimally small. With the help of equation (10) it can be seen that then $K_u D_u = K_m D_m$. In other words, for infinitesimally small cmc and Δ, equation (9b) reduces to equation (7) for micelles, and the flux of *unimers* towards the surface can be approximately described by equation (8) for *micelles.* Summarising the above results for a micellar system with relatively fast exchange between unimers and micelles: when the total polymer concentration is kept constant and the cmc is decreased, the total polymer flux at the surface decreases from a value corresponding to that of a system without micelles ($K_u D_u$) to a value corresponding to the flux of micelles ($K_m D_m$).

An experimentally more accessible quantity is the variation of the polymer concentration at constant cmc. For this situation we plotted in Figure 3 the flux of polymer towards the surface as a function of the total polymer concentration. The flux is scaled by the mean velocity U and the cmc. When the corona of the micelles is repelled by the surface and the exchange rate between micelles and unimers is very low, the flux is determined by the concentration of unimers solely, which results in a constant flux above the cmc (curve c). Even if micelles do not adsorb themselves, their presence can enhance the flux of unimers towards the surface considerably. If the exchange between micelles and unimers is fast curve a is obtained. It is remarkable that this curve shows a higher flux

than the sum of the individual fluxes of unimers and micelles (curve b). The adsorption kinetics of polymers forming non-adsorbing micelles with a fast exchange rate between micelles and solution, is thus faster than that of adsorbing micelles without exchange of unimers with the solution.

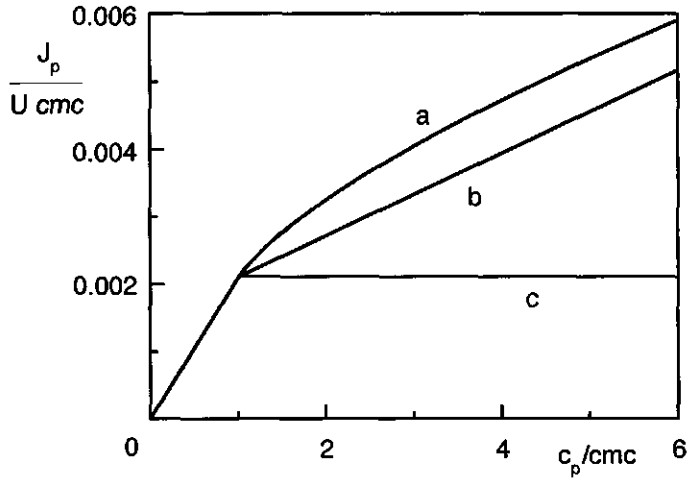

Figure 3. The flux of polymer towards the surface in a stagnation point flow as a function of the total polymer concentration. The flux and the concentration have been scaled by the mean velocity U and the cmc. Curve a was calculated with help of equations (9) and (10) and assumes fast exchange between unimers and micelles, curve b, calculated with equation (8), is for a system without exchange and in which also the micelles adsorb, in curve c it is assumed that no exchange occurs and that micelles do not adsorb. For the diffusion coefficients we assumed: $D_u = 10\ D_m$, and the streaming intensity parameter $\bar{\alpha}$ was taken as 2.

Whether the micelles and unimers can exchange or not depends on the relaxation time τ_r (which is inversely proportional to the exchange rate) and on the thickness of the micellar diffusive layer. The thickness of the diffusive or 'stagnant' layer (δ_u) for unimers is given by the difference in concentration in the bulk and at z = 0, divided by the concentration gradient at the surface. For the diffusive layer thickness of the micelles (δ_m) we have to take the concentration and the concentration gradient at $z = \Delta$ instead of z = 0.

$$\delta_m = \frac{c_m^b - c_m^\Delta}{\left(\frac{dc_m}{dz}\right)_\Delta} \qquad (11)$$

With this equation for the thickness of the diffusive layer we can calculate the time needed to diffuse across this layer, using the relation $\tau_m = \delta^2/2D_m$. If this time is much smaller than τ_r, the micelle will hardly supply new unimers. If τ_m is much larger than τ_r, most micelles will have broken up before they arrive at the surface, thereby enhancing the flux of adsorbing unimers towards the surface. Comparing the experimental initial adsorption rates of a range of polymers differing in chain length, and accordingly with a different τ_m and τ_r, gives us the opportunity to estimate the order of magnitude of the exchange rate constant.

Experimental

Materials

A series of four diblock copolymers of poly(dimethyl siloxane) (PDMS) and poly(2-ethyl-2-oxazoline) (PEtOx) was used. The polymers were kindly given to us by Dr. J.S. Riffle, Virginia State University, USA. The synthesis of these block copolymers proceeded by two steps, as described by Liu et al.[22] In the first step monofunctional poly(dimethyl siloxane) oligomers were synthesised by living anionic ring-opening polymerisation of hexamethyl trisiloxane and end functionalisation with benzyl chloride endgroups. In the second step these oligomers were used to initiate the cationic ring-opening polymerisation of 2-ethyl-2-oxazoline. The structural formula of the block copolymers is given in Figure 4, and some of the characteristics are given in Table 1. The refractive index increment of the block copolymers in solution must be known for reflectometry and is calculated from the values for the two different blocks, where we assumed the refractive index increment to be additive. For the poly(2-ethyl-2-oxazoline) block a value of 0.161 $cm^3\ g^{-1}$ was taken from reference [10]. For the poly(dimethyl siloxane) block we made a rough estimate by using $dn/dc = (n_p - n_s)/\rho_p$,[23] where n_p is the polymer refractive index (1.43)[24], n_s is the refractive index of the solvent (1.333) and ρ_p is the polymer density (970 kg m^{-3}, as determined with a low molar mass silicon oil). For the block copolymers this gives a refractive index increment of 0.15 $cm^3\ g^{-1}$. Polymer stock solutions of 10 g l^{-1} in demineralised water were stored in the refrigerator.

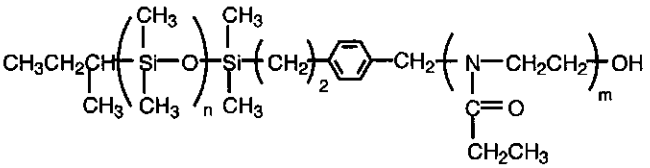

Figure 4 The structural formula of a poly(dimethyl siloxane)–poly(2-ethyl-2-oxazoline), PDMS-PEtOx, diblock copolymer.

Table 1. Some of the characteristics of the PDMS-PEtOx diblock copolymers. The first column gives the sample names in which the target molar mass for the blocks is indicated. The weight percentage PDMS was obtained from element analysis.[20] The number average molar mass of samples 2/8 and 5/20 was determined by ^{29}Si NMR,[29] the molar masses of the other samples were target values during synthesis. In the last two columns the degree of polymerisation of the PDMS block and the PEtOx block are given, respectively.

sample code	wt % PDMS	Mn PDMS (kg mol^{-1})	M_n PEtOx (kg mol^{-1})	N PDMS	N PEtOx
0.5/2	17.2	0.5	2	7	20
2/8	17.0	2.2	10.7	29	108
5/20	19.8	4.8	19.6	65	198
20/80	15.2	20	80	270	808

Light scattering

Dynamic light scattering experiments were done with an ALV light scattering apparatus using a 400 mW Argon ion laser tuned at a wavelength of 514 nm. All measurements were performed at T = 297 K.

Transmission electron microscopy

Cryogenic temperature transmission electron microscopy (cryo-TEM)[25,26] was used to study the structure of the polymeric micelles in solution. These measurements were performed by Dr. P.M. Frederik and Mr. P.H.H. Bomans at the Department of Pathology of the State University of Limburg, The Netherlands. The polymer samples were prepared as follows. A copper TEM grid was dipped in a 10 g l^{-1} polymer solution. The aqueous solution was blotted away from the grid with a strip of filter paper, so that only a thin film

of the sample spanned the holes. The grid was then immediately plunged into liquid ethane near its freezing point (T= 101K). In this way, the thin water film containing micellar particles is vitrified. The sample was transferred under liquid nitrogen to a cryotransfer stage which was inserted into the TEM. Judging from published data it is very likely that the structures seen on the sample grid are the same as those present in the polymer solution.[27]

Reflectometry

The polymer adsorption measurements were performed with a reflectometer in an impinging jet flow-cell as described in detail by Dijt et al.[28] For a stagnation point flow the transport of solute towards the adsorbing surface has been discussed by Dabros and Van de Ven.[20] In the previous section we discussed the influence of the presence of micelles on the flux in the stagnation point. The flux can be described analytically by equation (8a). When the cmc is of the same order of magnitude as the polymer solution concentration c_p the distance Δ must be calculated numerically from the experimental flux with equations (9) and (10). For the calculations some experimental parameters must be known: in our experimental set-up the viscosity $\nu = 10^{-6}$ m^2 s^{-1}, the dimensionless streaming intensity parameter $\bar{\alpha} = 2$, the Reynolds number Re = 10.6, and R = 0.5 mm. For the translational diffusion coefficients we used the values as measured by dynamic light scattering.

In a reflectometer[28] a polarised laser beam is reflected by the substrate in the cell. The substrate is a silicon wafer with a thin oxide layer. The reflected beam is split into its parallel and perpendicular components by a beam splitter; the respective intensities of these components, I_p and I_s, are detected separately and the signal S is calculated as $S = I_p/I_s = f\, R_p/R_s$, where f is an apparatus constant which can be found by calibration, and R_p and R_s are the reflectivities of the parallel and the perpendicular components. Upon adsorption a thin polymer layer is formed with a refractive index differing from that of the substrate and of the solution. The signal changes by an amount ΔS, and the relative change $\Delta S/S_0$ is proportional to the adsorbed amount Γ.

Macroscopically flat silicon wafers with a refractive index n = 3.8 from Aurel GmbH (Germany) were used. By thermal oxidation, we obtained an SiO_2 layer with a thickness of about 110 nm and n = 1.46. A TiO_2 layer with a thickness of about 25 nm and n = 2.33 was deposited by reactive sputtering of Ti in an oxygen atmosphere. This was carried out at Philips Laboratories in Eindhoven, The Netherlands. Strips cut from these wafers were cleaned by oxidation with UV-ozone, and could be cleaned and reused many times.

Results and Discussion

Block copolymer solutions

Dynamic light scattering

The block copolymers of PDMS-PEtOx are amphiphilic with a hydrophobic PDMS block and a hydrophilic PEtOx block. In an aqueous solution we therefore expect these polymers to form micellar structures. Indeed Nagpal et al.[29] found for two of these block copolymers micelles in solution. As in their paper, we also used dynamic light scattering to measure the size of these micelles. In Figure 5 we plot the micellar hydrodynamic radius (R_h) as a function of polymer concentration for the four polymer samples, measured at a scattering angle of 90°. In the data analysis we used the cumulant method described by Koppel[30]. The hydrodynamic radius of the micelles is calculated with the Stokes-Einstein relation for spherical particles. This may not be entirely correct for non-spherical micelles. Nevertheless, it gives a good impression of the size of these scattering particles.

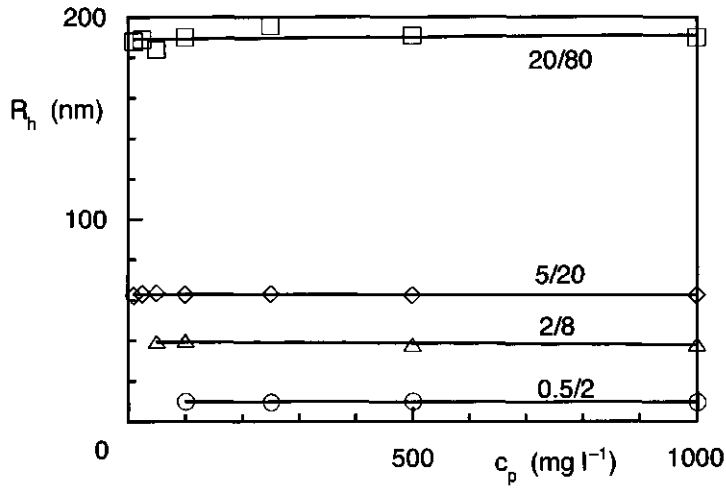

Figure 5. The hydrodynamic radius of four PDMS-PEtOx diblock copolymers in an aqueous solution as a function of the polymer concentration as measured by dynamic light scattering at a scattering angle of 90°.

The measured hydrodynamic radius and the scattered intensity were constant over a period of at least two weeks after preparation of the polymer solutions, indicating that the polymers in these solutions are very likely to have their equilibrium conformation. The average hydrodynamic radius of the PDMS-PEtOx polymer micelles is 10, 39, 63, and 190 nm for 0.5/2, 2/8, 5/20, and 20/80, respectively, and does not change with the polymer concentration. Nagpal et al.[29] found for 2/8 (in their paper denoted as PETOX-PDMS 11k-2k) an average hydrodynamic radius of 81 nm. This large value was attributed to the aggregation of relatively small micelles caused by the association of the PEtOx chains in the coronas. We find for 2/8 a smaller radius, 39 nm, and the particles are rather polydisperse as indicated by a considerable increase of the measured radius at a low scattering angle. For 5/20 Nagpal et al.[29] found an average hydrodynamic radius of 15 nm, considerably lower than the value of 62 nm measured by us. From the very small increase in radius at low scattering angle they concluded that this block copolymer forms rather compact micelles with a narrow size distribution. Again, our sample showed a considerable increase in hydrodynamic radius at decreasing scattering angle, indicating a broad size distribution. The radius reported by Nagpal et al. for compact micelles of 5/20 was 15 nm, which is even smaller than our result for 2/8, which has a lower molar mass. This also indicates that, although the size we find for 2/8 is smaller than reported by Nagpal et al., we probably have larger structures than that of compact single micelles. Also for the PDMS-PEtOx samples 0.5/2 and 20/80 we find a rather broad size distribution.

In order to find out whether there are two populations in the solution, compact single micelles and aggregates of micelles, we also performed a constrained regularisation analysis[31,32] on the light scattering data (with the regularised continuous inversion algorithm CONTIN). With this method a bimodal distribution can be revealed. However, this analysis showed only one peak at about the same radius as found by the cumulant analysis. Thus the solution contains only one population of rather polydisperse micelles. We cannot exclude the possibility that compact micelles are slightly aggregated in larger structures. However, it is also possible that the micelles have a non-spherical structure and are very polydisperse.

Transmission Electron Microscopy

The structure of the micelles in solution was investigated with cryo-TEM. The process of sample vitrification is very fast (of order 10 μs) which makes it very likely that the structures in the aqueous solution are kept in their original state. In Figure 6 we show the TEM pictures of 10 g l^{-1} aqueous PDMS-PEtOx diblock copolymer solutions of 2/8 (a), 5/20 (b), and 20/80 (c). For 0.5/2 the picture did not show any structure, indicating that particles are either absent or too small to be detected by cryo-TEM (i.e., the radius is smaller than a few nm). The density of PEtOx chains in the solubilised corona of the micelles is relatively low and this makes it unlikely that this corona can be seen on the TEM pictures.[33,34] The structures we see are therefore mainly the parts containing predominantly hydrophobic PDMS. In Figure 6a we see for 2/8 more or less spherical structures with a radius between 8 and 16 nm; the size distribution of the structures is rather broad. Polymer 5/20 gives spherical structures with a radius varying from 12 to 20 nm (Figure 6b). In Figure 6c we see that 20/80 forms oval structures with radii varying from 20 to 40 nm, however also long rods with a thickness of 30 nm are present. For none of the samples we see clusters of compact micelles. The structures are smooth and do not show dark spots which could be attributed to the existence of such small and compact micelles within one aggregate. The total size of the PDMS-PEtOx micelles is rather large if we take in account that the contribution of the PEtOx chains is not seen.

The size as measured by dynamic light scattering is much larger than found by TEM. This is partly due to the fact that TEM does not show the corona of the micelles. Also very important is the polydispersity of the structures seen by TEM. In light scattering the contribution of large structures is generally much higher than that of small objects. The existence of a few large structures can increase the measured average hydrodynamic radius considerably. For 20/80 we even find rods in solution. These long rods have a low diffusion coefficient and increase the radius as measured by dynamic light scattering substantially. The large structures may, among other reasons, arise from the fact that water is not a very good solvent for PEtOx: the solution show an LCST at 329 K and the solvency parameter χ at room temperature is 0.48,[35,36] which is rather close to phase separation conditions.

Figure 6. Cryo transmission electron micrograph pictures of 10 g l^{-1} aqueous PDMS-PEtOx diblock copolymer solutions of 2/8 (top), 5/20 (middle) and 20/80 (bottom). On the pictures 1 cm is equal to 80 nm.

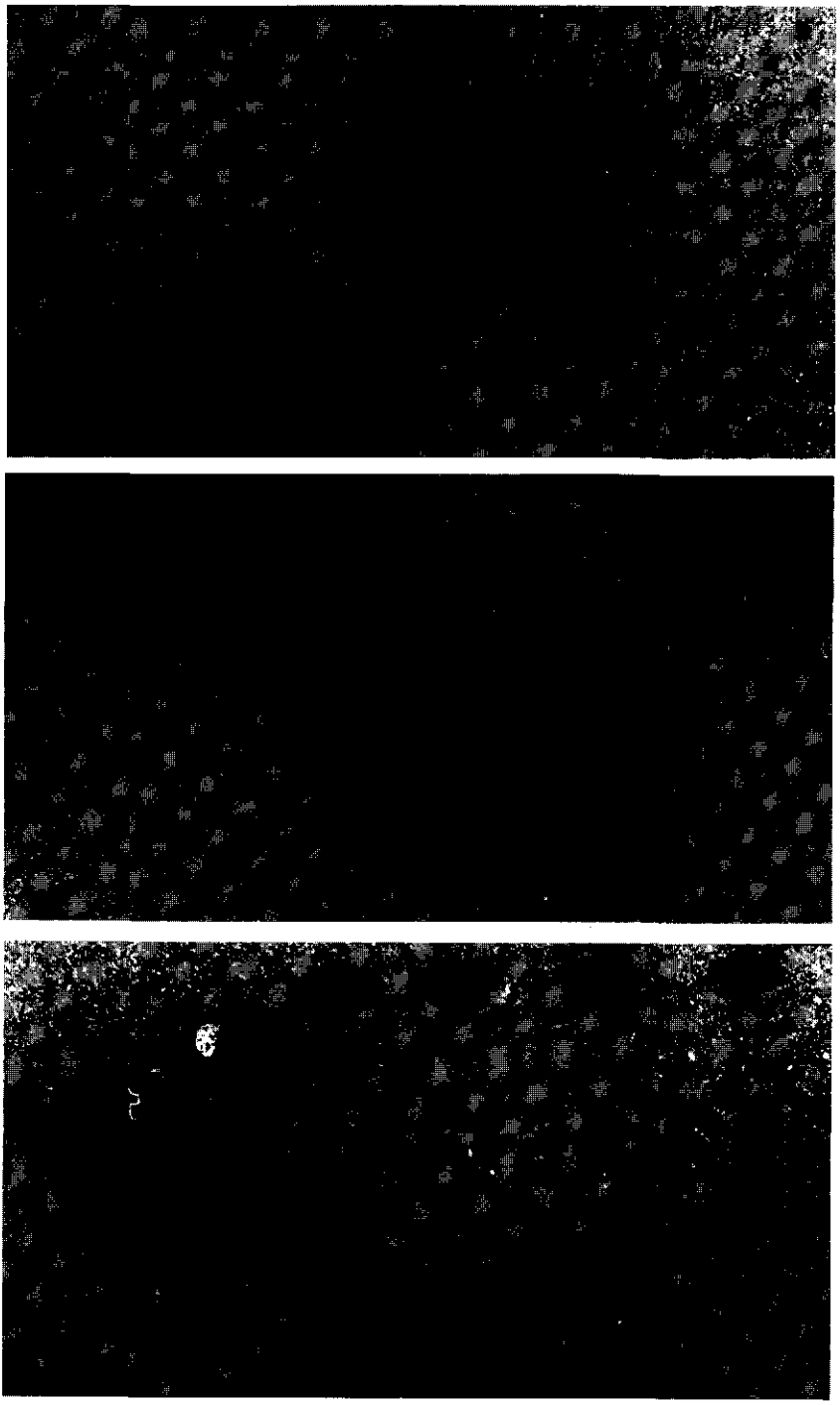

Scattered intensity

The critical micellisation concentration (cmc) of the block copolymer solutions can in principle be determined from a plot of the scattered light intensity as a function of the polymer concentration. This plot should have a linear part, the intersection of which with the concentration axis is at the cmc. Such a plot is given in Figure 7 for all polymer samples at a scattering angle of 90°.

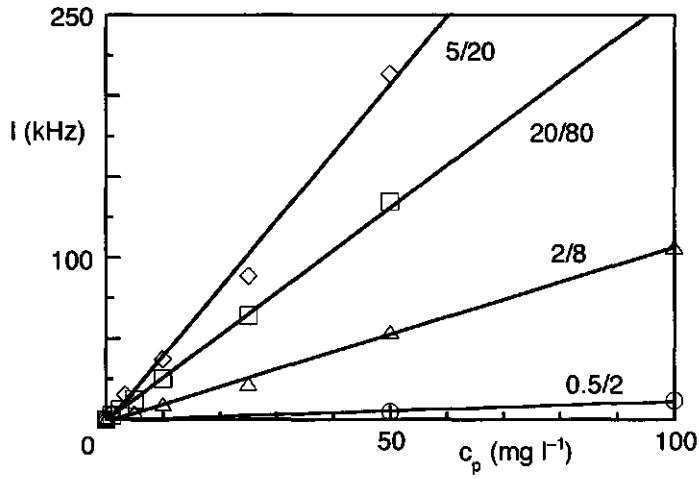

Figure 7. The scattered intensity of PDMS-PEtOx diblock copolymers in an aqueous solution as a function of the polymer concentration, measured by dynamic light scattering at a scattering angle of 90°.

The scattered intensity of the solution with the smallest polymer (0.5/2) is low and the lowest concentration at which we could do reliable measurements was 50 mg l^{-1}. For 2/8 the lowest concentration was 5 mg l^{-1}. For the two block copolymer samples with the highest molar mass (5/20 and 20/80) the lowest concentration was 1 mg l^{-1}. It can be seen that the intensity is a linear function of the polymer concentration for all polymers used. The intersection with the concentration-axis, which gives the cmc, is, within experimental error, at zero polymer concentration. The cmc of these polymer solutions is thus lower than the lowest concentration which gave reliable values: 50, 5, 1, and 1 mg l^{-1} for 0.5/2, 2/8, 5/20, and 20/80, respectively. Liu et al.[22] measured the surface tension of a solution of 0.5/2 as a function of the concentration. From these measurements they

obtained a cmc value of approximately 70 mg l^{-1}. This value is higher than the upper limit of the cmc from our light scattering data. For polymer solutions the determination of the cmc from surface tension measurements is problematic. As the diffusion coefficient of polymers is much lower than that of low molar mass surfactants, the time needed to obtain equilibrium can be rather large so that equilibrium between the solution and the surface is not guaranteed. For light scattering, equilibrium with the surface is not required. Also, it is not a problem to wait long before doing the measurements.

It is remarkable that the scattered intensity of 5/20 is higher than that of a 20/80 solution. This was expected to be just the reverse, as the scattered intensity is a function of the size of the scattering particle. The form factor of the micelles is not responsible for this result as we did not find minima and maxima as a function of the scattered angle, which is probably due to the polydispersity of the micelles. However, the scattered intensity at a certain angle is a complicated quantity in which not only the radius of the particles but also the difference between the refractive index of the scattering particle and that of the solvent plays an important role.[37] Increasing the difference between the refractive indices will increase the scattered intensity. The radius of 20/80 is three times larger than the radius of 5/20, nevertheless, the scattered intensity is lower. This may be explained by compacter micelles of 5/20 molecules compared to the aggregates formed by 20/80. The latter forms both oval particles and rodlike structures, as could be seen from the TEM-picture in Figure 6c. The rods decrease the diffusion coefficient (and hence increase the Stokes radius derived from it) but, on the other hand, decrease the average polymer density which, presumably, reduces the average refractive index. As a result, the scattered intensity could be relatively low, even when the hydrodynamic radius is rather large.

Adsorption

As we have seen in the previous section, the diblock copolymers used in this study form micellar structures in an aqueous solution. The corona of the micelles is formed by PEtOx chains whereas the core consists of PDMS, which forms a melt of flexible chains because the glass-transition temperature of PDMS (T_g = 146 K)[24] is well below room temperature. The micelles are rather large polydisperse structures. Before we turn to the adsorption of the block copolymers, we first investigate the behaviour of both homopolymers at a silica and a titania surface.

From a previous study[10] and from literature[35] we know that the homopolymer PEtOx adsorbs onto silica. We found an adsorbed amount of 0.58 mg m^{-2} for a molar mass of

6000. In the present work we also considered the system PEtOx/titania, but we did not observe any adsorption in this case. The hydrophobic PDMS is reported to have affinity for silica,[38] but for its interaction with titania we could not find any results in the literature.

For the micelles formed by block copolymers of PDMS-PEtOx this means that in the case of silica both the PEtOx corona and the PDMS core have surface affinity. This will cause a competition between PEtOx and PDMS for surface sites. In equilibrium the block with the highest adsorption energy will displace the other one. For these amphiphilic polymers the hydrophobicity of the PDMS block is an extra driving force which favours the adsorption of PDMS. For the polymer/silica system it therefore seems most likely that in the equilibrium situation the PDMS block will adsorb and the PEtOx block will remain in solution. In the case of titania the PEtOx corona does not have affinity for the surface. When the PDMS has affinity, the equilibrium adsorbed state will be similar to that on silica: an adsorbed block copolymer layer with a molten layer of PDMS in contact with the surface, and PEtOx blocks protruding into the solution. Because PEtOx adsorbs on silica but not on titania, we envisage different scenarios for the build-up of the adsorbed layer on either surface. Measurements of the kinetics of adsorption can tell us which scenario is adequate, and provides information about the adsorption mechanism of amphiphilic block copolymers.

Adsorption curves of the block copolymers

We measured the adsorbed amount as a function of time for all four PDMS-PEtOx diblock copolymer samples onto silica and titania with reflectometry. The adsorption curves for 0.5/2 on silica and titania are given in Figures 8a and 8b, for 2/8 in Figures 8c and 8d, for 5/20 in Figures 8e and 8f, and for 20/80 in Figures 8g and 8h, respectively.

Figure 8. The adsorption of PDMS-PEtOx block copolymers onto SiO_2 and TiO_2 from aqueous solution as a function of time. The polymer concentration was 10 or 40 mg l^{-1} and is indicated in the plot. The results for 0.5/2 on silica and titania are given in a and b, respectively, for 2/8 in plot c and d, for 5/20 in plot e and f, and for 20/80 in plot g and h. The meaning of the different regimes shown in plot g and h is given in the text.

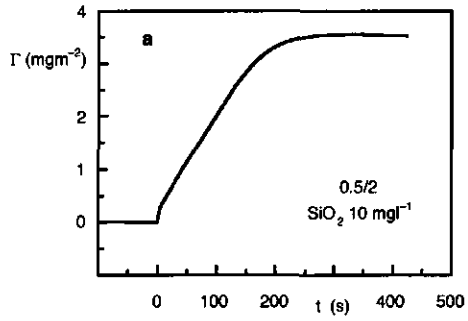
a
Γ (mgm⁻²)
0.5/2
SiO2 10 mgl⁻¹
t (s)

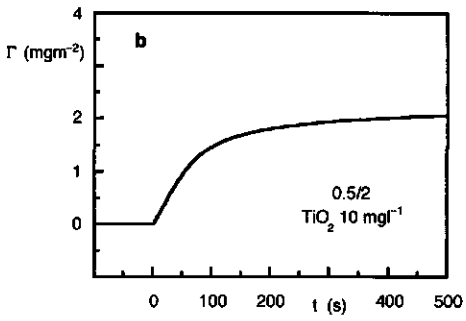
b
Γ (mgm⁻²)
0.5/2
TiO2 10 mgl⁻¹
t (s)

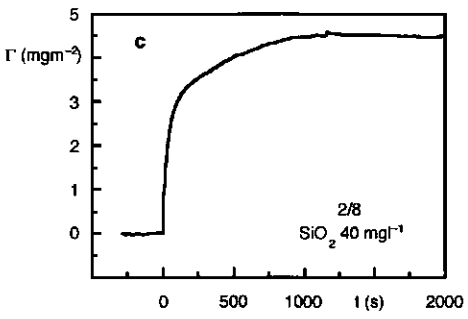
c
Γ (mgm⁻²)
2/8
SiO2 40 mgl⁻¹
t (s)

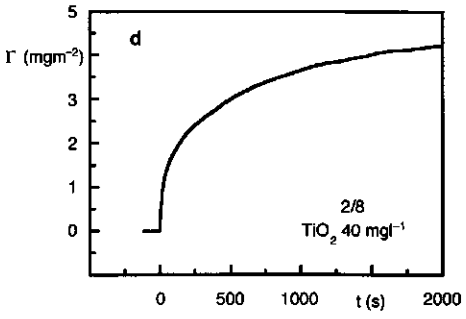
d
Γ (mgm⁻²)
2/8
TiO2 40 mgl⁻¹
t (s)

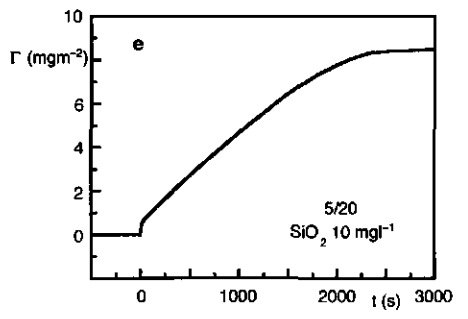
e
Γ (mgm⁻²)
5/20
SiO2 10 mgl⁻¹
t (s)

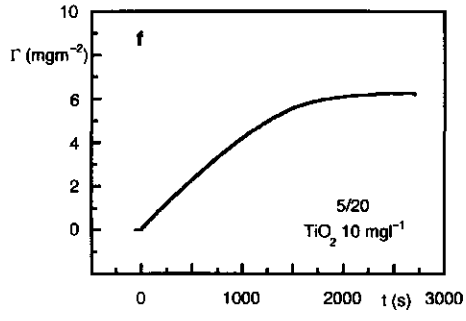
f
Γ (mgm⁻²)
5/20
TiO2 10 mgl⁻¹
t (s)

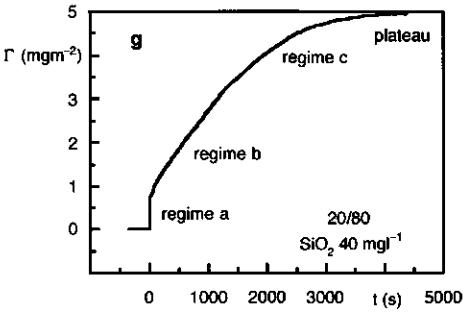
g
Γ (mgm⁻²)
plateau
regime c
regime b
regime a
20/80
SiO2 40 mgl⁻¹
t (s)

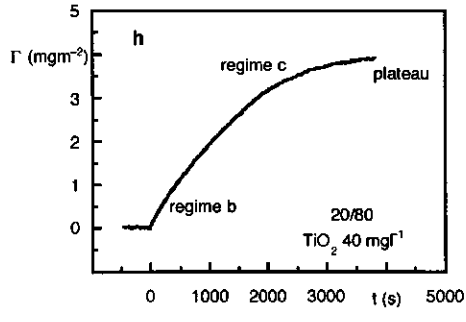
h
Γ (mgm⁻²)
regime c
plateau
regime b
20/80
TiO2 40 mgl⁻¹
t (s)

In order to discuss the different features of the adsorption curves, we first take a look at Figure 8g, for 20/80 onto silica. Several different regimes can be distinguished in one adsorption curve. In the first part of the curve the adsorption increases rapidly and linearly with time until an adsorbed amount of around 0.6 mg m^{-2} is reached (*regime a*). The slope of the adsorption curve then decreases rather abruptly to a new value. In this second regime (*regime b*) the adsorbed amount increases again more or less linearly with time up to a very high adsorbed amount, where we find a third regime (*regime c*) with a decreasing slope until a *plateau* is reached.

Figure 8h shows the corresponding adsorption curve on titania. The shape of this curve is different from that found on silica. The adsorption increases approximately linearly up to a rather high adsorbed amount (*regime b*), after which the slope decreases (*regime c*), and finally a *plateau* is reached. It is remarkable that the initial adsorption rate on titania is, on first approximation, equal to the adsorption rate in regime b on silica. This first regime on titania is therefore denoted regime b. Regime a, which was found on silica, is entirely missing on titania.

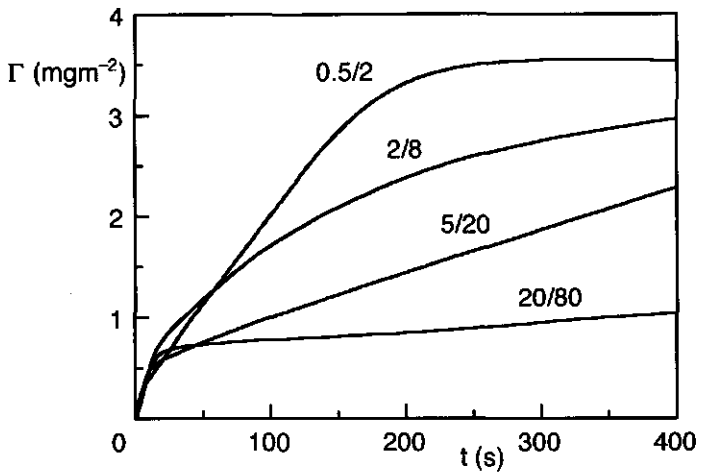

Figure 9. The first stages of the adsorption curves of four PDMS-PEtOx block copolymers onto silica as measured with reflectometry. The concentration of 0.5/2 and 5/20 was 10 mg l^{-1}, for 2/8 and 20/80 the measurements were done at 40 mg l^{-1} but the curves were rescaled to a polymer concentration of 10 mg l^{-1}.

In Figure 9 we enlarged the first stages of the adsorption curves of all four diblock copolymers on silica, emphasising regime a and (the beginning of) regime b. For all samples, the constant adsorption rate in regime a is the same up to an adsorbed amount between 0.2 (for 0.5/2) and 0.6 mg m^{-2} (for 20/80). There is a fairly sharp transition to regime b. The drop in adsorption rate from *a* to *b* is most pronounced for the diblock copolymer with the highest molar mass.

As is seen from Figures 8 and 9 the shape of the adsorption curves differs for the four polymer samples and depends also on the substrate. For 0.5/2 on silica we see that regime b lies between 0.4 and 3.0 mg m^{-2}. The adsorption rate then decreases rather abruptly in a narrow regime c; at the plateau of the curve the adsorbed amount is constant at 3.5 mg m^{-2}. On titania, regime b extends up to an adsorbed amount of approximately 1.0 mg m^{-2}. From this point, the adsorption rate decreases slowly, i.e., regime c is very wide. In the plateau the adsorbed amount is considerably lower than on silica (1.7 mg m^{-2}).

The shape of the adsorption curves of 2/8 is more rounded, the linear regimes are short and in most parts of the curve the adsorption rate is decreasing. This could be an indication that the polymers or the micelles are very polydisperse. The adsorbed amounts are higher than found for the short chains. The difference between the adsorbed amounts in the plateau on silica and titania is small: 4.9 and 4.2 mg m^{-2}, respectively.

The adsorption curve of 5/20 shows an extremely long regime b. On silica, the adsorption rate is constant up to an adsorbed amount of 6 mg m^{-2}. In regime c the adsorption rate decreases smoothly and the plateau is found to be around 8.5 mg m^{-2}. On titania, the adsorption increases linearly up to about 4 mg m^{-2} and the adsorbed amount in the plateau of the curve is 6.3 mg m^{-2}.

The shape of the adsorption curves of 20/80 on silica and titania is slightly rounded. Regime b extends up to approximately 3 mg m^{-2} for both silica and titania. The decrease of the adsorption rate in regime c is rather slow and the plateau value is only reached after a very long adsorption time, or with the use of a high polymer concentration. The adsorbed amounts in the plateau approximately 5.0 mg m^{-2} on silica and 3.7 mg m^{-2} on titania, respectively. The adsorbed amounts in the plateau of the adsorption curves on silica and titania for each of the polymers are collected in Table 2.

Table 2. The adsorption rate constants in regime b of the adsorption curves on silica and titania for the PDMS-PEOx diblock copolymers. In the fourth column the theoretical flux of micelles towards the surface is given, as calculated with equation (8). We assume that the total polymer concentration and the micelle concentration are equal (i.e., cmc is very small) and used the diffusion coefficient as measured by dynamic light scattering. The fifth and the sixth column show the plateau adsorbed amounts. In the last two columns the micellar diffusive layer thickness δ_m and the time τ_m a micelle needs to diffuse accross this layer are given. All measurements were done in an aqueous solution with a pH between 5 and 6 and a temperature of 295 K. The polymer concentrations were varied between 2 and 50 mg l^{-1}.

sample PDMS-PEtOx	$\frac{d\Gamma/dt}{c_p}$ regime b SiO_2 (10^{-6} m s^{-1})	$\frac{d\Gamma/dt}{c_p}$ regime b TiO_2 (10^{-6} m s^{-1})	J_m/c_p (10^{-6} m s^{-1})	Γ_{pl} SiO_2 (mg m^{-2})	Γ_{pl} TiO_2 (mg m^{-2})	δ_m (10^{-6} m)	τ_m (s)
0.5/2	1.75	1.82	3.62	3.5	1.7	6.6	0.9
2/8	1.53	1.70	1.46	4.9	4.2	4.2	1.4
5/20	0.40	0.45	1.06	8.5	6.3	3.5	1.7
20/80	0.038	0.056	0.508	5.0	3.7	2.5	2.4

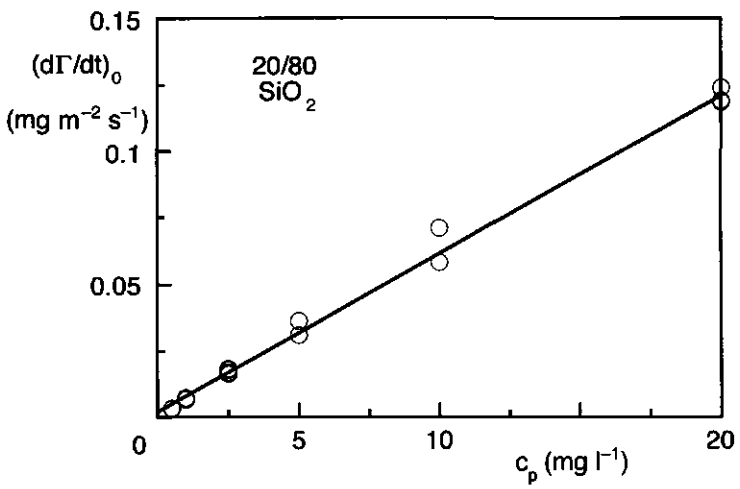

Figure 10. The initial adsorption rate $(d\Gamma/dt)_0$ on silica (in regime a) as a function of the polymer concentration for 20/80. The linear fit has a slope of $6.0*10^{-6}$ m s^{-1}.

Regime a

The adsorption rate in regime a for 20/80 is plotted in Figure 10 as a function of the polymer concentration in solution. It is clear that the initial adsorption rate increases linearly with concentration. The slope of the initial adsorption rate as a function of concentration (the rate constant) is $6.0*10^{-6}$ m s^{-1}. Also for the other block copolymers we found that the initial adsorption rate increases linearly with the polymer concentration; the adsorption rate appeared to be approximately equal for all samples (between 6.0 and $7.3*10^{-6}$ m s^{-1}).

A first attempt to interpretation is to ascribe the initial part of the adsorption curve on silica to the adsorption of micelles with a PEtOx corona that has affinity for the surface. This would also explain the absence of this regime in the adsorption curve on titania, as the PEtOx chains in the corona have no affinity for titania. We would then expect the initial rate to depend on the diffusion coefficient of the micelles. However, we do not find such a relation. Another argument against the adsorption of micelles in the initial part was obtained when we filtered the solution of the largest diblock copolymer 20/80 through an 0.22 μm millipore filter. Large micelles were no longer present. However, when we measured the adsorption of this sample onto silica, we found an adsorption curve with the same initial adsorption rate as for the unfiltered solutions. However, the adsorbed amount in the plateau was only 0.7 mg m^{-2}. This indicates that not micelles but something else adsorbs in the initial part of the adsorption curve on silica. As the cmc is very low it is most probable that there is some contamination in our samples that adsorbs on silica and not on titania. If the contamination is a low-molar-mass material, low concentrations give already a considerable flux towards the surface, comparable to the adsorption rate measured in regime a. So far, we have not been able to determine the exact nature of the contamination.

Regime b

Regime b in the adsorption curves on silica and on titania is linear in the polymer concentration. From Figures 8 and 9 it is seen that the adsorption rate in this regime depends on the type of polymer. For 20/80 this adsorption rate is extremely low. We plot this rate as a function of polymer concentration in Figures 11a and 11b for silica and titania, respectively. As the adsorption rate for this polymer is very low its determination is somewhat inaccurate. For the smallest polymer, 0.5/2 the rate is much higher and these results are given in Figure 11c and 11d. Within experimental error the same slope is found for regime b on both surfaces. From Figure 11 we determined the adsorption rate constants in regime b for 0.5/2 and 20/80. For the other two polymer samples the

rate constants were obtained in a similar way. The results are given in Table 2. For comparison we also included the theoretical flux as calculated for micelles with equation (8a), assuming that only micelles exist in solution (which is approximately correct when the cmc is low). In the same table we also give the adsorbed amounts in the final plateau.

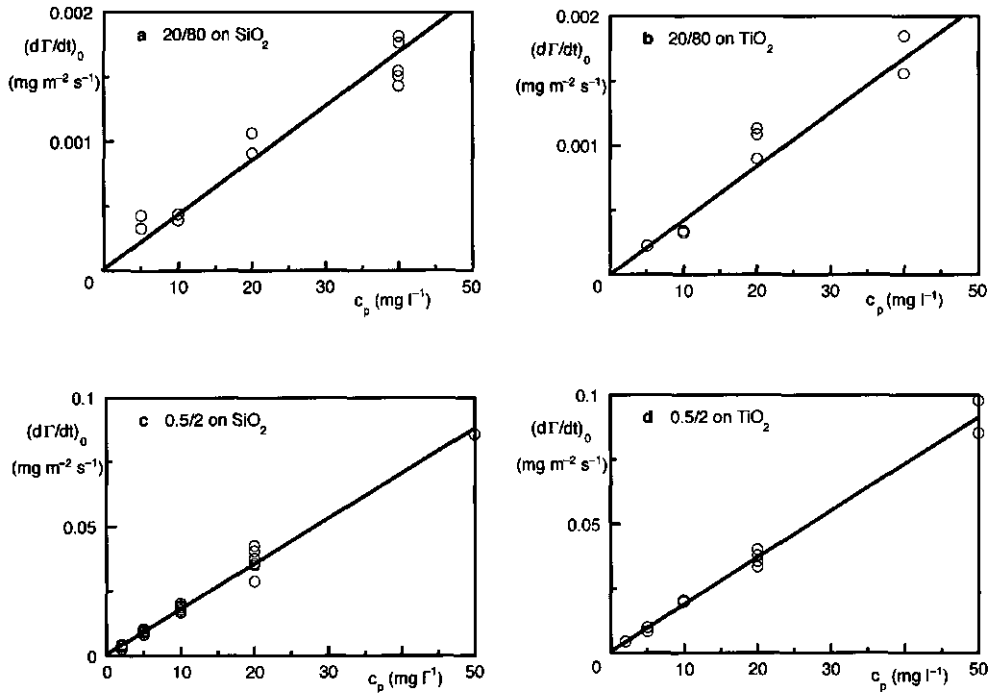

Figure 11. The adsorption rate in regime b for the largest polymer (20/80) and the smallest polymer (0.5/2) on both silica and titania as a function of the polymer concentration.

Adsorption on titania

Some interesting conclusions can be drawn from the adsorption kinetics. The adsorption from micellar solutions of the block copolymers onto titania, for which surface the corona has no affinity, most likely proceeds by the adsorption of free unimers[7]. The adsorption experiments were all performed well above the cmc, with the possible exception of the smallest polymer, where the concentration may be of the order of the cmc. If the exchange rate between micelles and unimers is relatively slow, we expect the initial adsorption rate in regime b to be very low. The rate would then be determined by the

cmc and would not vary with the total polymer concentration. However, we see in Figures 11b and d that the adsorption rates depend linearly on the concentration for all polymer samples. This result must be attributed to the presence of micelles, which supply new unimers, thereby contributing to the adsorption rate. Thus, the exchange of free unimers between micelles and solution must be taken into account.

When we take a look at Figure 3, which gives the theoretical flux of polymer towards the surface, we see that an inflection point is found at the cmc. The experimental results for titania in Figure 11 do not show such an inflection point, indicating that all polymer concentrations were indeed above the cmc, and that the cmc of all four polymer samples is below 2 mg l^{-1}. For the three largest polymers this was already known from the dynamic light scattering data, but for the smallest polymer 2 mg l^{-1} is considerably lower than the upper limit that we determined from our light scattering data.

For a relatively fast exchange of unimers between micelles and solution, we can describe the flux of polymer towards the surface with equation (8a) for micelles, curve b in Figure 3. When we compare the experimental adsorption rate constants on titania with the theoretical rate constant for the flux of micelles towards the surface, we see that for 20/80 the experimental value is about ten times lower than the calculated flux of micelles. For polymers 0.5/2 and 5/20 we find a value about half the theoretical flux. For polymer 2/8 the experimental value is close to the theoretical flux. However, this polymer showed a rather rounded adsorption curve, which indicates that the sample is rather polydisperse. Therefore, the experimental flux is likely to be dominated by the small micelles whereas the theoretical flux was calculated from the average diffusion coefficient as measured by dynamic light scattering, where large micelles are relatively more important. We realise that the values of the theoretical and experimental fluxes are not really quantitative. Roughly speaking, we can state that the experimental fluxes of the three smallest polymers is comparable to the theoretical flux, whereas the experimental flux of the largest polymer is an order of magnitude lower than the theoretical one. Thus, the exchange of unimers between micelles and solution must be relatively fast for the three polymers with the lowest molar mass, whereas for 20/80 the exchange is slower than the time needed to diffuse across the diffusive layer. Most micelles arrive at the surface before they have fallen apart and, as the corona does not have affinity for the titania surface, they will not contribute to the adsorption.

Micellar relaxation time

The thickness of the micellar diffusive layer δ_m can be calculated from equation (11b). For a concentration much higher than the cmc, Δ approaches zero, and δ_m can be

calculated easily. In Table 2 the thickness of the micellar diffusive layer for all polymer systems has been included. The thickness is between 2.5 μm for the large micelles of 20/80 and 6.6 μm for the small micelles of 0.5/2. From these values and the relation $\tau_m = \delta_m^2/2D_m$, it is now possible to estimate the average time τ_m a micelle needs to diffuse across this layer. This time has also been included in Table 2. The micellar relaxation time (τ_r) is the time a micelle needs to break up in free polymers. The three smallest polymers have a micellar relaxation time τ_r that is smaller than τ_m, as these micelles break up before they arrive at the surface. The largest polymer has a micelle relaxation time τ_r that is larger than the micellar diffusion time τ_m; we estimate it to be a few tens of seconds. The high relaxation time for the large micelles of 20/80 can be explained by the high molar mass of this polymer. The hydrophobic block has to diffuse out of the core into a non-favourable environment and to travel through the corona before it can enter the solution. By increasing the molar mass the barrier becomes higher due to the larger hydrophobic block for which the chance to 'escape' is much lower. Since the molar mass of the largest polymer is forty times higher than that of the smallest polymer, the micellar relaxation will be several orders of magnitude slower.[19] The time to diffuse across the diffusive layer depends also on the molar mass but this dependence is much weaker. In a plot of τ_m and τ_r as a function of molar mass for the polymers in this study these curves would probably cross.

Another factor contributing to the barrier is the viscosity of the micellar core. In our system the core is a true melt of flexible PDMS. Many stiffer hydrophobic polymers rather form a glassy core, in which the polymer motion is frozen. The exchange of free polymers between micelles and solution will then be extremely slow and equilibrium may not be attained. By changing the solvent conditions one can plasticise such a glassy core. The effect of solvent has been studied by Dewalt et al.[39] for polystyrene-poly(ethylene oxide) block copolymer adsorption onto polystyrene particles from an aqueous solution. In pure water they did not observe adsorption but by adding some THF, a good solvent for the PS core, they found that adsorption did occur. In the glassy state the adsorption from the micelles was probably kinetically blocked.

Adsorption on silica

For the silica surface the corona of the micelles can also attach to the surface. However, as we have seen from the results on titania, the micelles of the three smallest polymers will have broken up into unimers before they arrive at the surface. Hence, for the three smallest polymers the adsorption on silica also proceeds by the attachment of unimers. For the largest polymer the exchange of unimers between micelles and surface is not

fast enough, and part of the micelles will be able to reach the surface. These intact micelles can adsorb with their corona and the polymer could form a mixed layer of adsorbed unimers and micelles. One would then expect that the adsorption rate equals the theoretical flux of micelles towards the surface. The adsorption rate in regime b for 20/80 on silica would then be different from that found on titania. However, from Table 2 we see that this does not hold: the experimental rate on silica is much slower than the theoretical flux of micelles and equals that of titania. Apparently, the corona is inhibited from adsorbing to the surface. A possible explanation is the existence of the contamination in the polymer sample, as mentioned before. This contamination gives rise to regime a, and probably forms a thin layer which inhibits the adsorption of the PEtOx corona. The hydrophobic block of the unimers has a very high affinity for the surface and can displace the layer of contaminant molecules. As a consequence, the adsorption rate is, as for the adsorption on titania, governed by the exchange rate between micelles and unimers.

Adsorbed amount

The plateau adsorbed amount on silica is higher than on titania. This is an indication that the PDMS block has a higher affinity for silica than for titania. The adsorption curves on titania are more rounded than on silica, and especially regime c is longer. In this regime a barrier is formed by the brush of PEtOx chains. Although the lateral pressure in this brush may not be very high, as water is almost a theta solvent for the PEtOx chains, the brush could reduce the kinetics of adsorption considerably. However, the adsorbed amount on silica is higher than on titania, implying that the brush is denser and has a higher lateral pressure. We would then expect that regime c is wider for silica than for titania. As this is not the case the adsorption kinetics is more likely to be governed by the adsorption energy at the surface, rather than by the steric barrier of the brush.

The plateau adsorbed amounts are much higher than normally found for homopolymers. The presence of a long non-adsorbing block, in combination with a strongly anchoring block, gives rise to a real anchor-buoy structure with a high adsorbed amount, which is typical for diblock copolymer adsorption. For a constant composition, the adsorbed amount is expected to increase with the total length of the block copolymer.[3,5] For the three polymers with the lowest molar mass this trend is followed, but the plateau adsorbed amount for the largest polymer 20/80 is considerably lower than for sample 5/20. Probably the maximum adsorbed amount is not yet reached for the longest polymer. The barrier formed by the PEtOx chains of adsorbed molecules in this case extends over a very long distance. Although the density of this brush is less than for the

brush of the smaller polymer, the long distance over which unimers have to diffuse constitutes an enormous kinetic barrier. It can therefore take a very long time before equilibrium is obtained. Reflectometry is not suitable to measure on time scales more than a few hours, so that for such long polymers another technique should be used to study the equilibrium state.

Desorption

Desorption of the polymers upon dilution by pure solvent was also studied. For the three polymers with the highest molar mass the desorption was negligible. However, the desorption of 0.5/2 was rather large. In Figure 12 we plotted the desorption of this polymer upon dilution on silica and on titania. The adsorbed amount is scaled to the adsorbed amount at the plateau, the time-axis runs from the onset of desorption.

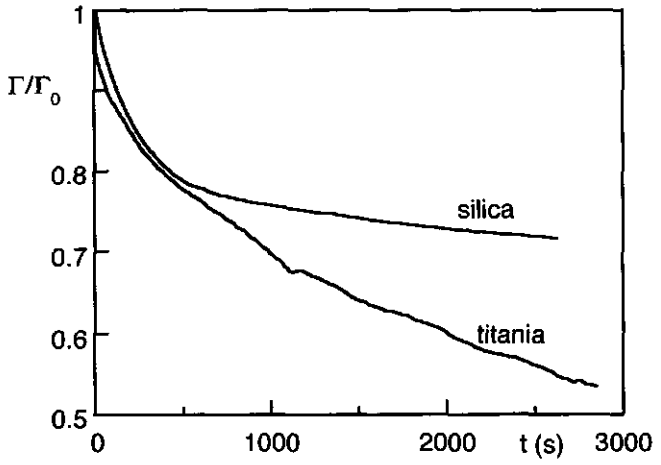

Figure 12. Desorption of 0.5/2 upon dilution with water from silica and titania.

The desorption on silica and titania is relatively fast until about 20 percent of the material has desorbed; from that point on the desorption behaviour on both surfaces is different. On titania the desorption continues, although the desorption rate gradually decreases. On silica the desorption rate falls rapidly and the adsorbed amount becomes almost constant. Nevertheless, even after 40 minutes polymers still desorb from both surfaces. The desorption from silica has roughly a log t dependence whereas the desorption from titania seems to be faster than logarithmically. The fact that the desorption rate on titania

is higher than on silica points to a stronger interaction of the polymer with silica. This interaction must be attributed to the hydrophobic block: in the saturated layer the hydrophilic blocks are not in contact with the surface. This conclusion is in agreement with the lower adsorbed amounts on titania, from which we already deduced that the adsorption energy on silica is higher than on titania.

The behaviour of the diblock copolymer 0.5/2 is similar to that of a surfactant. Because of the small number of segments surfactant molecules can easily be desorbed upon dilution[40]. The hydrophobic PDMS block contains only seven siloxane segments and the hydrophilic PEtOx block consists of 20 segments. This is more than for most common surfactants, but this sample is not really polymeric either. The intermediate behaviour between that of a small surfactant and a long polymer gives a very slow desorption of the molecule upon dilution.

Conclusions

In this paper we considered the solution and adsorption behaviour of amphiphilic diblock copolymers. Four diblock copolymers of hydrophobic poly(dimethyl siloxane) (PDMS) and hydrophilic poly(2-ethyl-2-oxazoline) (PEtOx) were studied. The block copolymers only differ in their total molar mass; the ratio PEtOx/PDMS was approximately constant (block length ratio between 5 and 6). In an aqueous solution these block copolymers form large polydisperse micelles. For the polymer with the highest molar mass we found oval micelles but also rods in the solution, as revealed with cryo-TEM. The critical micellisation concentration could not be determined but is lower than 2 mg l^{-1}.

Both blocks of the copolymers have affinity for silica and only the hydrophobic block has affinity for the titania surface. The adsorption of these polymers onto macroscopically flat oxide surfaces was studied with reflectometry in a stagnation point flow cell. We were able to follow the time-dependent adsorption up to several hours after the onset of adsorption. Apart from a small contribution of a low-molar-mass contaminant to the curve on silica, the adsorption curves on silica and titania show similar features. The contaminant prevents the corona of the micelles from adsorbing onto silica, so that on both surfaces the adsorption behaviour is governed by the adsorption of the hydrophobic blocks The adsorption kinetics are clearly affected by the exchange rate between micelles and free polymers. For the three smallest molar masses the exchange rate is fast compared to the time a micelle needs to diffuse across the diffusive layer. Before the micelles arrive at the surface they have already broken up into free polymers. Because the cmc is very low, the experimental adsorption rate is determined by the diffusion of

micelles towards the surface. For the longest polymer this is not the case: the exchange of unimers between micelles and solution is now relatively slow, the micelles do not adsorb directly, and the adsorption rate is retarded by the slow exchange process. We estimated the micellar relaxation time, i.e., the time a micelle needs to break up. For the largest polymer we found the relaxation time to be in the order of a few tens of seconds. The other polymers have a micellar relaxation time that is shorter than roughly one second.

In the initial regime of the adsorption curve the adsorption rate is diffusion limited (for the three smallest polymers) or exchange rate limited (for the largest polymer). This leads to a linear increase of the adsorption as a function of time. When the brush begins to develop, a steric barrier is created for new incoming polymer molecules. In principle, this could give rise to rather slow adsorption kinetics. However, on silica we find adsorption curves with a rather fast transition from the (second) linear regime to the plateau. For titania the transition that is more gradual, which points to a higher barrier for the adsorption. This is a surprising result as one would expect the barrier to be independent of the adsorption energy. The adsorbed amounts in the plateau of the adsorption curves are very high, as expected for strongly adsorbing diblock copolymers with a relatively short anchor block. The adsorption kinetics of the largest polymer are very slow; in this case the equilibrium adsorbed amount is probably not reached within the time scale of the measurements (up to several hours). The adsorbed amount on silica is considerably higher than on titania. The PDMS block is more strongly anchored to the silica surface, so that the brush density can become higher than on titania. Upon dilution with water, the three largest polymers do not desorb at all, only the shortest polymer molecule (with only 7 anchor segments) shows a considerable desorption. The desorption from titania is higher than from silica, in line with the lower adsorption energy on the former surface.

References

(1) Fleer, G. J.; Cohen Stuart, M. A.; Scheutjens, J. M. H. M.; Cosgrove, T.; Vincent, B. *Polymers at Interfaces*; Chapman & Hall: London, 1993.

(2) Napper, D. H. *Polymeric stabilisation of colloidal dispersions*; Academic Press: London, 1983.

(3) Marques, C. M.; Joanny, J. F.; Leibler, L. *Macromolecules* **1988**, *21*, 1051.

(4) Marques, C. M.; Joanny, J. F. *Macromolecules* **1989**, *22*, 1454.

(5) Van Lent, B.; Scheutjens, J. M. H. M. *Macromolecules* **1989**, *22*, 1931.

(6) Evers, O. A.; Scheutjens, J. M. H. M.; Fleer, G. J. *J. Chem. Soc., Faraday Trans* **1990**, *86*, 1333.

(7) Johner, A.; Joanny, J. F. *Macromolecules* **1990**, *26*, 5299.

(8) Kopf, A.; Baschnagel, J.; Wittmer, J.; Binder, K. *Macromolecules* **1996**, *29*, 1433.

(9) Amiel, C.; Sikka, M.; Schneider, J. W.; Tsao, Y. H.; Tirrell, M.; Mays, J. W. *Macromolecules* **1995**, *28*, 3125.

(10) Bijsterbosch, H. D.; Cohen Stuart, M. A.; Fleer, G. J.; Van Caeter, P.; Goethals, E. J. *Macromolecules* **1997**, *submitted*.

(11) Cosgrove, T.; Zarbakhsh, A.; Luckham, P. F.; Hair, M. L.; Webster, J. R. P. W. *Faraday Discussions* **1994**, 189.

(12) Guzonas, D.; Hair, M. L.; Cosgrove, T. *Macromolecules* **1992**, *25*, 2777.

(13) Huguenard, C.; Varoqui, R.; Pefferkorn, E. *Macromolecules* **1991**, *24*, 2226.

(14) Munch, M. R.; Gast, A. P. *Macromolecules* **1990**, *23*, 2313.

(15) Parsonage, E.; Tirrell, M.; Watanabe, H.; Nuzzo, R. G. *Macromolecules* **1991**, *24*, 1987.

(16) Tripp, C. P.; Hair, M. L. *Langmuir* **1996**, *12*, 3952.

(17) Tiberg, F.; Malmsten, M.; Linse, P.; Lindman, B. *Langmuir* **1991**, *7*, 2723.

(18) Milner, S. T. *Science* **1991**, *251*, 905.

(19) Halperin, A.; Alexander, S. *Macromolecules* **1989**, *22*, 2403.

(20) Dabros, T.; Vandeven, T. G. M. *Colloid and Polymer Science* **1983**, *261*, 694.

(21) Abramowitz, M.; Stegun, I. A. *Handbook of mathematical functions*, 1972.

(22) Liu, Q.; Wilson, G. R.; Davis, R. M.; Riffle, J. S. *Polymer* **1993**, *34*, 3030.

(23) Van Krevelen, D. W. *Properties of Polymers, Their Estimation and Correlation with Chemical Structure*; Elsevier: Amsterdam, 1976.

(24) Brandrup, J.; Immergut, E. H., Eds *Polymer Handbook, 3rd ed.*; Wiley and Sons: New York, 1989.

(25) Lin, Z.; Hill, R. M.; Davis, H. T.; Scriven, L. E.; Talmon, Y. *Langmuir* **1994**, *10*, 1008.

(26) Bellare, J. R.; Davis, H. T.; Scriven, L. E.; Talmon, Y. *J. Electron. Microsc. Techn.* **1988**, *10*, 87.

(27) Frederik, P. M.; Stuart, M. C. A.; Verkleij, A. J. *Biochim. Biophys. Acta* **1989**, *979*, 275.

(28) Dijt, J. C.; Cohen Stuart, M. A.; Fleer, G. J. *Adv. Colloid Interface Sci.* **1994**, *50*, 79.

(29) Nagpal, V. J.; Davis, R. M.; Liu, Q.; Facinelli, J.; Riffle, J. S. *Langmuir* **1994**, *10*, 4434.

(30) Koppel, D. E. *J. Chem. Phys.* **1972**, *57*, 4814.

(31) Provencher, S. W.; Hendrix, J.; De Maeyer, L.; Paulussen, N. *J. Chem. Phys.* **1978**, *69*, 4273.

(32) Provencher, S. W. *Comput. Phys. Commun.* **1982**, *27*, 213.

(33) Suss, D.; Cohen, Y.; Talmon, Y. *polymer* **1995**, *36*, 1809.

(34) Mortensen, K.; Talmon, Y. *Macromolecules* **1995**, *28*, 8829.

(35) Chen, C. H.; Wilson, J. E.; Davis, R. M.; Chen, W.; Riffle, J. S. *Macromolecules* **1994**, *27*, 6376.

(36) Chen, C. H.; Wilson, J. E.; Chen, W.; Davis, R. M.; Riffle, J. S. *Polymer* **1994**, *35*, 3587.

(37) Lyklema, J. *Fundamentals of interface and colloid science I. Fundamentals*; Academic Press: London, 1991.

(38) Cohen Addad, J. P.; Morel, N. *J.Phys. III France* **1996**, *6*, 267.

(39) Dewalt, L. E.; Ouyang, H. D.; Dimonie, V. L. *Journal of Applied Polymer Science* **1995**, *58*, 265.

(40) Tiberg, F.; Jonsson, B.; Lindman, B. *Langmuir* **1994**, *10*, 3714.

Chapter 5

Adsorption of graft copolymers onto silica and titania

The adsorption of graft copolymers of poly(acryl amide) (PAAm, backbone) and poly(ethylene oxide) (PEO, side chains) from aqueous solution onto silica and titania was studied with reflectometry. Two high-molar-mass copolymers were used with a different PEO graft density (10 and 18 % w/w PEO in copolymer G10 and G18, respectively). On titania only the PAAm backbone adsorbs and the PEO does not. This results in adsorbed amounts of 0.83 and 0.85 mg m^{-2}, respectively, which is about the same as for a PAAm homopolymer. On silica the situation is reversed: now the PEO side chains adsorb and the PAAm backbone does not. The adsorption as a function of time shows a maximum, before the stable plateau is reached. The adsorbed amount on silica is much higher than on titania: in the final plateau it is 1.35 and 1.2 mg m^{-2} for G18 and G10, respectively. On silica the polymers form longer loops and tails so that more molecules can be accommodated at the surface. The overshoot on silica depends on the polymer concentration, suggesting that it is not caused by a conformational change of the adsorbed layer but by exchange with polymer molecules from solution. Differences in graft distribution and graft density in the polymer sample are probably responsible for the displacement. The average number of grafts per polymer is rather low. On statistical grounds there should be an appreciable polydispersity in graft distribution and in graft density. Molecules in which the grafts are clustered in a few groups can displace molecules with more regularly separated grafts, and molecules with a high graft density can displace those with a lower number of side chains. The newly arriving molecules can then adsorb in a flatter conformation with a lower adsorbed amount as the extra loss in conformational entropy is compensated by the gain in adsorption energy.

Introduction

Polymers are extensively used for the stabilisation of colloidal dispersions. By forming a protective layer around the particles, they can prevent these particles to aggregate by Van der Waals force.[1,2] Especially diblock copolymers can be very effective in forming a thick stabilising layer. This feature arises from the fact that only a small part of the molecule, the anchor block, adsorbs to the surface. The other part, the buoy block, protrudes into the solution and forms a long dangling tail. For good steric stabilisation it is necessary that the polymer tails protrude far into the solution, as these tails determine the thickness of the adsorbed layer.[2] From this point of view, it is interesting to consider another type of copolymer; a *graft copolymer*. Such copolymers, also called comb copolymers, have a main chain of one type of segments, and side chains grafted to it consisting of another type of monomer units. Each graft copolymer has then many tails which makes them suitable as steric stabilisers of colloidal dispersions. So far, the adsorption and stabilisation by graft copolymers has received relatively little attention in literature.[3-6]

In a few theoretical papers the behaviour of graft (co)polymers was considered. Van der Linden et al.[6] found with a numerical self-consistent-field theory that graft *homopolymers* (with the same type of segments in backbone and side chains) adsorb preferentially with their backbone, the side chains dangling in the solution. These authors suggested that the opposite result found by Balasz and Siemasko[3] may be due to insufficient equilibration in the Monte-Carlo simulations. In both studies it was found that graft homopolymers form a thinner adsorbed layer than the equivalent linear polymer with the same total number of segments. Although the graft polymer has many more tails than the linear polymer, the extension of these tails into the solution is limited by the adsorption of the backbone. When the side chains are relatively long compared to the backbone spacing, a thick brush of non-adsorbing tails could be formed, comparable to that formed by diblock copolymers. Increasing the total length of the graft polymer eventually results in a thick layer because the backbone chain ends are no longer adsorbed and behave as tails (with attached side chains).[6] In the case of a graft *copolymer* with an adsorbing backbone and non-adsorbing grafts, the results are more or less similar to that obtained with the graft *homopolymer*. The picture, however, changes considerably for a graft copolymer with adsorbing grafts and a non-adsorbing backbone. In this case, the side chains adsorb to the surface and parts of the backbone dangle in the solution as loops and tails. The backbone prevents some of the side chains from adsorbing for entropical reasons. The loops and tails therefore contain both backbone and some grafts. The

resulting layer is less dense close to the surface and it extends further away in the solution than for a graft copolymer with non-adsorbing grafts. The adsorbed amount is mainly determined by the density in the first few layers and is therefore lower for a polymer with adsorbing side chains than for one with an adsorbing backbone.

In two experimental studies adsorption of graft copolymers was investigated. Eremenko et al.[4] considered the adsorption of copolymers of poly(acryl amide) grafted to poly(vinyl alcohol) and its effect on the electrokinetic potential of silica and the hydrodynamic layer thickness. They found that the adsorbed amount of the polymer with more adsorbing side chains is considerably higher. However, the graft density of their polymers is very low (2-6 side chains per molecule). Liang et al.[5] studied the adsorption of graft copolymers with a poly(methyl methacrylate-co-methacrylic acid) backbone and poly(ethylene oxide) side chains onto latex particles. The adsorbed amount and layer thickness increased with increasing graft density. This result is unexpected because the graft density mainly determines the density of the adsorbed layer, i.e., the adsorbed amount, but does hardly affect the layer thickness. For a better interpretation of the data more information about molar mass and graft density is essential.

In this study we compare the adsorption of graft copolymers with an adsorbing backbone and non-adsorbing side chains to the reverse situation of adsorbing side chains and a non-adsorbing backbone. In order to make a meaningful comparison we used a single type of graft copolymer on two different surfaces, with different affinity for the backbone and graft segments. The effect of graft density could be investigated by using two graft copolymers with about the same molar mass but a different number of side chains. The graft copolymers had a poly(acryl amide) backbone and poly(ethylene oxide) side chains. The graft density was low, with a weight percentage of the side chains of 10 and 18 % for the two polymers used. The adsorption of these polymers was studied with reflectometry. The adsorbent surfaces were silica, on which only the side chains adsorb, and titania, for which only the backbone has affinity.

Experimental

Polymers

The polymers used in this study were graft copolymers of poly (acryl amide) (PAAm) and poly (ethylene oxide) (PEO), which where synthesised and kindly made available by Prof. M. Möller (Twente University, The Netherlands, presently at Ulm University, Germany). The polymers were synthesised by radical copolymerisation of acryl amide

with a small amount of a PEO macro-monomer which had been end-functionalised with an acrylate moiety.[7] The PEO side chains had a molar mass of 6.34 kg mol^{-1} and a polydispersity index M_w/M_n = 1.11. Two polymer samples were used, differing in graft density. The PAAm-PEO graft copolymer with the highest PEO graft density (18 % in weight) is denoted as G18. The other graft copolymer, G10, has a weight percentage PEO of 10%. Considering the molar mass of the PEO side chains this means that a backbone part between two side chains has, on average, a rather high molar mass of 59 and 30 kg mol^{-1} for G10 and G18, respectively. The total molar mass of the copolymers is of the order of 1000 kg mol^{-1}. The molar mass of G18 is expected to be higher than that of G10 due to the presence of more side chains, despite the fact that the total length of the main chain is probably slightly smaller. The ratio m/n (number m of backbone units divided by the number n of grafts) is 832 for G10 and 416 for G18. The average number of grafts is therefore roughly 15 per molecule for G10, and about 30 per G18 chain, However, on statistical grounds there should be an appreciable dispersity in graft density. The structural formula of the graft copolymers is given in Figure 1 and a schematic impression of a chain of G10 and G18 is sketched in Figure 2.

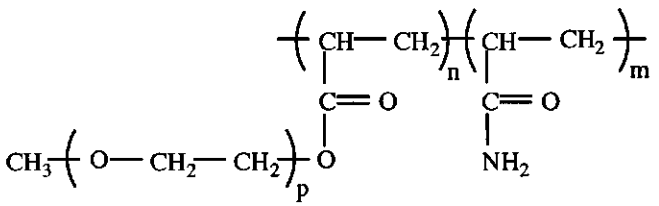

Figure 1. The structural formula of the PAAm-PEO graft copolymers. The PEO side chains are more or less randomly distributed along the main chain. For both polymers G10 and G18 the number of EO units per side chain (p) is 144. The number of side chains n is roughly 15 for G10 and 30 for G18, the total molar mass is of the order 1000 kg mol^{-1}.

The polymers are soluble in water, although cross-linking reactions may render the polymer insoluble.[8] It is possible that the main chain PAAm is, to a very small extent, hydrolysed so that the polymer contains a few acrylic acid groups. The ester link between the main chain and the PEO side chains can easily be hydrolysed with acid or base, resulting in a solution with a mixture of two soluble homopolymers: PAAm with a very high molar mass and PEO with a molar mass of 6.34 kg mol^{-1}. This polymer mixture is used to study the adsorption behaviour of the individual building blocks of the graft copolymers.

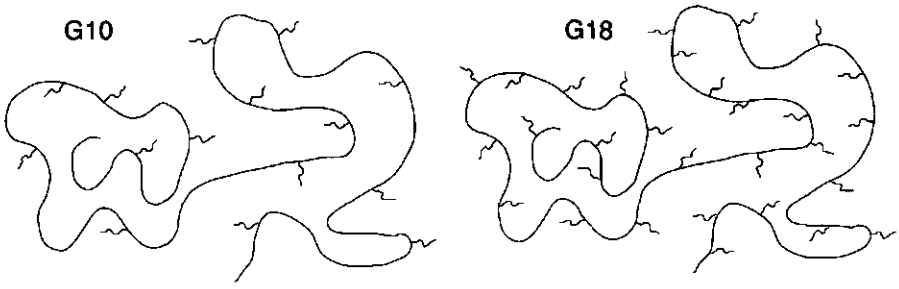

Figure 2. Schematic representation of copolymers G10 and G18. The side chain density is rather low but the molar mass per side chain is relatively high (6.34 kg mol^{-1}).

Measurements

The adsorption of the graft copolymers was measured with a reflectometer equipped with a stagnation point flow cell, a technique that has been described extensively elsewhere.[9,10] Macroscopically flat silicon wafers from Aurel GmbH (Germany) were used. By thermal oxidation, we obtained an SiO_2 layer with a thickness of about 110 nm. A TiO2 layer with a thickness of about 25 nm was deposited on a silicon wafer by reactive sputtering of Ti in an oxygen atmosphere. This was carried out at Philips Laboratories in Eindhoven, The Netherlands. Strips cut from these wafers were cleaned by oxidation with UV-ozone, and could be cleaned and re-used many times. Fresh solutions of the copolymers were stored in the refrigerator and used within one week. The adsorption measurements were performed with polymer concentrations varying from 5 to 100 mg l^{-1} in demineralised water. To screen the effect of any charged groups present we added KNO_3 up to a total concentration of 10 mM, except for one series of measurements were we studied the effect of different concentrations of salt. All measurements were performed at room temperature (T = 294 ±1 K).

Results and discussion

Reflectometry is a suitable tool to study the kinetics of polymer adsorption at time scales varying from a few seconds up to several hours. This technique measures the adsorbed amount of polymer at the surface, but any conformational changes at constant adsorbed amount are not detected.

The homopolymers PEO and PAAm have a different affinity for silica and titania surfaces. From earlier studies is known that PEO has a high adsorption affinity for silica[9-11] but we found no affinity at all for titania (results not shown). For the acryl amide homopolymer

the adsorption behaviour is the opposite: it has almost no affinity for silica, the adsorbed amount is very low, and on titania we found an adsorbed amount between 0.5 and 1 mg m^{-2} (results not shown). For the graft copolymers of PAAm-PEO we measured the adsorbed amount on both silica and titania as a function of time. In Figure 3 we show an example of kinetic adsorption curves of the copolymer with the higher graft density, G18, on both surfaces. Figure 4 gives similar data for the copolymer with the lower graft density, G10.

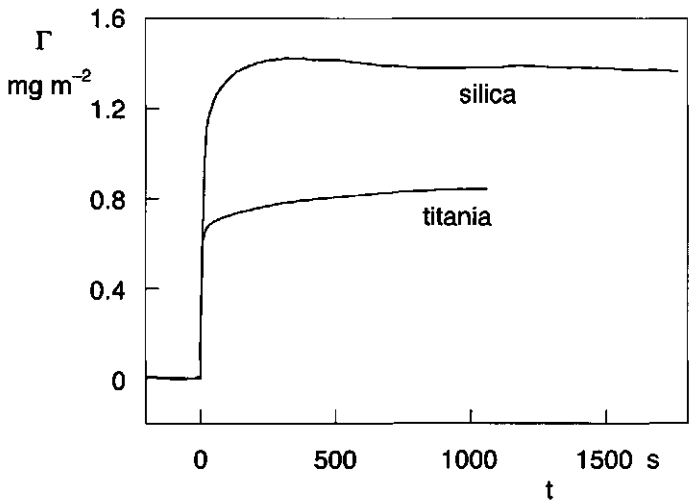

Figure 3. Kinetic adsorption curves of G18 on silica and titania. The polymer concentration is 50 mg l^{-1} in a 10 mM KNO_3 solution at pH 6.

The adsorption curves of G18 and G10 on titania are very similar. In the initial stages of the adsorption the adsorbed amount increases linearly with time, as expected for diffusion-limited adsorption in a stagnation point flow. Towards saturation of the surface the adsorption rate decreases abruptly and eventually the adsorbed amount does not change any longer: a plateau is reached. The plateau adsorbed amount for titania is almost equal for both copolymers: 0.84 and 0.81 mg m^{-2} for G18 and G10, respectively. This adsorption behaviour resembles that of a linear PAAm homopolymer with a molar mass of 500 kg mol^{-1}: the plateau adsorbed amount for this sample was 0.7 mg m^{-2} at the same salt concentration and pH. Apparently, the presence of the PEO side chains, which have no affinity for the titania surface, does hardly affect the adsorption behaviour

of the copolymers. The copolymers adsorb with the PAAm backbone to the surface and, as the graft density is low, the adsorption is similar to that of a linear PAAm homopolymer. This is in agreement with theoretical predictions by Van der Linden et al.[6] who found that, upon increasing the backbone spacing between the grafts, the polymer behaves more and more as a linear homopolymer.

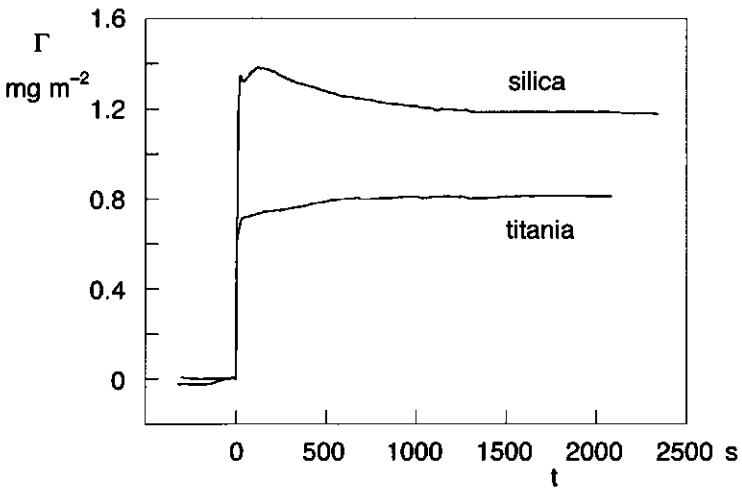

Figure 4. Kinetic adsorption curves of G10 on silica and titania. The polymer concentration is 50 mg l^{-1} in a 10 mM KNO_3 solution at pH 6.

The adsorption onto silica can, in contrast to that on titania, only occur through the presence of the PEO side chains. The initial parts of the adsorption curves of G18 and G10 increase again linearly with time, and the adsorption rate is the same as found on titania. This is the expected behaviour since the limiting step in this stage of the adsorption is the mass transport towards the surface. The low graft density does not reduce the initial attachment rate of the copolymer. The presence of a few long PEO side chains is already sufficient to 'trap' the polymer when it arrives at the surface. After the initial stage of the adsorption a maximum in the adsorbed amount is reached. After that, the adsorbed amount decreases to the final plateau level, where the adsorbed amount remains constant in time. The 'overshoot' around the maximum is far more pronounced for G10 than for G18: the difference in adsorbed amount between the maximum and the plateau is 0.2 and 0.05 mg m^{-2}, respectively. This overshoot is a very interesting phenomenon, which has only been reported occasionally before. A few cases have been

observed for compact proteins.[12-14] For these proteins, the overshoot was interpreted as a slow change of conformation of adsorbed molecules which spread on the surface and slowly displace later arriving weakly adsorbed protein molecules. Johnson et al.[15] found an overshoot for the adsorption of poly(dimethyl siloxane) and cis-poly(isoprene) onto germanium oxide and silica and interpreted it as a surface-induced crystallisation of the adsorbed homopolymers. We will return to the overshoot further on. The adsorbed amount on silica found for G10 in the maximum is slightly higher than found for G18, but at the plateau the adsorbed amount of G18 is higher. Both polymers have a considerably higher adsorbed amount on silica than on titania.

Ionic strength and pH

Before discussing the above results in more detail, we first consider the effect of the salt concentration and pH. For G10 we studied the adsorption from a 50 mg l^{-1} solution onto silica and titania as a function of pH at different concentrations of KNO_3. In Figure 5 we give the adsorbed amount in the final plateau of the adsorption curves on titania, and in Figure 6 we plot the adsorbed amount in the maximum of the adsorption curves on silica.

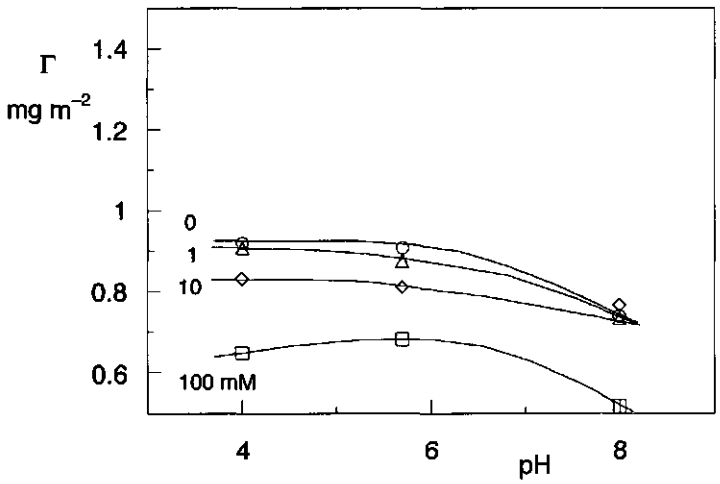

Figure 5. The adsorbed amount in the plateau of the adsorption curve of G10 on titania as a function of pH at different concentrations of KNO_3: 0 mM (circles), 1 mM (triangles), 10 mM (diamonds), and 100 mM (squares). The polymer concentration is 50 mg l^{-1}.

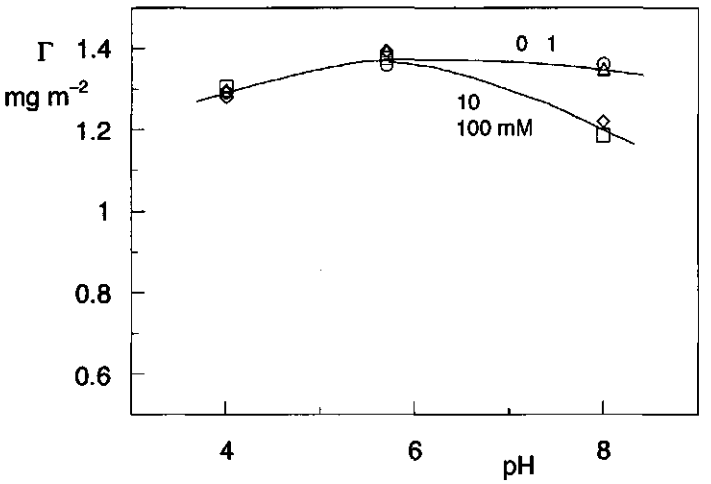

Figure 6. The adsorbed amount in the maximum of the adsorption curve of G10 on silica as a function of the pH at different concentrations of KNO_3: 0 mM (circles), 1 mM (triangles), 10 mM (diamonds), and 100 mM (squares). The polymer concentration is 50 mg l^{-1}.

Even though the polymers carry almost no charge, the salt concentration and pH can have an effect on the adsorption behaviour of the graft copolymers as the amide group has a delocated electron pair which makes the oxygen slightly negatively charged and the amine positive. In addition, some of the amides may be hydrolysed and converted into acidic carboxyls.

As can be seen from Figure 5 the pH has an effect on the adsorbed amount in the plateau of the adsorption curve. The highest adsorption is found at a low pH (with the exception of the highest salt concentration), which coincides with the iso-electric point of titania which is at pH 4.[16] The surface is then only weakly charged and the polymer carboxyl groups, if present, are dissociated for a small part, rendering the polymer main chain slightly negatively charged. The adsorption at this pH is mainly determined by the non-electrostatic interaction between polymer and surface. When the pH is increased to 5.7 the surface and the polymer are both negatively charged, which reduces the adsorbed amount (except for 100 mM, where the screening of electrostatic interactions is strongest). A further decrease of the adsorbed amount found at pH 8 can also be explained by the increase of charge on both adsorbent and adsorbate. However, these effects are small, from which we conclude that there are only few acidic groups present in the polymer. This is confirmed by the adsorption rates at different pH, which are, within

experimental error, not affected by the pH of the solution. Increasing the ionic strength decreases the importance of electrostatic interactions between polymer and surface. If this screening is the only effect, it would show up in the results as an increase of the adsorbed amount at a pH above 4, and no effect would be expected around pH = 4. However, this does not hold for the results shown in Figure 5. Clearly the role of salt is more complicated. For example, the ions can interfere with the polar amide groups of the main chain. Such an interference will affect the adsorption because it is this group which is probably responsible for the adsorption onto titania.

The adsorption curves of G10 onto silica at different pH and salt concentrations were all similar to the one plotted in Figure 4, the only difference is the adsorbed amount. The shape of the curves is the same, as is the relative difference between the adsorbed amounts in the maximum and at the plateau of the curve. In Figure 6 we see again an effect of varying pH and ionic strength of the solution. However, the effects are smaller than for the adsorption on titania. The ionic strength and the pH can have a direct effect on the acryl amide groups responsible for the adsorption on titania. For PEO, which is the adsorbing group on silica, we hardly expect any effect of salt and pH on the adsorption in the range in which we varied these parameters. Indeed, the pH has only a small effect on the adsorbed amount, and the ionic strength does not affect the adsorbed amount at pH 4 or 6. At pH 8, however, we find a small decrease in the adsorbed amount at the two higher ionic strength. The small differences in the adsorbed amounts found on silica are probably caused by a change in solution properties of the PAAm main chain. The results of varying pH and ionic strength for G18, with a higher graft density, are very similar to those obtained with G10; we do not show these results. For the remainder of the experiments we used polymer solutions with an ionic strength of 10 mM KNO_3 and a pH of 6.

Adsorption isotherms

The adsorption isotherm of a polymer is usually of the high-affinity type, due to the many segments that can contribute to the adsorption.[2] In Figure 7 we plot the adsorption isotherms of G18 on silica and on titania. The isotherm on titania shows that there is hardly any dependence on the polymer concentration used. The adsorbed amount in the plateau of the isotherm is around 0.85 mg m^{-2}, similar to what we found for the adsorption of a PAAm homopolymer.

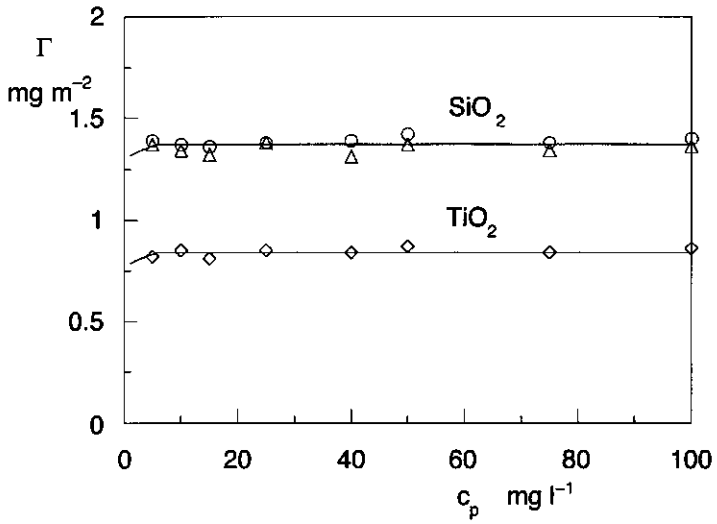

Figure 7. Adsorption isotherms of G18 on titania (diamonds) and on silica (triangles). For silica we give also the adsorbed amount in the maximum of the adsorption curve (circles), which in this case is not much higher than the plateau value. The solutions contain 10 mM KNO_3 and pH is around 6.

For the adsorption of G18 on silica also a high-affinity isotherm is found. The difference between the adsorbed amounts in the maximum and in the plateau of the adsorption curves is small for this polymer and it does hardly depend on the polymer concentration. The adsorbed amount in the plateau of the isotherm is 1.35 mg m^{-2}, which is considerably higher than on titania. Apparently, the polymer conformations at the two types of surfaces is different.

The analogous results for G10 are given in Figure 8. For this polymer the overshoot on silica is much larger than for G18, and the drop in Γ following the overshoot is around 0.2 mg m^{-2} over the entire concentration range.

The adsorption isotherm of G10 on titania is almost the same as for G18, with an adsorbed amount in the plateau of the isotherm around 0.83 mg m^{-2}, slightly lower than found for G18. This would agree well with the fact that the molar mass of G18 is somewhat higher than that of G10. However, the small difference is perhaps not significant, as it is within the experimental error of the technique used.

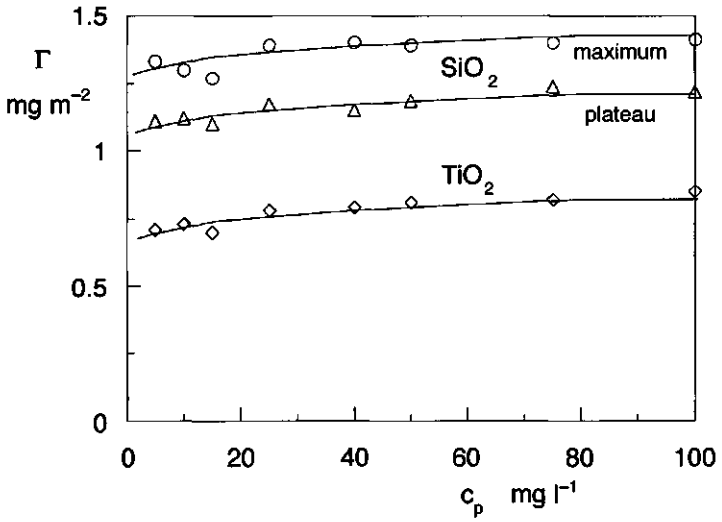

Figure 8. Adsorption isotherms of G10 on titania (diamonds) and on silica (triangles). For silica we give also the adsorbed amount in the maximum of the adsorption curve (circles). The solutions contain 10 mM KNO_3 and pH is around 6.

Also for sample G10 the adsorption on titania is thus similar to that of a PAAm homopolymer. The difference in graft density does hardly affect the adsorbed amount, as in both cases the number of side chains is low. The result of Liang et al.[5], in which the adsorbed amount (and layer thickness) increases with the density of non-adsorbing grafts, suggests that the graft density in their system is much higher. The similar behaviour of our copolymers and a PAAm homopolymer on titania suggests that the copolymers have a conformation which is not much different from that of an adsorbed homopolymer. Only a few PEO side chains protrude into the solution but their contribution to the adsorbed amount is small. A pictorial representation of the structure of the adsorbed polymer layer on titania is given in Figure 9a.

The adsorbed amount in the maximum of G10 on silica is about the same as that of G18. The decrease of the adsorbed amount following the overshoot is larger than for G18, which corresponds to a lower plateau value for G10. On silica the graft copolymers probably have a configuration in which only part of the side chains are adsorbed at the surface. The polymer would loose a considerable amount of configurational entropy if all grafts would have to be in contact with the surface. The surface is therefore only partly covered with PEO chains. The reason for the higher adsorbed amount on silica is that the

graft copolymer forms longer loops and tails. Only a fraction of the PEO chains is in contact with the surface; yet these adsorbed grafts attach the whole chain firmly to the surface, because of the relatively high adsorption energy of the (long) PEO chains. The PEO chains used in this study do indeed adsorb strongly on silica,[11] and they are probably long enough to secure attachment of the whole molecule. The resulting polymer layer could then be similar to that of a brush formed by the adsorption of diblock copolymers, where only one block attaches to the surface and the other protrudes into the solution.[17,18] The difference is that the graft copolymer used has a very high molar mass and that the brush contains many loops and not only tails. Consequently, the brush density is not very high. The configuration of the two polymers used in these experiments are probably similar as the adsorbed amounts do not differ much. As the graft density of G10 is lower than that of G18, less side chains per polymer are adsorbed to the surface. A sketch of the possible structure of the adsorbed layer on silica is given in Figure 9b.

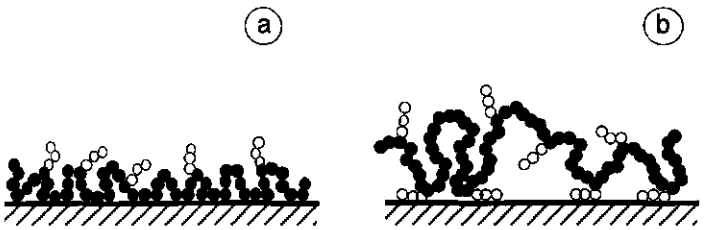

Figure 9. Schematic presentation of the adsorbed layer of PAAm-PEO graft copolymers on titania (a) and on silica (b). The PAAm main chain is represented by filled circles, the PEO grafts by open circles.

The adsorbed amounts on silica are higher than on titania, which could lead to the conclusion that the adsorption of side chains is more favourable than that of the backbone. This seems to be in contradiction with the numerical self-consistent field results presented by Van der Linden et al.[6] These authors concluded that the adsorbed amount is higher for an adsorbing backbone, although the layer thickness is less. However, their results were obtained with graft copolymers that did not differ in the relative amount of adsorbing segments, whereas in our system the ratio of the mass of potentially adsorbing segments to the total molar mass is 0.10 and 0.18 for silica and 0.90 and 0.82 for titania, respectively. If we would have decreased the relative number of adsorbing segments on titania, i.e., increased the graft density, this most likely would have given rise to an increase in the adsorbed amount, which eventually would have been higher than for silica in these experiments. We could not check these conjectures because graft copolymers with a higher graft density were not available.

Hydrolysis

The copolymers can easily be hydrolysed at the ester connection between the PAAm main chain and the PEO side chains by acid or base. We hydrolysed the grafts by adding NaOH to the stock solution of both G10 and G18 until a pH of 11 was reached. The solution was kept at this pH for one hour after which it was diluted to the desired concentration, and the pH and the ionic strength were again adjusted to 6 and 10 mM, respectively. From these solutions, which contain a mixture a short PEO homopolymers and long linear PAAm homopolymers, we measured the adsorption to both silica and titania. For both G10 and G18 we found on silica an adsorbed amount of 0.4 mg m^{-2}, which agrees well with earlier results obtained with PEO homopolymers with a similar molar mass.[9,19] On titania the adsorbed amount was, within experimental error, the same as found for the graft copolymers. These results clearly demonstrate that the adsorbance of the graft copolymer is a result of combining the two different segment types together in one single molecule.

Overshoot

In almost all cases, the adsorption of a polymer is accompanied by a partial flattening or spreading of the molecule. For flexible polymers, this is usually a very fast process, much faster than the rate of supply from solution. Therefore, highly coiled transient states with big loops are usually not observed on the experimental time scale. However, some spreading processes are relatively slow, such that they become comparable in rate to the polymer supply. Under such conditions overshoots may appear; some examples are found with compact molecules like proteins[12-14] and with surface induced crystallisation of polymers.[15] It is characteristic for these kind of overshoots that they only appear for sufficiently high polymer supply rate. If the polymer supply is slow the polymer can assume its most favourable conformation before all surface sites are occupied and there is no need to displace some of the already adsorbed polymers to obtain that conformation. The adsorption curves of PAAm-PEO graft copolymers show a measurable overshoot, which is most pronounced for the polymer with the lower side chain density.

In order to get a better insight in the overshoot phenomenon we take a closer look at the adsorption kinetics of the graft copolymers on silica. We plot a part of the adsorption curve of G10, the polymer with the lower graft density and a large overshoot, for different polymer concentrations in Figure 10. In this case we normalise the variable time by multiplying it with the polymer concentration; the abscissa then represents the integrated polymer flux, i.e., the total mass of polymer supplied.

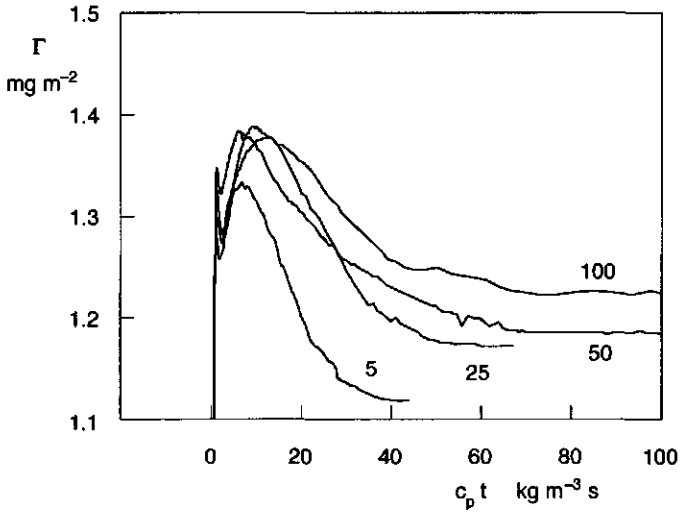

Figure 10. Part of the adsorption curves of G10 on silica as a function of the polymer flux for different polymer concentrations, which are indicated in the figure and are expressed in mg l^{-1}. The measurements were performed at an ionic strength of 10 mM and pH = 6.

The maxima in the adsorption curves of Figure 10 are all, by approximation, located at a constant $c_p t$, which means that the moment when the maximum is reached is mainly controlled by the integrated polymer flux. We also observe that the decay rate of the adsorbed amount after the maximum depends on the polymer concentration. This implies that it is the transport rate which controls the decay rate of Γ, rather than a process occurring at the surface. Another very important result seen in Figure 10 is that the overshoot does not disappear when the polymer is added very slowly, i.e., for low polymer concentrations.

From Figure 9b we know that probably only part of the PEO side chains is adsorbed on the silica surface and that the surface is only partly covered with adsorbed chains. The polymer layer can therefore gain some adsorption energy if it could bring more of the grafts in contact with the surface. This could be achieved by a reconformation of the adsorbed polymers such that more of the grafts are adsorbed to the surface. The polymers would then have to flatten their structure, thereby releasing some of the already adsorbed polymers. This would then lead to a decrease of the adsorbed amount. However, the results shown in Figure 10 do not support that the overshoot is caused by a conformational change of the adsorbed polymers. The polymer supply and the time

given to obtain this supply determine the decay rate of the adsorbed amount. This suggests that the decrease of the adsorbed amount is more likely to be caused by displacement of initially adsorbed polymer chains by newly arriving molecules from solution. Such a process must, of course, be driven by a decrease of the systems' Gibbs energy.

Differences in graft distribution and graft density in the polymer sample could be a reason for displacement by polymer molecules from solution. The average number of grafts per polymer is rather low, roughly 15 for G10 and 30 for G18. On statistical grounds there should be an appreciable polydispersity in graft distribution and in graft density. Thus the distribution of side chains along the PAAm chain is probably irregular, and also the number of grafts is not the same in the various molecules. Molecules in which the grafts are clustered in a few groups can displace molecules with more regularly separated grafts, and molecules with a high graft density can displace those with a lower number of side chains. The newly arriving molecules can then adsorb in a flatter conformation as the extra loss in conformational entropy is compensated by the gain in adsorption energy. Accordingly, the adsorbed amount decreases as the total number of adsorbed molecules becomes less.

The overshoot is most pronounced for the polymer with the lower graft density. This is to be expected as this polymer has probably a larger polydispersity in graft density and graft distribution. The adsorbed amount in the plateau of the adsorption curve of G18 is slightly higher than that of G10. This seems to be in contradiction with the fact that the higher chain density gives a higher adsorption energy and probably a more flattened conformation of the resultant polymer layer. However, the difference in plateau adsorbed amounts is only small and could possibly be explained by the difference in molar mass.

Conclusions

The adsorption of graft copolymers of poly(acryl amide) (PAAm) and poly(ethylene oxide) (PEO) from an aqueous solution onto silica and titania was studied with reflectometry. Two high-molar-mass polymers (M_w around one million g mol^{-1}) were used with different PEO side chain densities: G10 with a weight percentage of 10% PEO side chains and G18 with 18% (w/w) PEO grafts. On titania only the PAAm backbone adsorbs and the PEO chains do not. This results in an adsorbed amount of 0.85 and 0.83 mg m^{-2} for G18 and G10, respectively, which is about the same as that found for a PAAm homopolymer. This outcome is in agreement with self-consistent-field calculations reported by Van der Linden et al.[6] for a graft polymer with a low graft density and an adsorbing backbone.

On silica the PEO side chains adsorb and the PAAm backbone does have no affinity for the surface. In the initial part of the adsorption curves the adsorption rate is the same as on titania. For both polymers we observed a maximum in the adsorption as a function of time, after which the adsorbed amount decreases and a plateau is reached. The overshoot is small for G18 (0.05 mg m^{-2}) and more pronounced for G10 (0.2 mg m^{-2}). Such an overshoot phenomenon has only incidentally been reported before.[12-15]

The adsorbed amount on silica is much higher than found on titania: in the plateau the adsorbances are 1.35 and 1.2 mg m^{-2} for G18 and G10, respectively. Upon adsorption the graft copolymers adapt a conformation in which only part of the side chains are adsorbed. Following the overshoot, both graft copolymers show a decrease in the total adsorbed amount. The overshoot depends on the polymer concentration which suggests that it is not caused by a conformational change of the adsorbed layer but by exchange with polymer molecules from solution.

Differences in graft distribution and graft density in the polymer sample could be a reason for displacement by polymer molecules from solution. The average number of grafts per polymer is rather low, roughly 15 for G10 and 30 for G18. On statistical grounds there should be an appreciable polydispersity in graft distribution and in graft density. Molecules in which the grafts are clustered in a few groups can displace molecules with more regularly separated grafts, and molecules with a high graft density can displace those with a lower number of side chains. The newly arriving molecules can then adsorb in a flatter conformation with a lower adsorbed amount as the extra loss in conformational entropy is compensated by the gain in adsorption energy. The overshoot is most pronounced for the polymer with the lower graft density. This is to be expected as this polymer has probably a larger polydispersity in graft density and graft distribution.

The high adsorbed amount of the graft copolymers on silica makes it very probable that they can effectively be used as steric stabilisers of aqueous silica dispersions.[20] An advantage of these polymers above diblock copolymers is that the latter usually form micelles in solution. The occurrence of micelles can form a kinetic barrier which slows down the adsorption process[21] which is, for many applications, a major disadvantage. The adsorption of graft copolymers onto silica is a transport-limited process so that a stabilising steric layer may be obtained much faster than with block copolymers.

References

(1) Napper, D. H. *Polymeric stabilisation of colloidal dispersions*; Academic Press: London, 1983.

(2) Fleer, G. J.; Cohen Stuart, M. A.; Scheutjens, J. M. H. M.; Cosgrove, T.; Vincent, B. *Polymers at Interfaces*; Chapman & Hall: London, 1993.

(3) Balazs, A. C.; Siemasko, C. P. *J. Chem. Phys* **1991**, *95*, 3798.

(4) Eremenko, B. V.; Malysheva, M. L.; Rusina, O. D.; Kutsevol, N. V.; Zeltonozskaya, T. B. *Colloids and Surfaces A - Physicochemical and Engineering Aspects* **1995**, *98*, 19.

(5) Liang, W.; Bognolo, G.; Tadros, T. F. *Langmuir* **1995**, *11*, 2899.

(6) Van der Linden, C. C.; Leermakers, F. A. M.; Fleer, G. J. *Macromolecules* **1996**, *29*, 1000.

(7) De Vos, S. C.; Möller, M. *Makromol. Chem. Macrom. Symp.* **1993**, *75*, 223.

(8) Gramain; Frère *New Polymeric Materials* **1992**, *3*, 175.

(9) Dijt, J. C.; Cohen Stuart, M. A.; Hofman, J. E.; Fleer, G. J. *Colloids and Interfaces* **1990**, *51*, 141.

(10) Dijt, J. C.; Cohen Stuart, M. A.; Fleer, G. J. *Adv. Colloid Interface Sci.* **1994**, *50*, 79.

(11) Van der Beek, G. P.; Cohen Stuart, M. A. *J. Phys. (Paris)* **1988**, *49*, 1449.

(12) Walton, A. G.; Soderquist, M. E. *Croat. Chem. Acta* **1980**, *53*, 363.

(13) Van Dulm, P.; Norde, W. *J. Colloid Interface Sci.* **1983**, *91*, 248.

(14) Shirahama, H.; Lyklema, J.; Norde, W. *J. Colloid Interface Sci.* **1990**, *139*, 177.

(15) Johnson, H. E.; Clarson, S. J.; Granick, S. *Polymer* **1993**, *34*, 1960.

(16) Hoogeveen, N. G.; Cohen Stuart, M. A.; Fleer, G. J. *J. Colloid Interface Sci.* **1996**, *182*, 133.

(17) Evers, O. A.; Scheutjens, J. M. H. M.; Fleer, G. J. *J. Chem. Soc., Faraday Trans* **1990**, *86*, 1333.

(18) Marques, C. M.; Joanny, J. F. *Macromolecules* **1989**, *22*, 1454.

(19) Bijsterbosch, H. D.; Cohen Stuart, M. A.; Fleer, G. J.; Van Caeter, P.; Goethals, E. J. *Macromolecules* **1997**, *submitted.*

(20) Bijsterbosch, H. D.; Cohen Stuart, M. A.; Fleer, G. J. *in preparation* **1997**.

(21) Bijsterbosch, H. D.; Cohen Stuart, M. A.; Fleer, G. J. *In preparation* **1997**.

Chapter 6

Effect of block and graft copolymers on the stability of colloidal silica

We use dynamic light scattering to measure the time-dependent increase of the average hydrodynamic radius of colloidal silica particles in the presence of salt. This increase is linear in time up to twice the radius of unaggregated particles. The method is a very useful tool in monitoring the stabilising effect of adsorbed polymer. Four different series of diblock and graft copolymers were used to stabilise an aqueous silica dispersion against aggregation by salt. For two series of non-selectively adsorbing diblock copolymers we found a good correlation between the adsorbed amount and the stabilisation: a higher adsorbed amount provides a better steric stabilisation. Nevertheless, in these experiments the amounts are not high enough to stop the aggregation completely. Excellent steric stabilisation was obtained with a series of amphiphilic diblock copolymers and two graft copolymers. This result is in line with the large adsorbed amounts of these polymers

Introduction

The effect of polymers on the stability of colloidal dispersions is of great importance in many industrial processes and products. Polymers can dramatically change the stability of a colloidal dispersion because of their interfacial activity.[1] Both an increase and a decrease of this stability is possible.[2] In some applications destabilisation is the main purpose, for example in water purification and papermaking; in other cases the stabilisation of colloids is desired, for instance in the food and paint industry. Without polymer, a colloidal dispersion in a non-polar solvent is often unstable. In an aqueous dispersion the particles can be stabilised electrostatically without the need of polymer: if the range of the electrostatic repulsion, which depends mainly on the ionic strength, is higher than that of the attractive Van der Waals forces, the dispersion will be stable. In both polar and apolar solvents the colloidal particles can be stabilised sterically by the presence of polymers. These polymers must then adsorb on the surface of the colloidal particles and form a thick layer, thereby providing the particles with a stabilising repulsive sheath.

In previous papers we reported on the adsorption of different types of block and graft copolymers onto silica and titania.[3-5] In this paper we study the effect of these polymers on the stability of an aqueous silica dispersion in the presence of salt. Electrostatic stabilisation of the silica dispersion is eliminated by using a high ionic strength. The electrostatic repulsion then only has a very short range and does not protect the silica particles against coagulation. An adsorbed polymer layer can prevent the coagulation of the particles or, when the layer is not thick enough, may reduce the coagulation rate. By comparing the coagulation rate of particles with an adsorbed polymer layer to that of an unstable bare silica dispersion we get insight in the stabilising properties of the polymers.

We used dynamic light scattering to measure the average hydrodynamic radius of the silica particles as a function of time. This gives a good indication of the stability of a colloidal dispersion as during coagulation the average size of the aggregates will increase. The rate of increase of the radius in time is related to the coagulation rate of the dispersion.

Experimental

Materials

The polymers used are described in more detail in previous papers on the adsorption onto silica and titania.[3-5] Molar masses per block and the adsorbed amount on silica are given in Table 1, where for the graft copolymers the total molar mass is given.

Table 1. Characteristics of the polymers used. The adsorbed amount on silica as measured by *reflectometry has been included.*

sample	M_w kg mol^{-1}	Γ mg m^{-2}	sample	M_w kg mol^{-1}	Γ mg m^{-2}
PVME	99	0.78	PMeOx-PEO-PMeOx 75	3.0-2.0-3.0	0.70
PVME-PEtOx 63	15.7-9.2	1.23	PMeOx-PEO-PMeOx 57	1.3-2.0-1.3	0.65
PVME-PEtOx 42	7.5-10.3	0.88	PEO	7.1	0.36
PVME-PEtOx 17	2-8 [a]	0.69	PDMS-PEtOx 0.5/2	0.5-2 [a]	3.5
PEtOx	6.0	0.56	PDMS-PEtOx 2/8	2.18-10.7	4.9
PMeOx	6.0	0.53	PDMS-PEtOx 5/20	4.83-19.6	8.5
PMeOx-PEO 89	5.8-0.75	0.62	PDMS-PEtOx 20/80	20-80 [a]	5.0
PMeOx-PEO 67	4.3-2.1	0.61	PAAm-g-PEO G10	1000 [b]	1.2
PMeOx-PEO 17	1.0-5.0	0.47	PAAm-g-PEO G18	1000 [b]	1.35

(a) The molar mass of these polymers has not been determined, the value given is the target molar mass during synthesis.

(b) This is an order of magnitude for the total molar mass. The molar mass of the PEO grafts is 6.34 kg mol^{-1}. The number of PEO grafts per molecule is about 15 for G10 (10 % w/w) and 30 for G18 (18 % w/w)

We used a series of poly(vinyl methyl ether)-poly(ethyl oxazoline) (PVME-PEtOx) diblock copolymers where both blocks are soluble in water and have affinity for silica, leading to non-selective adsorption from a non-selective solvent.[3] Di- and triblock copolymers of poly(methyl oxazoline) (PMeOx) and poly(ethylene oxide) (PEO) also adsorb non-selectively on silica.[3] The adsorbed amount of this series of polymers is slightly lower than that of the first series. Very high adsorbed amounts are found for a series of amphiphilic diblock copolymers of poly(dimethyl siloxane) (PDMS) and poly(ethyl oxazoline). These polymers adsorb preferentially with the hydrophobic PDMS block and a very dense adsorbed layer is formed on the silica surface.[4] Intermediate values for the adsorbed amount are found for the last series of polymers used in this study: graft

copolymers with a backbone of poly(acryl amide) (PAAm) and side chains of poly(ethylene oxide).[5] The backbone of the graft copolymer has no affinity for silica and the adsorption of this polymer proceeds by the attachment of the PEO grafts. The graft density is low: the weight percentage of the side chains is 10 and 18 %.

Polymer solutions in demineralised water were stored in the refrigerator an were used within a few days after preparation.

Coagulation of silica

The aggregation of particles in a colloidal dispersion can be monitored by particle counting methods as used in the Coulter Counter[6] and Single Particle Optical Sizing.[7,8] Other techniques use a more indirect method to obtain information on the aggregation process by monitoring the turbidity[9] or the rheology[10] of the dispersion. In this study we used dynamic light scattering to measure the average hydrodynamic radius of the silica particles in the dispersion. In a stable dispersion the particles do not aggregate and the average radius is constant in time. If aggregation occurs, the particles form aggregates with a higher hydrodynamic radius than the single particles. The average hydrodynamic radius will thus increase as a function of time during the aggregation. With these measurements we are able to monitor the effect of the different polymers on the stability of the silica dispersion. The rate of increase of the average hydrodynamic radius of polymer covered particles compared to that of uncovered particles is taken as a measure of the stabilising effect of the adsorbing polymers.

The average hydrodynamic radius of colloidal silica particles is measured with an ALV light scattering apparatus equipped with a 400 mW Argon ion laser which was tuned at a wavelength of 514 nm. All measurements were performed at a scattering angle of 70° and a temperature of 295 ± 1 K. The pH of the solutions was 6.5. The coagulation experiments are performed with a colloidal Stöber silica. The average hydrodynamic radius as determined by dynamic light scattering was 306 nm.[11]

The silica dispersion was sonicated for one hour before use. The effect of the ionic strength was studied by adding different amounts of KNO_3 to a dispersion with a total silica concentration of 0.005 % w/w. The solution was gently mixed three times by end-over-end rotation, and the average hydrodynamic radius was subsequently recorded with time intervals of 22 seconds. The increase of the radius with time for the different concentrations is used to obtain the critical coagulation concentration of KNO_3.

The colloidal silica was equilibrated for two days in a 400 mg l^{-1} polymer solution. We then added KNO_3 up to a total concentration of 0.5 M to study the effect of the polymer on the stability of a dispersion which is not electrostatically stabilised. The solution was then gently mixed three times by end-over-end rotation. Subsequently, the average hydrodynamic radius was recorded with time intervals of 22 seconds. The final silica concentration is equal to that used for the measurements without polymer.

Results and Discussion

Coagulation of silica by salt

During aggregation of particles in a colloidal dispersion the size of the aggregates will increase. This leads to an increase of the average hydrodynamic radius as measured by dynamic light scattering. We first consider the coagulation of a silica dispersion by addition of salt. The coagulation process is controlled by the Brownian movement of the particles (perikinetic coagulation), except for the initial seconds where mixing of the dispersion with the KNO_3 solution was necessary. The coagulation rate depends on the particle concentration. By changing the concentration of the dispersion we determined a concentration where the aggregation rate is such, that a considerable increase of the average hydrodynamic radius within the time scale of the measurements is observed. With a silica concentration of 0.005 % w/w (about 2.5×10^8 particles per ml) the hydrodynamic radius increases up to twice its initial value within one hour. In Figure 1 we show the increase of the average hydrodynamic radius of a silica dispersion in 0.5 M KNO_3. This concentration is assumed to be enough to eliminate the electrostatic repulsion between the particles.

In is clearly seen that the increase of the radius is linear in time. This linear increase continues up to an average hydrodynamic radius of 600 nm, twice the initial value (not shown). The accuracy of the measurements is very good, the slope can be reproduced with a standard deviation of $\pm$ 0.2 nm min^{-1}.

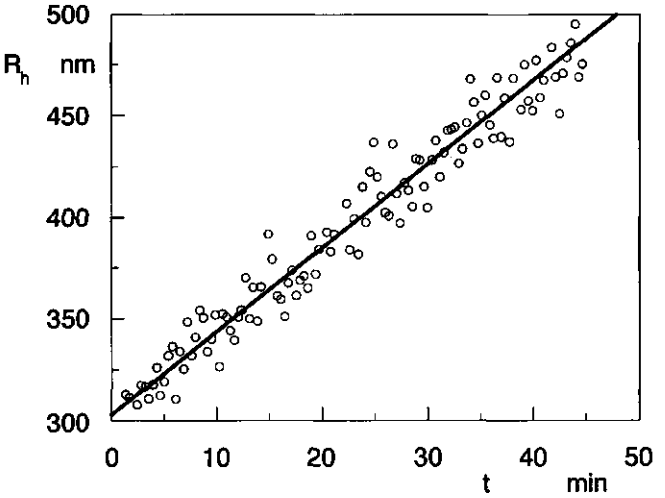

Figure 1. The increase of the average hydrodynamic radius (R_h) of an 0.005 % (w/w) silica dispersion in 0.5 M KNO_3 at pH 6.5, as measured by dynamic light scattering. The line is a linear fit; the slope is 4.1 nm min^{-1}.

In principle, we could obtain the overall rate constant k_s of the coagulation from a plot of the hydrodynamic radius as a function of time. As early as in 1916, Von Smoluchowski derived a theoretical expression for the change of the number of particles in perikinetic coagulation.[12,13] With this expression the intensity-weighted contribution of the different aggregates can be calculated as a function of time and an expression is obtained for the increase of the average hydrodynamic radius as a function of time.[14,15] The result can be compared to the experimental value. However, this expression is only valid for Raleigh scattering, hence for small particles, whereas we used silica particles with a size of the order of the wavelength of light. For these large particles the intensities have to be corrected for particle form factor effects, which complicates the expressions considerably. For this reason, we do not make a comparison with the theoretical prediction for the coagulation rate constant. Even without quantitative information on the coagulation rate constant, a plot of the hydrodynamic radius as a function of time is useful for qualitatively comparing the increase of the radius in (partly) stabilised dispersions with that in an unstable dispersion.

When the electric double layer which surrounds the silica particles is compressed sufficiently every collision leads to aggregation. This so-called rapid coagulation regime

can be found by measuring the increase of the hydrodynamic radius at different salt concentrations. When the increase depends no longer on the salt concentration, this regime is reached. In Figure 2 we plot the increase of the average hydrodynamic radius of a silica dispersion as a function of time for different salt concentrations. In the figure we only give the linear fits, in order to avoid an unreadable collection of data points.

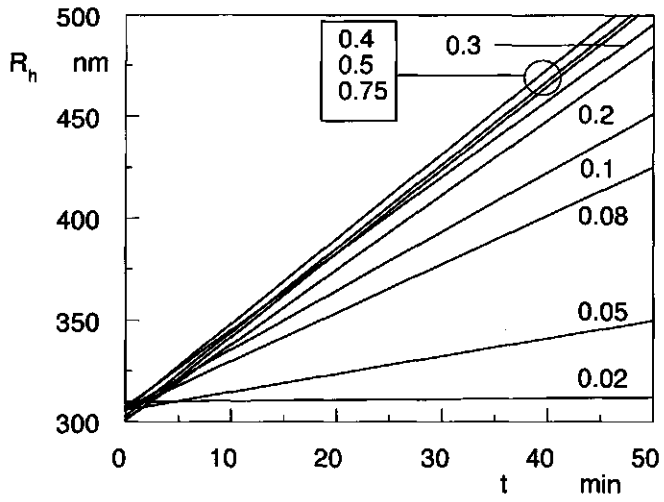

Figure 2. The increase of the average hydrodynamic radius (R_h) in an 0.005 % (w/w) silica dispersion with different concentrations of KNO_3 at pH 6.5 The lines are linear fits to the measured values of R_h, as in Figure 1. The salt concentrations are indicated in moles per litre.

For a low salt concentration the increase of the radius in time is slow, because only part of the collisions between the particles lead to an aggregate. Upon increasing the ionic strength the double layer becomes compressed and the repulsion between the particle decreases, which results in an increase of the slope in Figure 2. Rapid coagulation is reached when the salt concentration is above 0.4 M: the slope then becomes independent of the salt concentration since all collisions are effective. The slope m of the curves is a measure of the coagulation rate. This slope m can be used to deduce the stability ratio $W = m_r / m$, where m_r is the slope found for rapid coagulation at the same particle concentration. In Figure 3 we plotted this stability ratio W as a function of the salt concentration on a double-logarithmic scale. For m_r the average value of m at $[KNO_3]$ = 0.4, 0.5 and 0.75 M is used. The critical coagulation concentration, defined by the intersection of the two straight lines in Figure 3, is around 0.1 M.

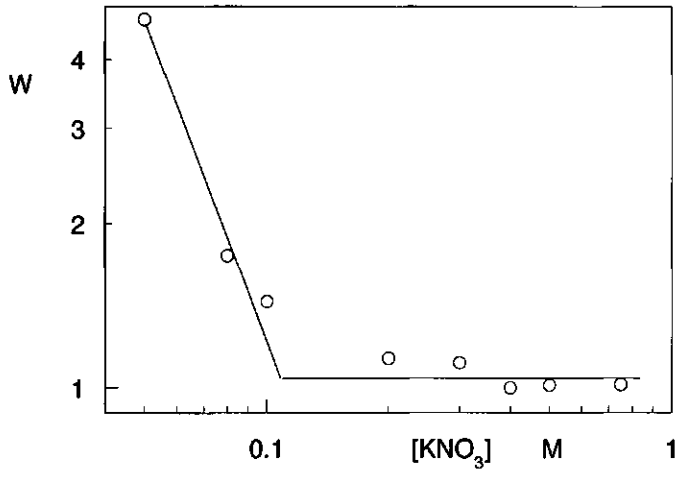

Figure 3. The stability ratio $W = m_r/m$ as a function of salt concentration in a double-logarithmic plot, for an aqueous 0.005 % (w/w) silica dispersion at pH 6.5.

Stabilisation by PVME-PEtOx diblock copolymers

In the previous section we have seen that measurements performed at 0.5 M KNO_3 are in the rapid coagulation regime. In the following sections we discuss the effect of adsorbed diblock and graft copolymers on the aggregation of silica in a dispersion with 0.5 M salt. Previously[3] we have shown that PVME-PEtOx diblock copolymers adsorb on silica with the PVME block as the adsorbed anchor block. However, also the PEtOx block adsorbs to the surface, which gives rise to a non-selective adsorption process with a relatively thin adsorbed layer. A real anchor-buoy structure, corresponding with a high adsorbed amount and a thick layer, is only found for a relatively high fraction of anchoring segments. This contrasts with the results obtained for selectively adsorbing diblock copolymers, where the highest adsorbed amount is formed at a relatively low fraction of anchoring segments.[16,17] For our non-selectively adsorbing system, the best stabilising effects may therefore be expected for the diblock copolymer with a relatively large PVME anchor block. In Figure 4 the stability ratio of silica covered with adsorbed PVME-PEtOx diblock copolymers is plotted as a function of the block copolymer composition. The stability ratio W is now defined as the ratio m_r/m, where m_r is the slope of a radius versus time curve of a bare silica dispersion in the rapid coagulation regime, and m is the slope of an aggregating silica dispersion with adsorbed polymer in 0.5 M KNO_3.

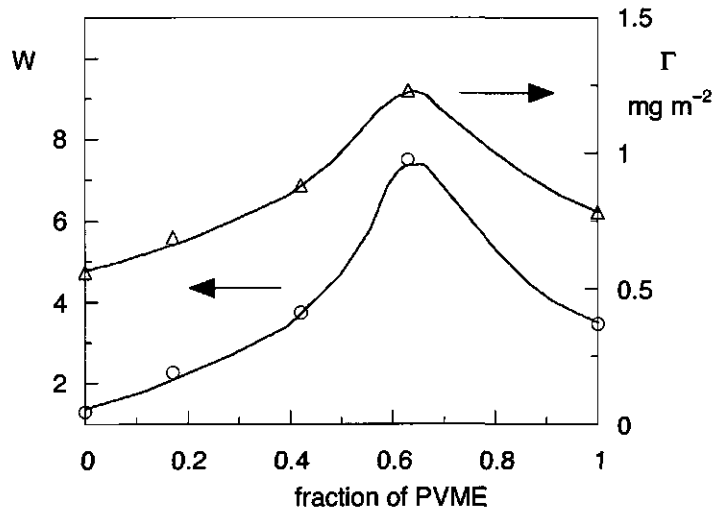

Figure 4. The stability ratio $W = m_r/m$ of an 0.005 % (w/w) silica dispersion saturated with an adsorbed polymer layer in 0.5 M KNO_3 at pH 6.5, as a function of the fraction of PVME in the diblock copolymers of PVME-PEtOx (circles, left axis). The adsorbed amount as measured by reflectometry[3] has been included (triangles, right axis).

The adsorbed polymers clearly slow down the aggregation of the silica dispersion. The PEtOx homopolymer, on the far left side of the figure, only has a very small effect. In this case the thickness of the layer and the adsorbed amount are very low due to the low molar mass (6000 g mol^{-1}). The PVME homopolymer (on the right side of the plot) provides some more steric stabilisation than PEtOx, which is not unexpected since this polymer has a much higher molar mass (99000 g mol^{-1}) and a higher adsorbed amount and layer thickness. We find a maximum in the stabilising effect for a diblock copolymer with a relatively large PVME block (around 60 % PVME). The trends in W are in excellent agreement with those for the adsorbed amount. Nevertheless, the dispersion does still aggregate to some extent, be it considerably slower than without adsorbed polymer. This insufficient stabilisation can be explained by the small thickness of the adsorbed layers, which was found to be around 7 nm in the maximum of Figure 4.[3] The attractive Van der Waals forces decrease in the direction away from the surface. We estimate that at 20 nm from the surface the attraction is of order kT, which is not enough to lead to particle aggregation as the particles also have kinetic energy and undergo Brownian motion. At shorter distances, however, the polymer layer is unable to completely screen these attractive forces.

Stabilisation by PMeOx-PEO block copolymers

The adsorption properties of PMeOx-PEO diblock copolymers on silica are very similar to those of the PVME-PEtOx.[3] Again, the highest adsorbed amount for this non-selectively adsorbing copolymer is found for a block copolymer with a relatively high fraction of anchor segments (i.e., PMeOx). The adsorption maximum is, however, far less pronounced than for PVME-PEtOx. Accordingly, the stabilising effect of these diblock copolymers is much lower than for the polymers in the previous section. This is demonstrated in Figure 5.

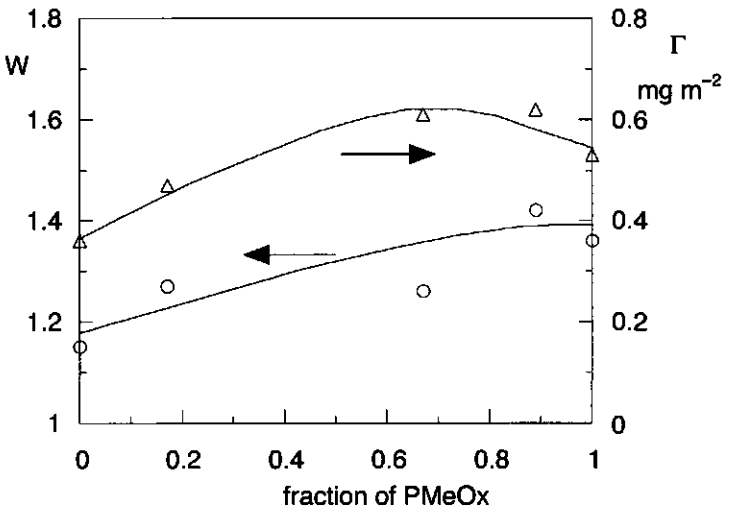

Figure 5. The stability ratio W = m_f/m of an 0.005 % (w/w) silica dispersion saturated with an adsorbed polymer layer in 0.5 M KNO_3 at pH 6.5, as a function of the fraction of PMeOx in the diblock copolymers of PMeOx-PEO (circles, left axis). The adsorbed amount as measured by reflectometry[3] has been included (triangles, right axis).

The weak maximum in the adsorbed amount is hardly reflected in the stabilising effect of these diblock copolymers. The steric stabilisation increases somewhat with the fraction of PMeOx, but the effect is only small and perhaps not significant, as it hardly exceeds the experimental error. Only the stability ratio of the PEO homopolymer (on the far left side of Figure 5) seems to be significantly lower than that of the others. This is in agreement with the low adsorbed amount of this polymer. The diblock copolymers of PMeOx-PEO are

much less effective stabilisers than the diblock copolymers of PVME-PEtOx, which again is in line with the results for the adsorbed amount.

Triblock copolymers with a middle block of PEO and two outer blocks of PMeOx have a slightly higher adsorbed amount than the diblock copolymers.[3] In principle, the steric stabilisation by these polymers could therefore be somewhat better. On the other hand, this triblock copolymer probably has shorter tails as the outer blocks have the highest affinity for the surface. Upon preparing the samples, however, some bridging flocculation occurred which made the samples unsuitable for the stability measurements. This bridging flocculation is more likely to occur with this type of triblock copolymers than with diblock copolymers as the former can more easily adsorb to two different particles.[18]

Stabilisation by PDMS-PEtOx diblock copolymers

Diblock copolymers of PDMS-PEtOX adsorb on silica with a very high adsorbed amount.[4] The series of four polymers adsorb with the hydrophobic PDMS block anchored to the surface, whereas the hydrophilic PEtOx block protrudes into the solution.[4] The hydrophilic block is larger than the hydrophobic block (the weight ratio is 4:1), so that very thick layers can be formed. The adsorbed layer is very effective in sterically stabilising the silica dispersion: no aggregation could be detected when the KNO_3 concentration of dispersion was increased to 0.5 M. Also after two days the average hydrodynamic radius was the same as before the salt had been added. The smallest copolymer has a very small molar mass, 2500 g mol^{-1}, but is as effective as the larger polymers. With the largest polymer, having a molar mass of 10^5 g mol^{-1}, however, no proper stability measurements could be performed. Before adding the salt solution, the average hydrodynamic radius had already increased to 700 nm, indicating that some aggregation had occurred. This aggregation is most probably caused by the presence of very large micelles and rod-like structures in a solution of this amphiphilic polymer.[4] The rods are very long and can probably trap the silica particles because also the hydrophilic chains have a high affinity for the silica surface. The process could thus be considered as the adsorption of silica particles onto a polymeric aggregate rather than the reverse. Upon addition of salt no additional aggregation is found. The three smallest diblock copolymers of PDMS-PEtOx did not pose such problems and can therefore be marked as excellent steric stabilisers. Again, this feature corresponds nicely with the observed very large adsorbed amounts.

Stabilisation by PAAm-PEO graft copolymers

Another type of polymer for which we studied the adsorption onto silica were graft copolymers with a non-adsorbing backbone of PAAm and adsorbing side chains of PEO[5]. The graft copolymers have a low grafting density, which results in a conformation where only a few of the side chains are actually adsorbed whereas the remainder of the molecule protrudes into the solution. This results in relatively high adsorbed amounts of about 1.3 mg m^{-2}, depending slightly on the graft density. When we increased the salt concentration of the silica dispersion with adsorbed graft copolymer to 0.5 M KNO_3 at pH 6.5, no aggregation was observed. Also after two days in this salt solution the average hydrodynamic radius was the same as before addition of salt. Although the adsorbed amount of these graft copolymers is not as high as that of the amphiphilic polymers, the thickness of the adsorbed layer may be relatively high because only a few of the side chains are adsorbed to the surface and the molar mass is quite high. These PAAm-PEO graft copolymers can thus be considered as very good steric stabilisers of a silica dispersion.

Conclusions

The coagulation of an aqueous silica dispersion by adding salt can successfully be monitored by measuring the increase of the hydrodynamic radius with dynamic light scattering. The radius increases linearly with time up to twice its initial value. Dynamic light scattering is suitable to study the stabilising effects of polymers adsorbed to silica particles. To this end, the increase of the average hydrodynamic radius in time for this 'protected' silica is compared with that of uncovered silica particles. Four different series of diblock and graft copolymers were used to stabilise the silica dispersion. For two series of non-selectively adsorbing diblock copolymers, poly(vinyl methyl ether)-poly(ethyl oxazoline) and poly(methyl oxazoline)-poly(ethylene oxide), we found a good correlation between the adsorbed amount and the stabilisation by the polymers. A higher adsorbed amount provides a better steric stabilisation. Nevertheless, for those polymers the adsorbed amounts, up to about 1.2 mg m^{-2}, are not high enough to protect the dispersion completely against aggregation. A series of amphiphilic diblock copolymers of poly(dimethyl siloxane)-poly(2-ethyl-2-oxazoline) with very high adsorbed amounts (between 3.5 and 8 mg m^{-2}) give excellent steric stabilisation of the dispersion. For the largest polymer in this series, however, some aggregation occurred as this polymer forms long rod-like micellar structures in solution to which the particles can probably adhere. Adsorbed layers of two graft copolymers of poly(acryl amide)-poly(ethylene oxide), with a non-adsorbing backbone and adsorbing side chains, are also effective in

preventing the silica from aggregating. Although the adsorbed amount of these graft copolymers is not as high as that of the amphiphilic polymers, the thickness of the adsorbed layer is relatively high because only a few of the side chains are adsorbed to the surface, and long loops and tails are formed.

References

(1) Fleer, G. J.; Cohen Stuart, M. A.; Scheutjens, J. M. H. M.; Cosgrove, T.; Vincent, B. *Polymers at Interfaces*; Chapman & Hall: London, 1993.

(2) Napper, D. H. *Polymeric stabilisation of colloidal dispersions*; Academic Press: London, 1983.

(3) Bijsterbosch, H. D.; Cohen Stuart, M. A.; Fleer, G. J.; Van Caeter, P.; Goethals, E. J. *Macromolecules* **1997**, *submitted.*

(4) Bijsterbosch, H. D.; Cohen Stuart, M. A.; Fleer, G. J. *In preparation* **1997**.

(5) Bijsterbosch, H. D.; Cohen Stuart, M. A.; Fleer, G. J. *in preparation* **1997**.

(6) Adachi, Y.; Matsumoto, T. *Colloids and Surfaces A - Physicochemical and Engineering Aspects* **1996**, *113*, 229.

(7) Pelssers, E. G. M.; Cohen Stuart, M. A.; Fleer, G. J. *J. Colloid Interface Sci.* **1990**, *137*, 350.

(8) Pelssers, E. G. M.; Cohen Stuart, M. A.; Fleer, G. J. *J. Colloid Interface Sci.* **1990**, *137*, 362.

(9) Smith, N. J.; Williams, P. A. *J. Chem. Soc., Faraday Trans.* **1995**, *91*, 1483.

(10) Miano, F.; Bailey, A.; Luckham, P. F.; Tadros, T. F. *Colloids and Surfaces* **1992**, *68*, 9.

(11) De Keizer, A.; Van der Ent, E. M.; Koopal, L. K. *in preparation* **1997**.

(12) Von Smoluchowski, M. *Phys. Z.* **1916**, *17*, 557, 585.

(13) Von Smoluchowski, M. *Z. Phys. Chem.* **1917**, *92*, 129.

(14) Versmold, H.; Hartl, W. *J. Chem. Phys.* **1983**, *79*, 4006.

(15) Killmann, E.; Adolph, H. *Colloid and Polymer Science* **1995**, *273*, 1071.

(16) Marques, C. M.; Joanny, J. F. *Macromolecules* **1989**, *22*, 1454.

(17) Evers, O. A.; Scheutjens, J. M. H. M.; Fleer, G. J. *J. Chem. Soc., Faraday Trans* **1990**, *86*, 1333.

(18) Wijmans, W. M.; Leermakers, F. A. M.; Fleer, G. J. *J. Colloid Interface Sci.* **1994**, *167*, 124.

Summary

The main aim of the work described in this thesis is to study the effect of different types of copolymers on the stability of aqueous oxide dispersions. Such dispersions are a major component in water-borne paints. In order to obtain a better insight in steric stabilisation we first investigated the relation between the adsorbed amount and layer thickness, and paid attention to the effect of the type of copolymer on the adsorbed amount. We also studied the adsorption kinetics as these are relevant for industrial purposes.

An introduction on steric stabilisation is given in Chapter 1. For block copolymers the solvent may be *non-selective* or *selective*. In a non-selective solvent both blocks are solvated and the polymer molecules are likely to be in a non-aggregated conformation. However, in a selective solvent the molecules form micelles in which the non-soluble blocks are clustered together, surrounded by a layer of solubilised chains. The adsorption kinetics are expected to be affected by the existence of such micelles. Another important feature for the adsorption of block copolymers is the selectivity of the surface. When only one of the blocks has affinity for the surface this will give rise to *selective adsorption*. On the other hand, the adsorption of a block copolymer in which both blocks have affinity for the surface is *non-selective*. The resultant polymer layer will differ for both cases. In thesis we studied selective and non-selective adsorption from a selective and a non-selective solvent. As the architecture of the copolymers is also relevant we paid attention to the adsorption of both block copolymers and graft copolymers.

In Chapter 2 we describe the properties of spread monolayers of polystyrene-poly(ethylene oxide) (PS-PEO) diblock copolymers at the air-water interface. The surface pressure and the thickness of the layer were measured as a function of the adsorbed amount. The thickness was determined with neutron reflectivity measurements.

Upon compression of the polymer monolayer the surface pressure increases over the entire experimental range of compression. At low coverage the adsorbing PEO block forms a flat "pancake" structure at the surface. When the surface area per molecule is decreased the PEO is pushed out of the surface layer into the solution to form a "cigar" or "brush" structure, which is firmly anchored by the PS block. Some scaling analysis have suggested that this desorption occurs as a first-order surface phase transition. When the polymer layer is compressed further, so that the surface density σ increases, the chains stretch and the thickness H of the layer increases too. Theories predict that H scales as $N\sigma^{1/3}$, where N is the number of monomers per polymer chain. This is confirmed by our

results. However, our experimental data do not show the first-order surface phase transition between pancake and brush. Numerical self-consistent-field calculations also show a gradual transition rather than a first-order phase transition.

In Chapter 3 we present a study on the non-selective adsorption of two series of diblock copolymers, poly(vinyl methyl ether)-poly(2-ethyl-2-oxazoline) and poly(2-methyl-2-oxazoline)-poly(ethylene oxide), from aqueous solution on a macroscopically flat silicium oxide surface. The adsorbed amounts in this study, and in that of Chapters 4 and 5, were measured with an optical reflectometer in an impinging jet flow cell. The hydrodynamic layer thickness was determined by dynamic light scattering.

The different blocks in the copolymers all have affinity for the silica surface. In all cases there is a small difference between the segmental adsorption energies of the two blocks, giving rise to *non-selective* adsorption of the block copolymers. For the two types of block copolymers used in this study, the adsorbed amount as a function of block copolymer composition shows a shallow maximum; at this maximum the longest block is also the more strongly adsorbing block. The same trend is found for the hydrodynamic layer thickness. These findings differ from theoretical predictions concerning *selective* adsorption, where a pronounced maximum is found for a short anchor block. With numerical self-consistent field calculations we demonstrate that the same trends as in our experimental findings can be predicted by theory. In non-selective adsorption of diblock copolymers, with a small difference between the adsorption energies of the blocks, both blocks compete for the same adsorption sites on the surface. When the blocks are incompatible they try to avoid each other, which promotes an anchor-buoy structure. These factors then give rise to a maximum in the adsorbed amount as a function of the block copolymer composition. At this maximum the longest block is also the more strongly adsorbing block. The adsorbed layer has the typical anchor-buoy structure which is necessary for an effective steric stabilisation, but this structure is less pronounced than for selective adsorption.

The kinetics of adsorption of diblock copolymers can be very slow if the polymers form micelles in solution. In Chapter 4 we compare the experimental adsorption rates on silica and titania with the theoretical flux of copolymer molecules towards the surface for four poly(dimethyl siloxane)-poly(2-ethyl-2-oxazoline) diblock copolymers with the same block length ratio but different molar masses. In aqueous solution these block copolymers form large polydisperse micelles with a very low critical micellisation concentration (lower than 2 mg l^{-1}).

On both surfaces the adsorption behaviour is governed by the anchoring of the hydrophobic siloxane blocks The adsorption kinetics are affected by the exchange rate of free polymer molecules between micelles and solution. For the three smallest molar masses the exchange rate is fast compared to the time a micelle needs to diffuse across the diffusive layer. Before the micelles arrive at the surface they have already broken up into free polymers. Because the cmc is very low, the experimental adsorption rate is determined by the diffusion of micelles towards the surface. For the longest polymer this is not the case: the exchange of polymer molecules between micelles and solution is now relatively slow. As the micelles do not adsorb directly, the adsorption rate is retarded by the slow exchange process. We were able to make an estimate of the micellar relaxation time, i.e., the time a micelle needs to break up. For the largest polymer the relaxation time is of the order of a few tens of seconds. The other polymers have a micellar relaxation time that is shorter than roughly one second.

The adsorption increases linearly as a function of time, up to very high adsorbed amounts where it reaches a plateau. Such high adsorbed amount is expected for strongly (and selectively) adsorbing diblock copolymers with a relatively short anchor block. The adsorbed amount on silica is considerably higher than on titania. The reason is probably that the hydrophobic block is more strongly anchored to a silica surface than to titania, so that the density of the adsorbed layer can become higher on silica.

In Chapter 5 we investigate the interfacial behaviour of *graft* or *comb copolymers*. We compare the adsorption of graft copolymers with an adsorbing backbone and non-adsorbing side chains to the reverse situation of adsorbing side chains and a non-adsorbing backbone. Two high-molar-mass poly(acryl amide)-graft-poly(ethylene oxide) copolymers with different side chain densities were used in this study.

On titania only the backbone of these polymers adsorbs and the side chains do not. The adsorbed amount is then about the same as that found for the homopolymer without side chains. On the other hand, on silica the side chains adsorb and the backbone does have no affinity for the surface. For both polymer samples we observe a maximum in the adsorbed amount as a function of time ("overshoot"), after which the adsorbed amount decreases and a plateau is reached. The plateau adsorbed amount on silica is much higher than on titania and also much higher than for both types of homopolymers. Upon adsorption the graft copolymers initially adopt a conformation in which only part of the side chains are adsorbed. Following the overshoot, the graft copolymers show a decrease in the total adsorbed amount. The overshoot depends on the polymer concentration, which suggests that it is not caused by conformational changes in the adsorbed layer but by an exchange process between surface and solution.

Differences in graft distribution and graft density in the polymer sample are probably responsible for the displacement of adsorbed chains by polymer molecules from solution. The average number of grafts per molecule is rather low in our polymer samples. On statistical grounds there is probably an appreciable polydispersity in graft distribution and in graft density. Molecules in which the grafts are clustered to some extend can displace molecules with more regularly separated grafts, and molecules with a high graft density can displace those with a lower number of side chains. The newly arriving molecules can then adsorb in a flatter conformation with a lower adsorbed amount as the extra loss in conformational entropy is compensated by the gain in adsorption energy.

The effect of the polymers used in Chapters 3 to 5 on the stability of an aqueous silicium oxide dispersion is described in Chapter 6. The time-dependent increase of the average hydrodynamic radius of silicium oxide aggregates in the presence of electrolyte was measured. The increase of this radius with time is a measure of the aggregation rate of the dispersion. The effect of polymers on the stability of a dispersion was studied by adding polymer to the dispersion and recording the effect in the aggregation rate. Comparison of the aggregation rate of this "protected" silica with that of uncovered silica particles gives then an indication of the steric stabilisation by the adsorbing polymers.

Four different series of diblock and graft copolymers were used in these stability measurements. For two series of non-selectively adsorbing diblock copolymers, poly(vinyl methyl ether)-poly(2-ethyl-2-oxazoline) and poly(2-methyl-2-oxazoline)-poly(ethylene oxide), we find a good correlation between the adsorbed amount and the stabilising effect. A higher adsorbed amount provides a better steric stabilisation. Nevertheless, for these polymers the adsorbed amounts are not high enough (up to about 1.2 mg m^{-2}) to protect the dispersion completely against aggregation. A series of amphiphilic diblock copolymers of poly(dimethyl siloxane)-poly(2-ethyl-2-oxazoline) with very high adsorbed amounts (between 3.5 and 8 mg m^{-2}) give excellent steric stabilisation of the dispersion. Adsorbed layers of the two graft copolymers of poly(acryl amide)-poly(ethylene oxide), with a non-adsorbing backbone and adsorbing side chains, are also effective in preventing the silica from aggregating. Even though the adsorbed amount of these graft copolymers is only around 1.3 mg m^{-2}, which is much lower than that of the amphiphilic polymers, aggregation is completely prevented.

The best steric stabilisation is found for those systems in which either the surface or the solvent is selective. In practical aqueous systems, however, it is difficult to synthesise diblock copolymers in which both blocks are soluble and where only one of the blocks has affinity for the surface. We have shown that copolymers with a different architecture,

graft copolymers, also can provide good steric stabilisation and may be a good alternative to diblock copolymers. Very good steric stabilisers are amphiphilic diblock copolymers in a selective solvent. However, it is important that the hydrophobic blocks are flexible enough for fast adsorption kinetics and that they completely wet the surface. Which copolymer should be chosen for the steric stabilisation of a practical colloidal system depends largely on the nature of the particles and the solvent, and on the availability of suitable copolymers.

Samenvatting

Copolymeer Adsorptie en het Effect op Colloïdale Stabiliteit

In dit proefschrift is een onderzoek naar de adsorptie van verschillende soorten copolymeren en het effect van deze polymeren op de stabiliteit van colloïdale dispersies beschreven. Een inleiding in dit onderwerp wordt gegeven in Hoofdstuk 1.

Colloïdale stabiliteit speelt een belangrijke rol bij tal van verschijnselen in de wereld om ons heen. Zonder colloïdale stabiliteit zou er bijvoorbeeld geen melk kunnen bestaan, zou ons bloed klonteren en zouden er geen wolken kunnen zijn. Dat laatste betekent bijvoorbeeld ook geen regen en dat zou landbouw een stuk moeilijker maken. Ook bij het maken van verf is colloïdale stabiliteit van groot belang. In een verf zijn pigmentdeeltjes zeer fijn verdeeld in een vloeistof, zodat een zogenaamd colloïdaal systeem gevormd wordt. Bij een watergedragen verf is, de naam zegt het al, die vloeistof water. De verdeling van vaste deeltjes in water is moeilijk omdat de deeltjes elkaar aantrekken door Van-der-Waalskrachten. Door de deeltjes te voorzien van een beschermend laagje kan voorkomen worden dat ze aggregeren (samenklonteren).

Polymeren zijn macromoleculen die opgebouwd zijn uit een groot aantal identieke segmenten. Indien alle segmenten van hetzelfde soort zijn spreken we van een *homopolymeer*. Komen er meer soorten segmenten in één macromolecuul voor dan wordt dit een *copolymeer* genoemd. Polymeren hebben vaak de neiging zich aan een grensvlak op te hopen (*adsorptie*). Middels adsorptie van een polymeer aan het oppervlak van een pigmentdeeltje kan zo'n deeltje voorzien worden van een polymeer-laag. Door de aanwezigheid van deze laag kunnen twee deeltjes elkaar niet meer zo dicht naderen dat ze door de Van-der-Waalskrachten aggregeren. Dit verschijnsel heet *sterische stabilisatie*, waarvan een schematische voorstelling gegeven wordt in Figuur 1b van Hoofdstuk 1. Het is essentieel dat de polymeerlaag dik genoeg is om aggregatie volledig uit te sluiten: de polymeren moeten goed vastzitten en een dikke laag vormen. Dit kan bereikt worden door een copolymeer te gebruiken. Er kunnen diverse variaties van copolymeren onderscheiden worden, voorbeelden hiervan zijn *blokcopolymeren* en *kamcopolymeren*. In een blokcopolymeer zijn verschillende soorten segmenten gegroepeerd in lange blokken in hetzelfde macromolecuul, waarbij elk blok bestaat uit slechts één enkel soort segment. Een kamcopolymeer heeft een lange hoofdketen met identieke segmenten en zijketens die opgebouwd zijn uit een ander type segment. In

Figuur 2 van Hoofdstuk 1 is een schematische voorstelling gegeven van een aantal verschillende soorten polymeer.

Als de verschillende blokken van één en hetzelfde macromolecuul zo gekozen worden dat er één grote affiniteit voor het oppervlak heeft en de ander niet, dan spreken we van *selectieve adsorptie* en kan er een heel dikke geadsorbeerde laag gevormd worden. Het niet-adsorberende blok (het *boeiblok*) draagt namelijk wel bij in de laagdikte omdat het vastgehouden wordt door het andere blok (het *ankerblok*). Voorbeelden van de structuur van een geadsorbeerde laag van copolymeren worden gegeven in Figuren 3 en 4 van Hoofdstuk 1.

Het oplosmiddel speelt een belangrijke rol bij de adsorptie van blokcopolymeren. Indien beide blokken oplosbaar zijn wordt het oplosmiddel *niet-selectief* genoemd en zullen de polymeermoleculen waarschijnlijk vrij in de oplossing bewegen. In een *selectief* oplosmiddel daarentegen, vormen de moleculen micellen waarin de niet-oplosbare blokken bij elkaar zitten, omgeven door een laag gesolvateerde ketens. We verwachten dat de aanwezigheid van zulke micellen van invloed zal zijn op de *adsorptiekinetiek*. Ook de selectiviteit van het oppervlak is van belang bij de adsorptie van blokcopolymeren. Voor selective adsorptie hebben we al gezien dat er een zeer dikke geadsorbeerde laag gevormd kan worden. Wanneer echter beide blokken affiniteit hebben voor het oppervlak zal dit aanleiding kunnen zijn voor *niet-selectieve* adsorptie. De structuur van de uiteindelijk polymeerlaag zal in dat geval waarschijnlijk anders zijn.

Om een beter inzicht te verkrijgen in het verschijnsel sterische stabilisatie bestuderen we in dit proefschrift het verband tussen de geadsorbeerde hoeveelheid en de polymeerlaagdikte en het effect van het het soort copolymeer op de geadsorbeerde hoeveelheid. We beschouwen hierbij selectieve en niet-selectieve adsorptie vanuit zowel een selectief als een niet-selectief oplosmiddel. Er wordt ook aandacht besteed aan de adsorptiekinetiek omdat deze een belangrijke rol speelt bij industriële toepassingen.

In Hoofdstuk 2 beschrijven we de eigenschappen van gespreide monolagen van polystyreen-poly(ethyleenoxide) (PS-PEO) diblokcopolymeren aan het grensvlak tussen water en lucht, een vloeibaar en samendrukbaar grensvlak. De oppervlaktedruk en de laagdikte zijn gemeten als functie van de geadsorbeerde hoeveelheid. De dikte is bepaald met neutronenreflectiemetingen.

Bij het langs het oppervlak (lateraal) samendrukken van de polymeermonolaag neemt de oppervlaktedruk continu toe. Bij een lage oppervlaktebedekking vormt het geadsorbeerde PEO blok een platte "pannnenkoekstructuur" aan het oppervlak. Wanneer het beschikbaar oppervlak per molecuul kleiner wordt, wordt de PEO van het oppervlak de

oplossing ingeduwd, waar het een "sigaarstructuur" vormt, stevig verankerd door het niet-oplosbare PS blok. Volgens bepaalde theoretische beschouwingen zou deze desorptie verlopen als een eerste-orde fase-overgang. Bij het verder samendrukken van de polymeerlaag, zodat de oppervlaktedichtheid σ toeneemt, strekken de ketens zich en neemt de dikte H van de laag ook toe. De laag van gestrekte polymeerketens wordt doorgaans "borstel" genoemd. Theorieën voorspellen dat H evenredig is met $N\sigma^{1/3}$, waarin N het aantal monomeren per polymeermolecuul is. Dit wordt bevestigd door onze resultaten. Wij vinden echter geen eerste-orde fase-overgang tussen de pannenkoek- en de sigaarstructuur. Ook met numerieke zelf-consistente-veld berekeningen vinden we een geleidelijke overgang en geen eerste-orde fase-overgang.

In Hoofdstuk 3 onderzoeken we de niet-selectieve adsorptie van twee reeksen blokcopolymeren, poly(vinylmethylether)-poly(2-ethyl-2-oxazoline) en poly(2-methyl-2-oxazoline)-poly(ethyleenoxide), vanuit een waterige oplossing op een vast oppervlak, nl. een macroscopisch vlak silica plaatje. De geadsorbeerde hoeveelheid is, evenals die in Hoofdstukken 4 en 5, gemeten met een optische reflectometer in stagnatiepuntstroming. De hydrodynamische laagdikte is bepaald met dynamische lichtverstrooiing.

De verschillende blokken van de copolymeren hebben alle affiniteit voor silica. Dit geeft aanleiding tot *niet-selectieve* adsorptie van deze blokcopolymeren. Toch is er ook een klein verschil tussen the adsorptie-energieën van de twee blokken in hetzelfde molecuul. Voor de twee soorten blokcopolymeren die in dit hoofdstuk zijn gebruikt vinden we een maximum als we de geadsorbeerde hoeveelheid uitzetten als functie van de samenstelling van het blokcopolymeer; in dit maximum is het langste blok ook het sterker adsorberende blok. We vinden eenzelfde trend voor de hydrodynamische laagdikte. Deze bevindingen verschillen van wat men verwacht op grond van theoretische beschouwingen aangaande *selectieve* adsorptie, waar een uitgesproken maximum gevonden wordt voor een relatief kort ankerblok. Met numerieke zelf-consistente-veld berekeningen tonen we aan dat de experimenteel waargenomen trends ook theoretisch verklaard kunnen worden. Bij niet-selectieve adsorptie van diblokcopolymeren met een klein verschil tussen de adsorptie-energieën, wedijveren beide blokken voor dezelfde adsorptieplekken. Als beide blokken niet compatibel zijn (d.w.z. niet spontaan mengbaar) zullen ze elkaar proberen te mijden, wat een anker-boei structuur bevordert. Dit heeft tot gevolg dat in de geadsorbeerde hoeveelheid als functie van polymeersamenstelling een maximum gevonden wordt waarbij het langste blok ook het sterker adsorberende blok is. De geadsorbeerde laag heeft de typische anker-boei structuur die nodig is voor effectieve sterische stabilisatie. Deze structuur is echter minder uitgesproken dan met selectieve adsorptie.

De adsorptiekinetiek van diblokcopolymeren kan heel langzaam zijn als de polymeren micellen vormen. In Hoofdstuk 4 vergelijken we de experimentele adsorptiesnelheid op silica en titania met de theoretische flux van moleculen naar het oppervlak. Dit doen we voor vier poly(dimethylsiloxaan)-poly(2-ethyl-2-oxazoline) diblokcopolymeren met dezelfde bloklengteverhouding maar met verschillende molaire massa's. In water vormen deze polymeren grote polydisperse micellen met een zeer lage kritische micelvormingsconcentratie (lager dan 2 mg l^{-1}). De hydrofobe siloxaanblokken vormen de kern van de micellen, omgeven door een gesolvateerde oxazolinelaag.

Op zowel silica als titania vormen de siloxaanblokken uiteindelijk de ankerende laag. De siloxaan moet echter eerst door de micellen "losgelaten" worden. De adsorptiekinetiek van deze blokcopolymeren wordt daarom beïnvloed door de uitwisselingssnelheid van vrije polymeermoleculen tussen micellen en oplossing. Voor de drie kleinste molaire massa's is deze uitwisselingssnelheid snel vergeleken met de tijd die een micel nodig heeft om over de diffusielaag naar het oppervlak te diffunderen. Voordat de micellen bij het oppervlak aankomen zijn ze al opgebroken in vrije moleculen, die vervolgens met hun hydrofobe blok kunnen adsorberen. Omdat de kritische micelvormingsconcentratie heel laag is, wordt de experimentele adsorptiesnelheid bepaald door de diffusie van micellen naar het oppervlak. Dit is niet het geval voor het langste polymeer: de uitwisseling van moleculen tussen micellen en oplossing is nu relatief langzaam. Omdat de micellen, in ieder geval op titania, niet zelf kunnen adsorberen wordt de adsorptie vertraagd door het langzame uitwisselingsproces. We zijn in staat een schatting te maken van de micellaire relaxatietijd, de tijd die een micel nodig heeft om op te breken. Voor micellen van het langste polymeer is de relaxatietijd enige tientallen seconden. De micellen van de andere polymeren hebben een relaxatietijd die korter is dan ruwweg één seconde.

De adsorptie neemt tot een zeer grote geadsorbeerde hoeveelheid lineair toe met de tijd, waarna een plateau bereikt wordt. Zo'n grote geadsorbeerde hoeveelheid is in overeenstemming met wat we verwachten voor sterk (en selectief) adsorberende diblokcopolymeren met een relatief kort ankerblok. De geadsorbeerde hoeveelheid op silica is aanzienlijk groter dan op titania. Het hydrofobe blok is waarschijnlijk sterker verankerd op silica dan op titania, zodat de dichtheid van de geadsorbeerde laag groter kan worden op silica.

In Hoofdstuk 5 onderzoeken we het grensvlakgedrag van kamcopolymeren. We vergelijken de adsorptie van kamcopolymeren met een adsorberende hoofdketen en niet-adsorberende zijketens met de omgekeerde situatie van adsorberende zijketens en een niet-adsorberende hoofdketen. Twee copolymeren met een hoofdketen van

poly(acrylamide) en zijketens van poly(ethyleenoxide) zijn in dit onderzoek gebruikt. De polymeren hebben beide een grote molaire massa maar verschillen in zijketendichtheid.

Op titania adsorbeert alleen de hoofdketen van deze polymeren en de zijketens niet. Omdat de zijketendichtheid klein is heeft dit als gevolg dat de geadsorbeerde hoeveelheid ongeveer dezelfde is als gevonden is voor een poly(acrylamide) homopolymeer zonder zijketens. Op silica is de situatie omgedraaid: de zijketens adsorberen en de hoofdketen niet. Voor beide polymeren nemen we nu een maximum in de geadsorbeerde hoeveelheid als functie van de tijd waar, waarna de geadsorbeerde hoeveelheid afneemt en een plateau bereikt wordt. De geadsorbeerde hoeveelheid in het plateau is veel groter dan op titania en ook veel groter dan voor de PEO homopolymeren op silica. De geadsorbeerde kamcopolymeren hebben een conformatie waarin slechts een deel van de zijketens in direct contact is met het oppervlak.

Het is opmerkelijk dat de geadsorbeerde hoeveelheid kamcopolymeer als functie van de tijd een maximum vertoont. De vorm van de curve hangt af van de polymeerconcentratie, wat er op wijst dat dit maximum niet wordt veroorzaakt door een conformatieverandering aan het oppervlak maar door een uitwisselingsproces tussen oppervlak en oplossing.

Verschillen in de zijketendistributie en -dichtheid tussen de individuele moleculen in het polymeermonster zijn waarschijnlijk verantwoordelijk voor de verdringing van geadsorbeerde ketens door ketens uit de oplossing. Het gemiddelde aantal zijketens per molecuul is tamelijk klein in onze polymeermonsters. Statistisch is het aannemelijk dat er een behoorlijke polydispersiteit is in de zijketendistributie en -dichtheid. Moleculen met gegroepeerde zijketens kunnen moleculen met een meer regelmatige verdeling verdringen en moleculen met een grotere zijketendichtheid kunnen moleculen met een kleinere zijketendichtheid verdringen. De nieuwkomers kunnen dan in een vlakkere conformatie adsorberen omdat het extra verlies van conformatie-entropie wordt gecompenseerd door winst in adsorptie-energie. Dit heeft een kleinere geadsorbeerde hoeveelheid tot gevolg.

Het effect van polymeren op de stabiliteit van een silica dispersie in water is beschreven in Hoofdstuk 6. We hebben daarbij gebruik gemaakt van de polymeren waarvan we het adsorptiegedrag in Hoofdstukken 3 tot en met 5 hebben beschreven. De tijdafhankelijke toename van de gemiddelde hydrodynamische straal van silica aggregaten in de aanwezigheid van electroliet is gemeten. De toename van deze straal als functie van tijd is een goede maat voor de aggregatiesnelheid van de dispersie. Het effect van polymeren op de stabiliteit van een dispersie is bestudeerd door polymeer toe te voegen en het effect op de aggregatiesnelheid vast te leggen. Vergelijking van de aggregatiesnelheid

van deze "beschermde" silica met die van onbedekte silicadeeltjes geeft dan een indicatie van de sterische stabilisatie door de adsorberende polymeren.

Voor twee reeksen niet-selectief adsorberende diblokcopolymeren, poly(vinylmethyl-ether)-poly(2-ethyl-2-oxazoline) en poly(2-methyl-2-oxazoline)-poly(ethyleenoxide), vinden we een goede correlatie tussen de geadsorbeerde hoeveelheid en de sterische stabilisatie. Desalniettemin is de geadsorbeerde hoeveelheid niet groot genoeg (maximaal ongeveer 1.2 mg m^{-2}) om de dispersie geheel tegen aggregatie te beschermen. De reeks van amfifiele poly(dimethylsiloxaan)-poly(2-ethyl-2-oxazoline) diblokcopolymeren, met een grote adsorptie op silica (tussen 3.5 en 8 mg m^{-2}), geeft een uitstekende sterische stabilisatie. Geadsorbeerde lagen van de twee poly(acrylamide)-poly(ethyleenoxide) kamcopolymeren, met adsorberende zijketens en een niet-adsorberende hoofdketen, zijn ook heel effectief in het voorkomen van aggregatie van de silicadispersie. Hoewel de geadsorbeerde hoeveelheid van deze polymeren slechts ongeveer 1.3 mg m^{-2} is, veel lager dan voor de amfifiele polymeren, is de dispersie toch volledig stabiel.

De beste sterische stabilisatie hebben we gevonden voor die systemen waarin of het oppervlak of het oplosmiddel selectief is. In de praktijk is het echter moeilijk om een diblokcopolymeer te synthetiseren waarvan beide blokken oplosbaar zijn in water en waarbij slechts één van de blokken affiniteit heeft voor het oppervlak. Wij hebben aangetoond dat kamcopolymeren ook een goede sterische stabilisatie kunnen geven en daarom een alternatief kunnen zijn voor diblokcopolymeren. Uitstekende sterische stabilisatoren zijn amfifiele diblokcopolymeren in een selectief oplosmiddel. Het is echter met dit soort polymeren belangrijk dat het hydrofobe blok flexibel genoeg is om een snelle adsorptiekinetiek te kunnen garanderen. Ook moet het hydrofobe blok het oppervlak goed bevochtigen. Een lage glas-overgangstemperatuur (T_g) en enige polariteit kunnen daarbij van nut zijn. Welk polymeer uiteindelijk gekozen moet worden voor de stabilisatie van een praktisch (industrieel) colloïdaal systeem hangt grotendeels af van het soort deeltjes en het oplosmiddel, en uiteraard van de beschikbaarheid van geschikte copolymeren.

Curriculum vitae

Henri Derk Bijsterbosch werd geboren op 5 december 1967 te Heerde. In 1986 behaalde hij het VWO diploma aan "De Heertganck" te Heerde, waarna hij de studie Moleculaire Wetenschappen aan de Landbouwuniversiteit te Wageningen begon. De doctoraalstudie omvatte de afstudeervakken Kolloïd- en Grensvlakchemie en Levensmiddelen-natuurkunde, alsmede een praktijktijd van zes maanden bij de afdeling Grensvlakfysica van het Akzo Research Laboratorium in Arnhem. De studie werd in 1992 met succes afgerond. Van oktober 1992 tot november 1996 was hij als Assistent in Opleiding werkzaam bij de vakgroep Fysische en Kolloïdchemie van de Landbouwuniversiteit. In die periode werd het in dit proefschrift beschreven onderzoek uitgevoerd. Sinds maart 1997 is hij werkzaam bij Unilever Research in Port Sunlight, Merseyside, Groot brittannië.

Nawoord

Met het proefschrift dat voor u ligt is een lange periode van onderzoek en schrijven afgesloten. Het is dan ook met een heel prettig gevoel dat ik dit nawoord schrijf. Een nawoord dat bedoeld is om mijn waardering uit te spreken voor de mensen om mij heen die mij hebben geholpen dit proefschrift te maken tot wat het nu is.

De betrokkenheid van Martien Cohen Stuart bij het in dit proefschrift beschreven onderzoek was groot. Zijn enthousiasme en vele ideeën waren een bron van inspiratie en richting. Gerard Fleer speelde een belangrijke rol bij de interpretatie van de resultaten en het corrigeren van de manuscripten. Martien, Gerard, ik ben er trots op met jullie te hebben samengewerkt.

Met Ad van Well en Victor de Haan van het Interfacultair Reactor Instituut te Delft heb ik een zeer prettige samenwerking gehad die uiteindelijk heeft geresulteerd in Hoofdstuk 2. Eric Goethals en Peter van Caeter hebben mij van een aantal blokcopolymeren voorzien waarmee een deel van het onderzoek beschreven in Hoofdstukken 3 en 6, is uitgevoerd.

Het onderzoek is deels gefinancierd door het Innovatiegericht Onderzoek Programma Verf (IOP-v). De halfjaarlijkse voortgangsbijeenkomsten met de expertgroep dispergeren was zeer nuttig om de link met de praktijk van verfmaken in te zien. De oprechte belangstelling van de leden van de expertgroep was een grote stimulans voor het onderzoek. De samenwerking heeft duidelijk een brug geslagen tussen wetenschappelijk onderzoek en de industriële praktijk; en dat is de belangrijkste doelstelling van het IOP-v.

Michel Mellema, Martine van den Berg en Corien Struijk hebben een doctoraalvak bij mij gedaan. Hun bijdragen zijn her en der over het proefschrift verspreid terug te vinden. Ik hoop dat jullie van mij geleerd hebben; ik heb het leuk gevonden en er veel van opgestoken om jullie te begeleiden.

De vakgroep Fysische en Kolloïdchemie waar ik het onderzoek heb uitgevoerd is een bijzondere werkplek. De diversiteit van de mensen op de vakgroep maakt dat er een prettige sfeer is. Aan hulp voor allerhande zaken was nooit gebrek en gelukkig was er ook altijd tijd en belangstelling voor andere dingen dan werk. Jullie hebben er met z'n allen voor gezorgd dat ik met plezier terugkijk op mijn verblijf bij de vakgroep.

De laatste woorden in dit proefschrift zijn voor Mireille. Je hebt me altijd volledig gesteund. Als het eens niet wilde vlotten motiveerde je me weer om door te gaan. Nog belangrijker was dat je samen met Lotte het geheel wist te relativeren. Jouw bijdrage aan dit proefschrift is van onschatbare waarde geweest. Daarom kan ik nu met recht zeggen: Ons boekje is af!